1-1-2013

Experimental and Simulation Predicted Crack Paths For AL-2024-T351 Under Mixed-Mode I/II Fatigue Loading Using An Arcan Fixture

Eileen Miller
University of South Carolina - Columbia

EXPERIMENTAL AND SIMULATION PREDICTED CRACK PATHS FOR AL-2024-T351 UNDER MIXED-MODE I/II FATIGUE LOADING USING AN ARCAN FIXTURE

by

Eileen Miller

Bachelor of Science
University of South Carolina, 2011

Submitted in Partial Fulfillment of the Requirements

For the Degree of Master of Science in

Mechanical Engineering

College of Engineering and Computing

University of South Carolina

2013

Accepted by:

Michael A. Sutton, Director of Thesis

Xiaomin Deng, Co-director of Thesis

Lacy Ford, Vice Provost and Dean of Graduate Studies

ACKNOWLEDGEMENTS

There are many people who have made this work possible for me. I would first like to express my greatest appreciation for my advisor, Dr. Michael Sutton, for his mentorship through my career at the University of South Carolina. He has provided opportunities for me to work, learn, and grow as an engineer as well as proving support educationally, financially, and personally. I would also like to thank Dr. Xiaomin Deng for his guidance in this research project and in the classroom. His patience and expectations of excellence have been invaluable to this work and my preparation for future endeavors.

I would also like to extend my appreciation to Mr. Haywood Watts and Mr. Brendan Croom for their assistance conducting experiments in the laboratory. Dr. Anthony Reynolds provided valuable guidance in conducting the experiments, and Dan Wilhelm played an instrumental role in troubleshooting with the test stand. Their help is also greatly appreciated.

I also would like to acknowledge the financial support provided by NASA's South Carolina Space Grant Consortium through the Graduate Student Fellowship which helped fund my education. Also the financial support provided by an Air Force Research Lab SBIR project and specifically AFRL engineers Dr.. Robert Reuter and Dr. James Harter is deeply appreciated. Finally, I would like to extend my thanks to the College of Engineering and Computing at the University of South Carolina where the experiments were performed.

Abstract

Mixed mode I/II fatigue experiments and simulations are performed for an Arcan fixture and a 6.35mm thick Al-2024-T351 specimen. Experiments were performed for Arcan loading angles that gave rise to a range of Mode I/II crack tip conditions from $0 \leq \Delta K_{II}/\Delta K_{I} \leq \infty$. Measurements include the crack paths, loading cycles and maximum and minimum loads for each loading angle. Simulations were performed using three-dimensional finite element analysis (3D-FEA) with 10-noded tetrahedral elements via the custom in-house FEA code, CRACK3D. While modeling the entire fixture-specimen geometry, a modified version of the virtual crack closure technique (VCCT) with automatic crack tip re-meshing and a maximum normal stress criterion was used to predict the direction of crack growth. Results indicate excellent agreement between experiments and simulations for the measured crack paths during the first several millimeters of crack extension.

Table of Contents

Acknowledgements iii

Abstract iv

List of Tables vii

List of Figures viii

List of Symbols xi

List of Abbreviations xvi

Chapter 1 Introduction 1

1.1 Motivation 1

1.2 Background 3

1.3 Current Work 10

Chapter 2 Experimental Work 12

2.1 Fixture and Specimen Preparation 12

2.2 Setup 14

2.3 Experimental Procedure 16

2.4 Load Prediction 18

2.5 Determination of Experimental Crack Paths 21

2.6 Experimental Results 26

Chapter 3 Theoretical Work 32

3.1 Crack3D 32

3.2 Geometry, Mesh Generation, and Boundary Conditions 38

3.3 Simulation Procedure 42

3.4 Post-Processing of Simulation Results 44

3.5 Theoretical Results 44

Chapter 4 Discussion 50

4.1 Discussion of Experimental Results 50

4.2 Discussion of Theoretical Results 52

Chapter 5 Conclusions 60

Chapter 6 Recommendations for Future Work 62

References 65

Appendix A – Experimental Data Recorded 69

Appendix B – Details and Tips for CRACK3D Input Files Generation 91

Appendix C – Files Associated with CRACK3D for Φ = 45° 95

LIST OF TABLES

Table 2.1 Scale factors used to convert digitized points from pixels to meters................25

Table 2.2 Percent error in crack path position 25

Table 3.1 Table of applied displacements for line on top fixture 41

Table 3.2 All combinations of simulations performed to verify convergence of solution 43

Table A.1. Experimental data recorded data for Φ = 15°. 69

Table A.2. Experimental data recorded data for Φ = 30°. 73

Table A.3. Experimental data recorded data for Φ = 45°. 82

Table A.4. Experimental data recorded data for Φ = 60°. 87

Table A.5. Experimental data recorded data for Φ = 90°. 90

LIST OF FIGURES

Figure 1.1 The three fracture modes for nominally elastic conditions 3

Figure 1.2 A schematic of a typical log-log plot of Paris' Law..5

Figure 1.3 Diagram of Arcan fixture and specimen 7

Figure 1.4 Specimen for Arcan fixture with single edge crack 7

Figure 1.5 Schematic of kinked crack...8

Figure 2.1 Mixed mode I/II Arcan test fixture and butterfly shaped test specimen. Angle Φ = 0° corresponds to far-field tension and Φ = 90° is far-field shear 13

Figure 2.2 (a) Dimension of specimens in inches (b) Diagram of notch and pre-crack 13

Figure 2.3 Images of experimental set up for 45° loading angle 14

Figure 2.4 (Top) One degree-of-freedom slide apparatus; (Bottom) Two degree-of-freedom slide apparatus...15

Figure 2.5 Schematic of coordinate system in which the crack tip was tracked during Pre-cracking (solid line) and testing (dotted line)...17

Figure 2.6 Visual representations of the actual geometry and loading (solid line) And the assumed geometry and loading (dotted lines) 18

Figure 2.7 Diagram of geometry for Tada's empirical expression 19

Figure 2.8 Schematic of the images digitized and an exaggerated view of how the points Were selected for determining the scale factor from pixels to meters...........................22

Figure 2.9 Coordinate system used to define crack paths from the tip of the pre-crack ...25

Figure 2.10 Crack growth rate along crack path for 30° loading case..............................26

Figure 2.11 Crack growth rate along crack path for 45° loading case..............................27

Figure 2.12 Crack growth rate along crack path for 60° loading case..............................27

Figure 2.13 Originally digitized crack path data for 15° loading case 28

Figure 2.14 Digitized crack path and polynomial fit for 15° loading case 29

Figure 2.15 Digitized crack path and polynomial fit for 30° loading case 29

Figure 2.16 Digitized crack path and polynomial fit for 45° loading case 30

Figure 2.17 Digitized crack path and polynomial fit for 60° loading case 30

Figure 2.18 Crack path for Φ = 60° determined by slide apparatus experimentally versus the crack path determined by digitization 31

Figure 3.1 An exaggerated local 2D view of a crack-front finite element mesh on the Plane normal to the crack-front, where the rigid springs between the node pairs have Zero length 34

Figure 3.2 A local view of a crack front mesh on the extended crack surface, where the Local coordinate system for a mid-node on the crack front has its origin at the node 35

Figure 3.3 Diagram of crack growth direction for MCS criterion 37

Figure 3.4 Diagram of a picture of actual Arcan fixture and specimen (left) and image of Finite element model geometry (right) 39

Figure 3.5 Image of the 3D mesh...40

Figure 3.6 A 2D view of the initial 3D finite element mesh in the specimen region 40

Figure 3.7 Boundary conditions at Φ = 30° 41

Figure 3.8 Crack path for Φ = 15° with various initial meshes, minimum element sizes, And crack increments 45

Figure 3.9 2D view of the 3D deformed mesh for Φ = 45° (top) and a close up of the Crack path and re-meshing zone around the crack front 45

Figure 3.10 The experimental and predicted crack path for the 15° loading case.............46

Figure 3.11 The experimental and predicted crack path for the 30° loading case.............46

Figure 3.12 The experimental and predicted crack path for the 45° loading case.............47

Figure 3.13 The experimental and predicted crack path for the 60° loading case.............47

Figure 3.14 Plot of ΔK_I and ΔK_{II} along the crack path for the 15° loading case................48

Figure 3.15 Plot of ΔK_I and ΔK_{II} along the crack path for the 30° loading case................48

Figure 3.16 Plot of ΔK_I and ΔK_{II} along the crack path for the 45° loading case................49

Figure 3.17 Plot of ΔK_I and ΔK_{II} along the crack path for the 60° loading case................49

Figure 4.1 Plot of crack path for $\Phi = 30°$ and edge of top fixture.....................................51

Figure 4.2 Plot of ΔK_{eq} and da/dN along crack length for 30° loading case......................56

Figure 4.3 Plot of ΔK_{eq} and da/dN along crack length for 45° loading case......................57

Figure 4.4 Plot of ΔK_{eq} and da/dN along crack length for 60° loading case......................57

Figure 6.1 Schematic of Arcan fixture with proposed tension bar for $\Phi = 75°$.................64

Figure B.1 A 2D schematic diagram of volumes in the specimen region used to create the Initial finite element mesh 92

LIST OF SYMBOLS

$\sigma_{\theta\theta\, max}$ Maximum circumferential stress defined in polar coordinates around the crack tip.

K Stress intensity factor.

K_I Stress intensity factor for Mode I.

K_{II} Stress intensity factor for Mode II.

K_{III} Stress intensity factor for Mode III.

σ Far field tensile stress.

a Crack length.

w Specimen width.

ΔK Difference in maximum applied stress intensity factor and minimum applied stress intensity factor for fatigue loading.

K_{max} Maximum applied stress intensity factor for fatigue loading.

K_{min} Minimum applied stress intensity factor for fatigue loading.

R Loading ratio, also known as R-ratio.

σ_{max} Maximum applied far-field tensile stress for fatigue loading.

σ_{min} Minimum applied far-field tensile stress for fatigue loading.

N Number of loading cycles.

da/dN Crack growth rate which is the differential amount of crack growth per number of stress cycles.

C Material and R-ratio dependent proportionality constant for Paris' Law.

m Material and R-ratio dependent power constant for Paris' Law.

ΔK_{TH} Threshold ΔK. The value below which the fatigue crack will not propagate.

K_c Fracture toughness. The value which, if K_{max} exceeds, rapid crack propagation ensues and final fracture occurs.

F_I Function of loading, geometry, and crack orientation for determining K_I empirically.

F_{II} Function of loading, geometry, and crack orientation for determining K_{II} empirically.

t Specimen thickness.

P Pin load applied using Arcan fixture.

α Angle from the vertical direction to the first segment of a kinked crack.

β Angle from the first segment of a kinked crack to the second segment.

b Crack length for the second segment of a kinked crack.

Φ Loading angle for Arcan fixture.

h Distance from crack to uniform tensile stress for Tada's empirical solution for K_I.

ΔK_{eq} Equivalent ΔK for the mixed mode loading condition.

γ, γ_1, $\gamma 2$ Parameters for ΔK_{eq}.

$x_{i,f}^{\Phi}$ The ith x-position in pixels of the crack path for the font of the specimen for loading case Φ.

$x_{i,b}^{\Phi}$ The ith x-position in pixels of the crack path for the back of the specimen for loading case Φ.

$y_{i,f}^{\Phi}$ The ith y-position in pixels of the crack path for the font of the specimen for loading case Φ.

$y_{i,b}^{\Phi}$ The ith y-position in pixels of the crack path for the back of the specimen for loading case Φ.

Δx_i^{Φ} The standard deviation in pixels for all the x-positions of the crack path for the font of the specimen for loading case Φ.

Δy_i^{Φ} The standard deviation in pixels for all the y-positions of the crack path for the font of the specimen for loading case Φ.

$s_{v,f}^{\Phi}$ The average vertical scale factor used for converting crack path y-position from pixels to meters for the front of the specimen for loading case Φ.

$s_{h,f}^{\Phi}$ The average horizontal scale factor used for converting crack path x-position from pixels to meters for the front of the specimen for loading case Φ.

$s_{v,b}^{\Phi}$ The average vertical scale factor used for converting crack path y-position from pixels to meters for the back of the specimen for loading case Φ.

$s_{h,b}^{\Phi}$ The average horizontal scale factor used for converting crack path x-position from pixels to meters for the back of the specimen for loading case Φ.

$\Delta s_{v,f}^{\Phi}$ The standard deviation of the vertical scale factor used for converting crack path y-position for the front of the specimen for loading case Φ.

$\Delta s_{h,f}^{\Phi}$ The standard deviation of the horizontal scale factor used for converting crack path x-position for the front of the specimen for loading case Φ.

$\Delta s_{v,b}^{\Phi}$ The standard deviation of the vertical scale factor used for converting crack path y-position for the back of the specimen for loading case Φ.

$\Delta s_{h,b}^{\Phi}$ The standard deviation of the horizontal scale factor used for converting crack path x-position for the back of the specimen for loading case Φ.

$X_{i,f}^{\Phi}$ The average i^{th} x-position in meters of the crack path for the front of the specimen for loading case Φ.

$X_{i,b}^{\Phi}$ The average i^{th} x-position in meters of the crack path for the back of the specimen for loading case Φ.

$Y_{i,f}^{\Phi}$ The average i^{th} y-position in meters of the crack path for the front of the specimen for loading case Φ.

$Y_{i,b}^{\Phi}$ The average i^{th} y-position in meters of the crack path for the back of the specimen for loading case Φ.

$\Delta X_{i,f}^{\Phi}$ The standard deviation for the i^{th} x-position in meters of the crack path for the front of the specimen for loading case Φ.

$\Delta X_{i,b}^{\Phi}$ The standard deviation for the i^{th} x-position in meters of the crack path for the back of the specimen for loading case Φ.

$\Delta Y_{i,f}^{\Phi}$ The standard deviation for the i^th^ y-position in meters of the crack path for the front of the specimen for loading case Φ.

$\Delta Y_{i,b}^{\Phi}$ The standard deviation for the i^th^ y-position in meters of the crack path for the back of the specimen for loading case Φ.

$\Delta a/\Delta N$ Crack growth rate which is the discrete amount of crack growth per number of stress cycles.

K_x Spring constant assumed in VCCT used in calculating the force in the x-direction.

K_y Spring constant assumed in VCCT used in calculating the force in the y-direction.

K_z Spring constant assumed in VCCT used in calculating the force in the z-direction.

F_x Reaction force in the x-direction on each node on the crack front and the mid-nodes attached to the element just ahead of the crack front in VCCT.

F_y Reaction force in the y-direction on each node on the crack front and the mid-nodes attached to the element just ahead of the crack front in VCCT.

F_z Reaction force in the z-direction on each node on the crack front and the mid-nodes attached to the element just ahead of the crack front in VCCT.

u_x Nodal displacement in the x-direction.

u_y Nodal displacement in the y-direction.

u_z Nodal displacement in the z-direction.

G_I Strain energy release rate for Mode I.

G_{II} Strain energy release rate for Mode II.

G_{III} Strain energy release rate for Mode III.

E Young's modulus of elasticity.

ν Poisson's Ratio.

Δa Crack growth increment.

θ_c Angle which the crack will propagate according to MCS criterion.

$\sigma_{\theta\theta}$ Circumferential normal stress defined in polar coordinates around the crack tip.

$\sigma_{r\theta}$ Shear stress defined in polar coordinates around the crack tip.

LIST OF ABBREVIATIONS

3D-FEA .... 3 – Dimensional Finite Element Analysis

SIF .... Stress Intensity Factor

2D-DIC .... 2 – Dimensional Digital Image Correlation

VCCT .... Virtual Crack Closure Technique

MCS .... Maximum Circumferential Stress

LT .... Longitudinal-Transverse

MTS .... Material Test System

NASA .... National Aeronautics and Space Administration

CCD .... Charge-Coupled Device

CHAPTER 1

INTRODUCTION

1.1 MOTIVATION

The aerospace industry has experience with a range of structural failures, oftentimes due to fatigue cracks in aircraft fuselage components that are exposed to relatively high stress levels during cyclic loading effects incurred during repeated take-off and landing events that lead to fatigue crack initiation at material defects and near stress concentrations. One of the first incidents that raised public awareness occurred in April of 1988 when 18 feet of the fuselage ripped off one of Aloha Airlines' Boeing 737s in midflight. The cabin quickly decompressed resulting in one fatality and eight serious injuries. The National Transportation Safety Board reported that undetected dis-bonding and widespread fatigue damage between rivets led to the failure of a lap joint [1]. A few months later, Continental Airlines found several 30 inch long cracks in a Boeing 737 aircraft in the same general area where damage occurred in the Aloha Airlines incident [2].

Ten years later, in October 1998, structural fatigue cracks in the fuselage of a Boeing 737s were reported [3], prompting the Federal Aviation Administration to propose the Airworthiness Directive [3]. The directive required aircraft with less than 60,000 flight cycles to be inspected initially and then inspected again every 3,000 cycles. Furthermore, aircraft would be required to receive modifications to strengthen the bulkhead before

75,000 cycles. Considering only Boeing 737s in the United States, the estimated cost of the inspections could be up to $26 million per inspection cycle and $71 million for modifications [3].

Despite the efforts of airlines and the Federal Aviation Administration to monitor fatigue cracks in aging aircraft, the danger of structural failure in fuselages continues into the 21st century. In 2009, fatigue at the top of the fuselage just in front of the vertical tail fin caused a 12 inch hole to rip open midflight, causing decompression of the cabin and an emergency landing of a Southwest Airline Boeing 737 [4]. Southwest Airline had another fuselage failure during flight just two years later. A section near the top of the fuselage, about five feet long and one foot wide, ripped off due to the sudden propagation of fatigue cracks in the skin of the aircraft [5].

The presence of fatigue cracks is not exclusive to commercial jetliners. In 2004, Lockheed Martin made the switch from titanium to aluminum for some structural features of the F-35 [6]. In 2010, fatigue cracks were discovered on the bulkhead of a Lockheed Martin ground test aircraft [6]. Although no structural failure occurred in these cases, the presence of fatigue cracks must be monitored to avoid potential catastrophes.

In fact, fatigue cracks are expected to form in the fuselage of modern airplanes due to repeated (a) pressurization and decompression of the cabin during every flight and (b) loading effects during take-off and landing. Thus, the propagation of cracks into critical joints continues to be an area of concern, especially since such propagation under complex stress states is not completely understood. Although procedures are currently in place to inspect and repair fatigue cracks, the ability to better predict how far a crack will propagate and in which direction it would grow when subjected to various loading conditions could save millions of dollars in premature inspection and repair, while also identifying the severity of an existing flaw in an aero-structure.

1.2 BACKGROUND

As noted in Section 1.1, flaws in aircraft components oftentimes are exposed to complex stress states. For nominally elastic conditions, the crack tip stress states generally are decomposed into three modes of loading which are shown schematically in Figure 1.1. Mode I, the opening mode, is such that the crack surfaces move away from

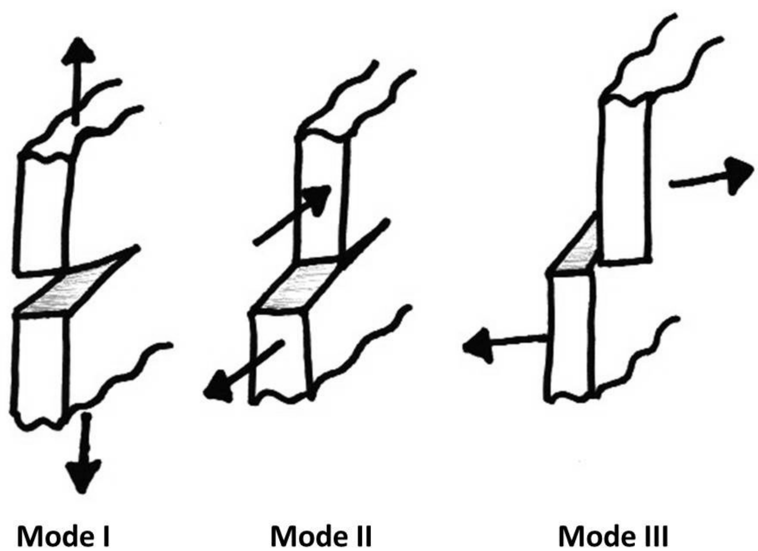

Figure 1.1. The three facture modes for nominally elastic conditions.

each other and the material directly ahead of the crack is subjected to a dominant tensile stress. Mode II, the in-plane sliding mode, is such that shear loading is applied parallel to the direction of crack growth and the material directly ahead of the crack tip is subjected to a dominant in-plane shear stress. Mode III, the out-of-plane shearing mode, is designated either out-of-plane or transverse shear, with the crack surfaces moving parallel to and across each other. Mode I crack tip conditions are generally the dominant influence on fatigue crack propagation in most aerospace metallic components (e.g., aluminum, titanium).

Crack propagation under Mode I loading is reasonably well understood [7]. Using a maximum circumferential stress (MCS) criterion, the predicted and actual crack trajectories during fatigue loading are perpendicular to the local $\sigma_{\theta\theta\ max}$ direction where $\sigma_{\theta\theta\ max}$ is the maximum circumferential stress ahead of the crack tip [8]. This direction nominally coincides with the loading direction when local conditions are not influenced by stress concentrations, material defections/inclusions, or other factors.

For high cycle fatigue, it is generally assumed that the far field stress remains linear elastic, while the local stress also remains mostly linear elastic with a small plastic zone around the crack tip (ideally, the plastic zone size would be no more than one tenth of the thickness of the specimen). The stress intensity factor (SIF), K, is a value which describes the magnitude of the local elastic stress field and is a function of the stress and geometry of the structure and crack. For Mode I loading, K_I is defined by [7]

$$K_I = \sigma\sqrt{\pi a}\, f(^a/_W) \qquad [1.1]$$

where σ is the far field tensile stress; a is the crack length; and $f(^a/_W)$ is a parameter which depends on the geometry of the specimen and crack orientation. Since the loading is cyclic for fatigue studies, the loading parameter, ΔK, is considered the driving force for fatigue crack propagation and is defined as follows;

$$\Delta K = K_{max} - K_{min} \qquad [1.2]$$

where *max* and *min* refer to the maximum and minimum applied values of *K*. Another loading parameter that has been shown to be important in fatigue studies is the loading ratio, also known as the R-ratio. The R-ratio is defined as

$$R = \frac{\sigma_{min}}{\sigma_{max}} = \frac{K_{min}}{K_{max}} \quad [1.3]$$

Therefore ΔK can be expressed as

$$\Delta K = (1 - R)K_{max} \quad [1.4]$$

The use of ΔK as the primary driving force in high cycle fatigue was introduced by Paul Paris in his pioneering work [9]. Paris' Law defines the relationship between ΔK and the differential amount of crack extension per stress cycle, *da/dN*, and is written;

$$\frac{da}{dN} = C\Delta K^m \quad [1.5]$$

Paris' Law parameters, C and m, are determined experimentally for each material and may or may not be dependent on the loading ratio, R.

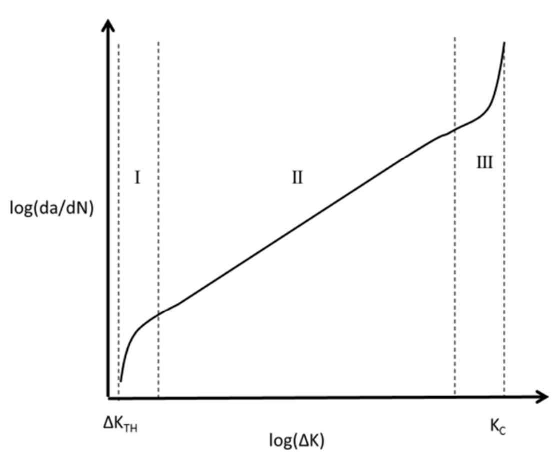

Figure 1.2. A schematic of a typical log-log plot of da/dN vs. ΔK.

As shown in Figure 1.2, a typical plot of the fatigue crack propagation process has three regions. Below threshold, ΔK_{TH}, the crack will not propagate. Then in region I, the crack growth begins to transition to region II where crack propagation occurs in a manner that is predicted by Eq 1.5. In region III, the crack growth again transitions as K_{max} approaches the fracture toughness, K_c. When $K_{max} \geq K_c$, rapid crack propagation ensues until final fracture occurs.

Now consider the case where a crack is under mixed-mode loading, that is, under any combination of two or more loading types (see Figure 1.1). For the combination of Mode I and Mode II loading conditions, methods for obtaining a mixed-mode I/II stress state experimentally when applying uniaxial tensile loading include (a) use of kinked cracks, (b) use of cracks propagating away from a hole, and (c) use of an Arcan fixture [9-18].

Independent mixed mode loading studies by both Zhang *et al.* [10] and Lopez-Crespo *et al.* [11] have used an Arcan fixture to statically load an existing crack while 2D digital image correlation (2D-DIC) was used to determine K_I and K_{II} from measured displacement fields around the crack tip for various degrees of Mode I/II loading. Zhang *et al.* used an Arcan fixture with a through thickness edge notch as the one shown in Figure 1.3. Lopez-Crespo *et al.* used the same fixture with a center notched specimen. Experimental SIFs were compared to values obtained from empirical expressions for the Arcan fixture. The edge cracked solution takes the following form [12] .

$$K_I = F_I \frac{P}{Wt}\sqrt{\pi a}\ ,\ K_{II} = F_{II} \frac{P}{Wt}\sqrt{\pi a} \qquad [1.6]$$

where t is specimen thickness and F_I and F_{II} are provided graphically as a function of various loading angles and $0.45 \leq a/W \leq 0.7$ [12]. There are some limiting factors for this model. First, it is only valid for a range of relatively large cracks. Secondly, it only considers straight cracks. Finally, it is only valid for static cracks. Thus, this model can only be used for determining the kinking angle for the initial crack propagation event.

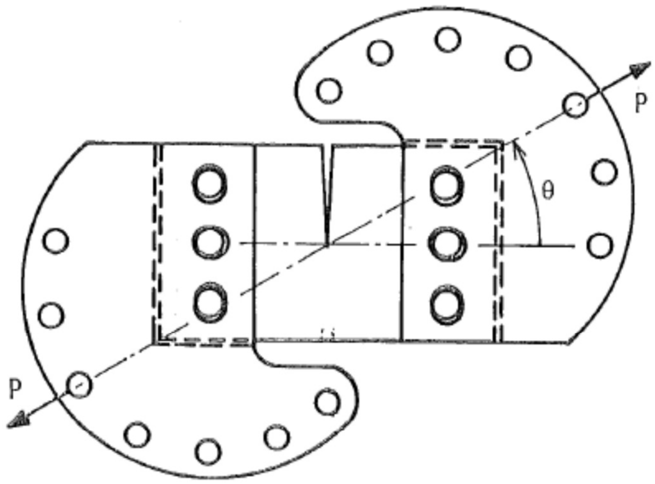

Figure 1.3. Diagram of Arcan fixture and specimen.

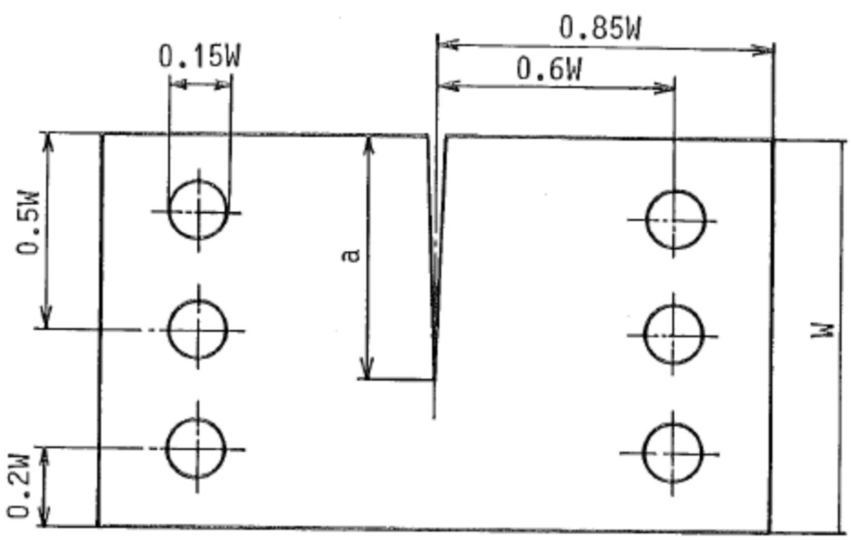

Figure 1.4. Specimen for Arcan fixture with single edge crack.

For the case of a kinked crack under uniform tensile loading (see Figure 1.5), another empirical model exits [12]

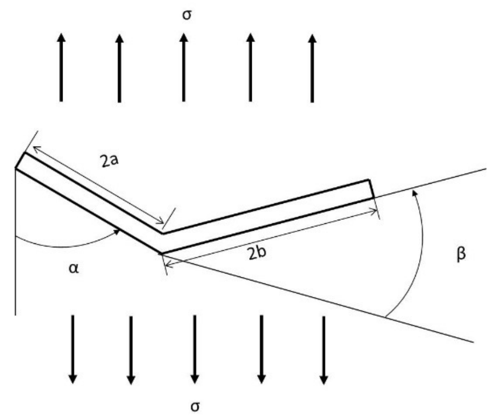

Figure 1.5. Schematic of kinked crack.

$$K_I = \sigma\sqrt{\pi a}F_I(\alpha, \beta, \frac{b}{a}) \ , \ K_{II} = \sigma\sqrt{\pi a}F_{II}(\alpha, \beta, \frac{b}{a}) \qquad [1.7]$$

$$\begin{pmatrix} F_I\left(\alpha,\beta,\frac{b}{a}\right) \\ F_{II}\left(\alpha,\beta,\frac{b}{a}\right) \end{pmatrix} = \frac{1-\cos 2\alpha}{2}\begin{pmatrix} F_I^1\left(\beta,\frac{b}{a}\right) \\ F_{II}^1\left(\beta,\frac{b}{a}\right) \end{pmatrix} - \cos 2\alpha \begin{pmatrix} F_I^2\left(\beta,\frac{b}{a}\right) \\ F_{II}^2\left(\beta,\frac{b}{a}\right) \end{pmatrix} - \frac{\sin 2\alpha}{2}\begin{pmatrix} F_I^3\left(\beta,\frac{b}{a}\right) \\ F_{II}^3\left(\beta,\frac{b}{a}\right) \end{pmatrix} \qquad [1.8]$$

$$\begin{pmatrix} F_I^K\left(\beta,\frac{b}{a}\right) = \sum_{n=0}^{2} F_{I,n}^k(\beta)\left(\frac{b}{a}\right)^n \\ F_{II}^k\left(\beta,\frac{b}{a}\right) = \sum_{n=0}^{2} F_{II,n}^k(\beta)\left(\frac{b}{a}\right)^n \end{pmatrix} \ for\ k = 1,3 \qquad [1.9]$$

$$\begin{pmatrix} F_I^K\left(\beta,\frac{b}{a}\right) = \sum_{n=0}^{2} F_{I,n}^k(\beta)\left(\frac{b}{a}\right)^{n+1/2} \\ F_{II}^k\left(\beta,\frac{b}{a}\right) = \sum_{n=0}^{2} F_{II,n}^k(\beta)\left(\frac{b}{a}\right)^{n+1/2} \end{pmatrix} \ for\ k = 2 \qquad [1.10]$$

where $F_{I,n}{}^k$ and $F_{II,n}{}^k$ for n=0, 1, and 2 and k=1, 2, and 3 are provided in a table for 0°≤ β≤ 180° [12]. Equation 1.7 is valid for $0 \leq \frac{b}{a} \leq 0.2$. Limitations to this model are that (a) it is applicable to kinked cracks in an infinite plate, (b) b « a, and (c) the loading must be distributed in such a way that uniform stress is applied to the region in which the crack is located. [12]

Gaylon et al. [13] performed fatigue tests using the Arcan fixture. In this study, the authors determined the crack growth trajectory for various degrees of mixed-mode I/II loading. Their results indicate that the crack trajectory is curvilinear and the stress distribution applied to the crack is non-uniform. Therefore, the two empirical models provided by Murakami and discussed previously are not applicable to quantify the mixed mode SIFs. Also, the measured crack trajectories suggest that for all combinations of Mode I/II loading, the fatigue cracks propagate in a manner that was locally dominated by K_I, while no crack propagation occurred for the pure Mode II loading case. However, there was such large scatter in the experimental data that it is difficult to definitively identify the trends. One cause of the inconsistency in the results was determined to be the three pin loading configuration used by the authors. It was suggested that future studies use only one pin for fixing the Arcan fixture to the test stand [14]; the use of a single pin is consistent with the work of Amstutz, Boone and others at the University of South Carolina [13, 14, 18, 21-23].

Chao et al. [15] also used the Arcan fixture with the one-pin configuration to study fatigue crack propagation under various mixed-mode loading conditions. Crack trajectories were compared to stable tearing results obtained under mixed-mode monotonic loading conditions. It was observed that cracks under fatigue loading propagate in a local Mode I direction for all loading cases including pure Mode II, unlike Gaylon's results. In Chao's studies, the amount of crack growth in fatigue for $\Phi=75^o$ and 90^o was quite small, indicating that the crack surfaces interfered after a small amount of crack extension and impeded further crack growth. For stable tearing, after Mode II loading becomes dominant, cracks in aluminum alloys tended to propagate in the local shear direction; that is, approximately parallel to the direction of the pre-crack. This transition from Mode I dominated crack growth to Mode II dominated crack growth under stable tearing conditions is consistent with results obtained by Amstutz et al [16] [17]. In Amstutz's work, the authors used the Arcan fixture to study mixed Mode I/II stable tearing crack growth. The results show that for most loading cases, where $K_{II}/K_{I,} <$ 1, the crack propagates under local Mode I conditions. However, as K_I approaches zero and K_{II}/K_I reaches a critical value ($\Phi=75^o$ and 90^o for Al 2024-T351), the crack begins to grow in Mode II. While this study included crack propagation, stable tearing occurs outside of the linear elastic range, and results suggest that the Mode II component has different effects in the linear elastic range than it does under elastic-plastic conditions.

Boljanovic [18] performed finite element analysis to model the results of Gaylon et al. The crack trajectories were simulated using MSC/NASTRAN [19] in a step-by-step method while applying the maximum circumferential stress (MCS) criterion to predict crack trajectory. Results of Boljanovic's work agree with Gaylon's experimental crack paths. However, the SIFs were not obtained at each step using the local crack tip field data, but were determined analytically after the simulation was performed since the step-by-step method of crack path prediction is quite time consuming. It is unclear if the analytical solution for the SIFs accounted for curvilinear crack paths.

1.3 CURRENT WORK

The objective of the current study is to (a) perform experiments and measure the crack path and (b) perform simulations and predict the fatigue crack path in an aerospace aluminum alloy undergoing applied, far-field mixed-mode I/II conditions. The Arcan fixture will be utilized to achieve far-field mixed-mode I/II conditions in 6.35mm thick Al-2024-T351 specimens. Crack paths, cycle count, and maximum and minimum loads will be measured during experiments, with loading ranging from $0 \leq K_{II}/K_I \leq \infty$. Simulations will then be performed using 3D-FEA. Crack trajectories will be predicted using virtual crack closure techniques (VCCT) and a MCS criterion. Local re-meshing will be used to extend the crack. The whole fixture and specimen will be modeled using 10-noded tetrahedral elements. Predicted crack paths will be compared to the results obtained experimentally, and the results will be discussed.

CHAPTER 2

Experimental Work

2.1 FIXTURE AND SPECIMEN PREPARATION

The Arcan fixture shown in Figure 2.1 was used to achieve mixed-mode I/II loading for discrete values of K_{II}/K_I in the range $0 \leq K_{II} / K_I \leq \infty$. The butterfly-shaped specimen shown in Figure 2.1 is machined to have tight contact with the upper and lower grips along all four straight, angled sides. Once tightly fitted into the grips, the specimen is further tightened into place using ten small bolts; five on the top part of the fixture and five on the bottom part. Around the edges of the stainless-steel grips are pairs of holes located every 15^o. With loading angle Φ defined as shown in Figure 2.1, the $\Phi = 0^o$ pin holes correspond to nominally Mode I crack conditions and the $\Phi = 90^o$ pin holes represent nominally Mode II crack loading conditions. The fixture was machined from 15-5PH stainless steel with Young's modulus =2.07×10^{11} Pa and Poisson's ratio = 0.30.

As shown in Figure 2.2, each butterfly-shaped specimen is 224.28 mm tall, 275.30 mm wide at the top and bottom of the specimen and 6.35mm thick. Each specimen is manufactured from Al-2024-T351 to form an LT orientation crack configuration (crack is along the transverse direction (T) and perpendicular to the rolling direction (L) in the aluminum specimen) [20] with Young's modulus = 7.11×10^{10} Pa and Poisson's ratio = 0.33. A jeweler's saw blade, size 0/6, was used to create an initial through-thickness edge notch 6.35mm long in the width direction on the left side of the specimen in the vertical center (see Figure 2.2). The front and back surfaces of the specimens were sanded with 600 grit sand paper before final sanding with 800 grit sandpaper to remove small surface defects. Metal polish was used to create a mirror finish on the surfaces for visually tracking crack tip progression during the experiment.

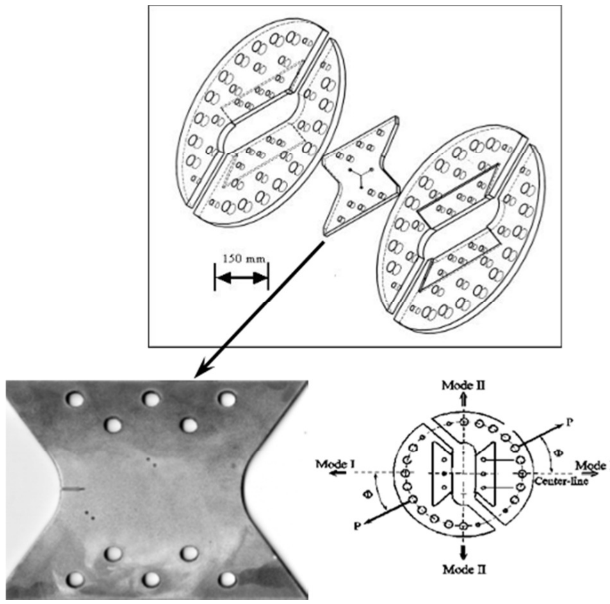

Figure 2.1. Mixed mode I/II Arcan test fixture and butterfly shaped test specimen. Angle $\Phi=0^0$ corresponds to far-field tension and $\Phi=90^0$ is far-field shear.

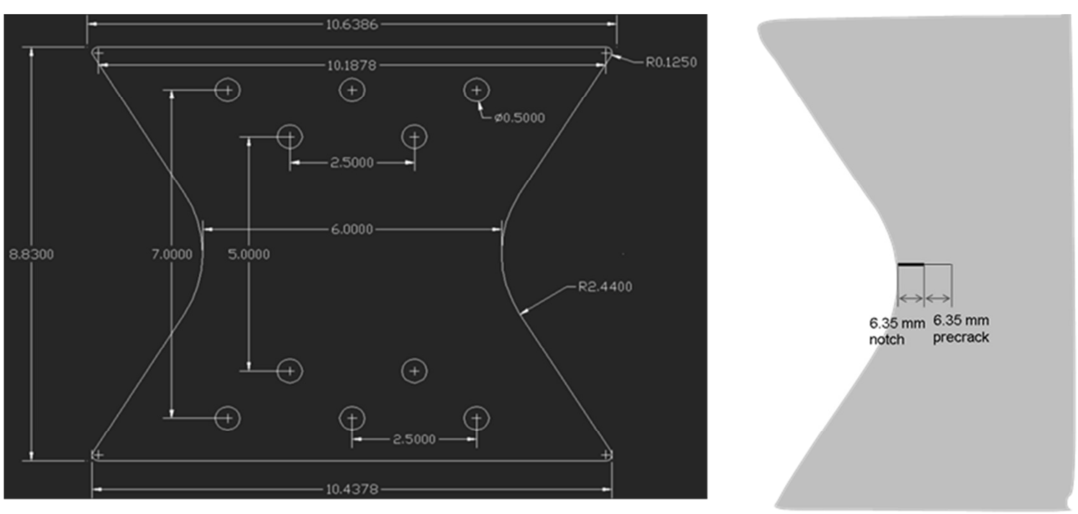

Figure 2.2. (a) Dimensions of specimens in inches (b) Diagram of notch and pre-crack

2.2 SETUP

As shown in Figure 2.3, a 50 kip (227 kN) servo-hydraulic Material Test System (MTS) controlled by TestStar II software was used to apply tensile loads in displacement control to the Arcan fixture and specimen. Stainless steel clevises were placed in the hydraulic grips of the MTS test frame, and the fixture was attached with one pin on the top and another pin on the bottom. . The top image of Figure 2.3 is of the complete test set-up with (a) the specimen and Arcan fixture pinned into the clevises of the test stand and (b) microscope objectives and slide apparatus for optical tracking of the propagating crack tip clamped to the test stand. The bottom image of Figure 2.3 shows the set up without the microscope objectives. The backing plate (not visible in Fig 2.3) is attached to the top and bottom pieces of the Arcan fixture and is oriented at 45°.

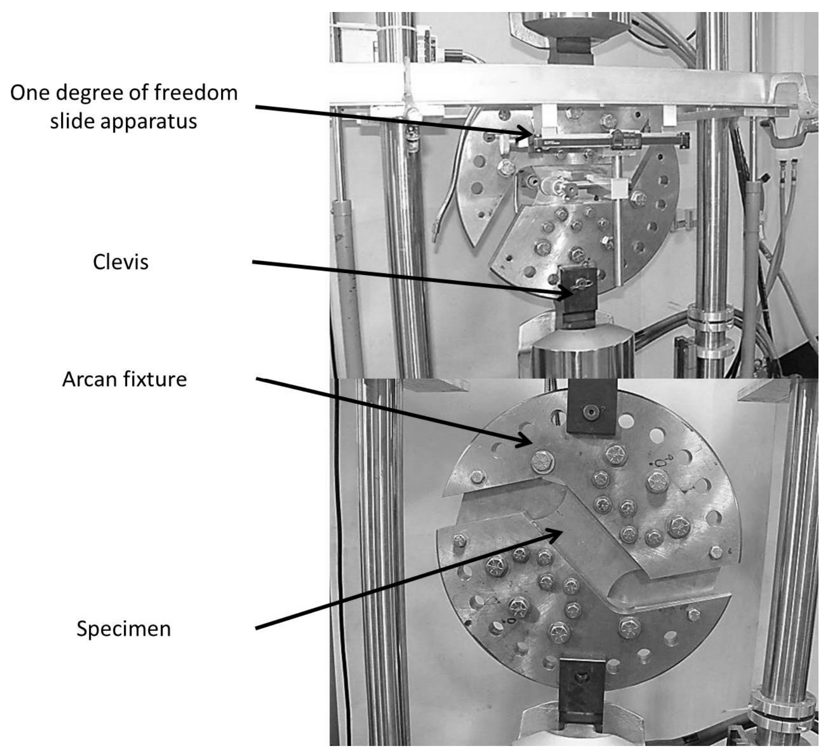

Figure 2.3. Images of experimental set up for a 45° loading angle.

During testing, the crack tip was tracked using the microscope objective and the slide apparatus. The objective is attached to the dual slide apparatus shown in Figure 2.4. The dual slide apparatus was designed and constructed by Mr. Haywood Watts. The apparatus consists of (a) a single, horizontally mounted manual screw driven slide manufactured by Velmex with a digital caliper to provide a metric positional measurement, (b) a second vertically-oriented Velmex slide with digital caliper that was mounted to the horizontal slide. The microscope objective was then connected to the vertical slide. Both vertical and horizontal slides operate independently, allowing for horizontal and vertical measurements of the crack tip position during the fatigue process.

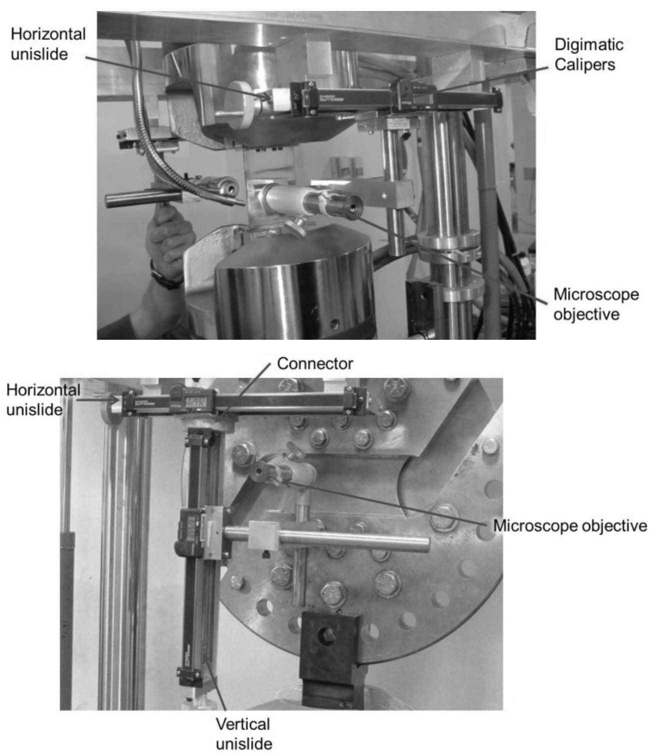

Figure 2.4. (Top) One degree-of-freedom slide apparatus; (Bottom) Two degree-of -freedom slide apparatus.

2.3 EXPERIMENTAL PROCEDURE

To mount the notched specimen into the Arcan fixture, it was first bolted into the top and bottom Arcan fixtures that were held in place by a backing plate designed to connect the top and bottom halves of the fixture and keep the assembly from moving during installation of the specimen into the fixture, minimizing initial distortions/stresses in the specimen prior to the experiment. The fixture-specimen-backing plate combination was pinned to the upper clevis, rotated about the pin to align with the bottom clevis and then the lower pin was put in place to fully install the specimen-fixture combination in the MTS test stand. Initially, the specimen is oriented to be in the Mode I configuration. Once fully installed, the backing plate is removed. Then, two sets of dual slide apparatuses were clamped to the test stand – one for tracking the crack on the front of the specimen and the other for tracking the crack on the back of the specimen. The calipers attached to the slides were zeroed at the center of the notch on the edge of the specimen, see Figure 2.5. After everything is in place, the specimens were fatigue pre-cracked an additional 6.35mm for a total crack length of 12.7mm. Fatigue loading was applied in force control according to the loads outlined in the following section at 10Hz.

After pre-cracking, the crack front was marked by cycling at a higher loading ratio (R=0.8 or R=0.9), and at about 90% of the pre-crack load. Then the backing plate was reattached to the fixture, the fixture was rotated in the test stand to the appropriate loading angle (e.g. see Figure 2.5). Once the specimen-fixture combination is correctly positioned for the specific loading angle, Φ, of interest, the backing plate was again removed and the microscope objectives were repositioned. The microscopes were re-zeroed at the center of the notch along the edge of the specimen and the length of the pre-crack was re-measured.

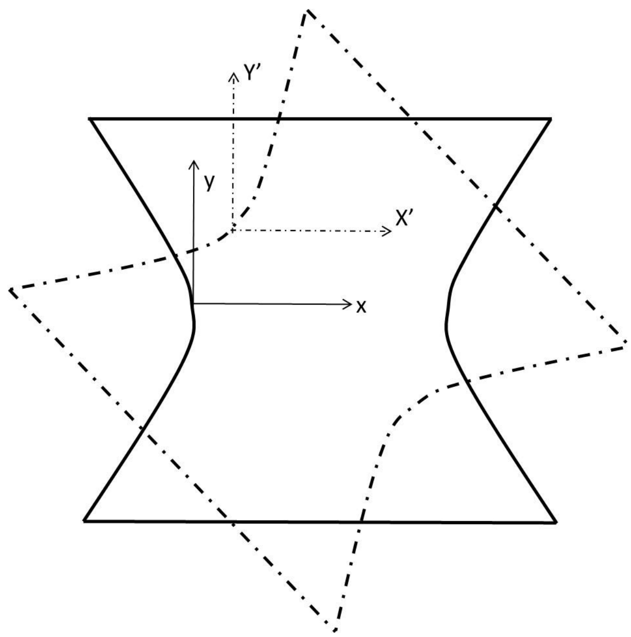

Figure 2.5. Schematic of coordinate system in which the crack tip was tracked during pre-cracking (solid line) and testing (dotted line)

Following the procedure outlined in the previous steps, a total of 6 experiments were performed at loading angles $\Phi = 15^o$, 30^o, 45^o, 60^o, 75^o, and 90^o, with $\Phi = 90^o$ degrees being nominally Mode II crack loading. For the loading cases $\Phi = 15^o$, 30^o, and 45^o, the one degree of freedom slide apparatus was used for tracking the crack tip. The two degree of freedom slide apparatus was built and used to track the crack tip for $\Phi = 60^o$, 75^o, and 90^o. Again, fatigue loading at 10Hz was applied in force control according to the loads outlined in the following section. The crack tip position was measured approximately every 5,000 to 20,000 cycles.

2.4 LOAD PREDICTION

Load data was predicted for fatigue pre-cracking and testing based on the load predictions for tests performed previously for NASA Langley Research Center and the US Air Force [21]. Load shedding was performed to avoid the risk of initiating stable tearing or formation of a large plastic zone at the crack tip. The loading ratio, *R,* and the amplitude of ΔK_I were held constant at 0.17 and 359 Pa*m$^{1/2}$ respectively, by allowing the load to decrease as the crack length increased.

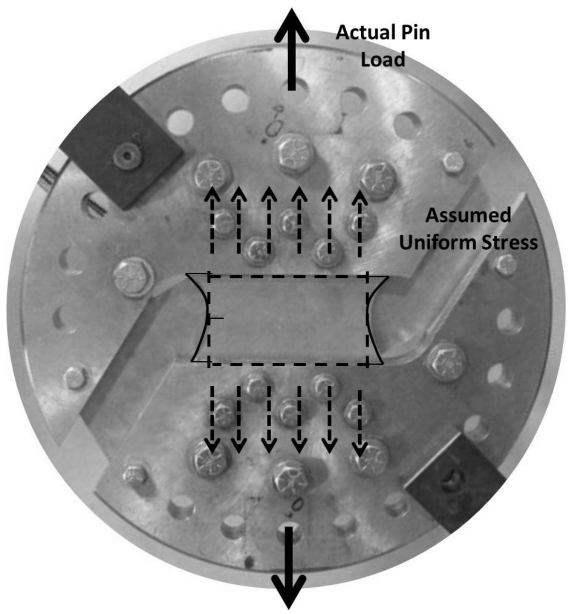

Figure 2.6. Visual representation of the actual geometry and loading (solid lines) and the assumed geometry and loading (dotted lines).

The SIF was estimated using an empirical expression from Tada [22] that is valid for a through-thickness edge crack under uniform uniaxial tension. It was assumed that the width was the transverse dimension of the butterfly specimen at its smallest cross-section, which is also where the notch is located. As shown schematically in Figures 2.6 and 2.7, an estimate for the uniform applied stress was obtained using the load applied at the pin divided by the cross-sectional area of the specimen using the assumed width and actual thickness, w = 152.4 mm and t = 6.35 mm.

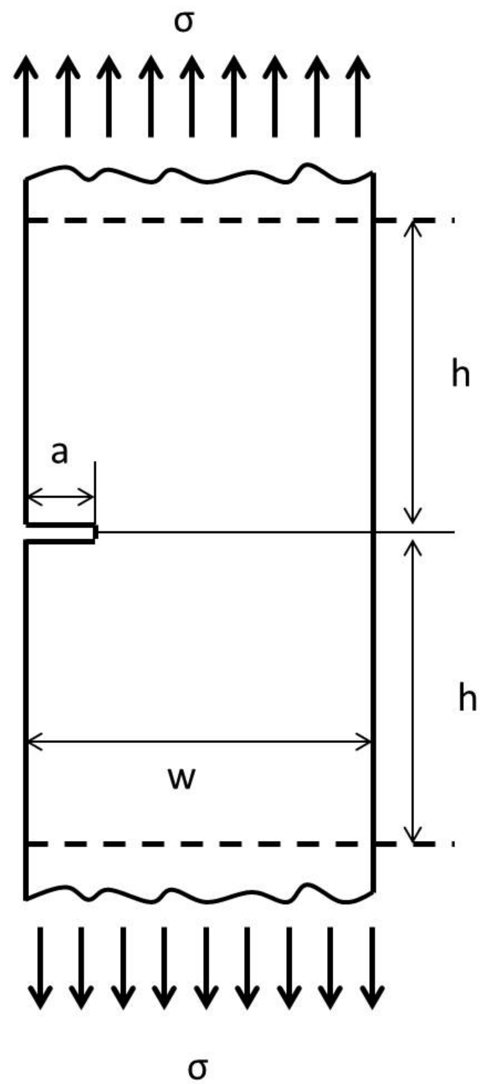

Figure 2.7. Diagram of geometry for Tada's empirical expression.

$$f\left(\frac{a}{w}\right) = \sqrt{\frac{2w}{\pi a}\tan\frac{\pi a}{2w}} * \frac{0.752+2.02(a/w)+0.37\left(1-\sin\frac{\pi a}{2w}\right)^3}{\cos\frac{\pi a}{2w}} \qquad [2.1]$$

Using Eqs 1.1, 1.2 and 2.1 [22], ΔK was estimated.

While performing the first experiment, which was for the 15° loading case, it was observed that the crack path on the front of the specimen deviated from the crack path measured on the back surface after a few millimeters of crack extension. These observations led to the implementation of a different approach for load prediction to avoid unusual crack propagation in future experiments. The goal of the modified approach was to keep ΔK constant in order to avoid excessive plasticity in the crack tip region, crack slanting, or crack tearing. Since the method for estimating the SIF was quite crude, and did not account for the various loading angles and resulting K_I and K_{II} values, it was determined that following Paris' Law for the material was a more accurate method of crack growth control for ΔK_{eq} which is defined as follows [23];

$$\Delta K_{eq} = \gamma \Delta K_I + (1-\gamma)\sqrt{(\Delta K_I)^2 + \gamma_1(\Delta K_{II})^2 + \gamma_2(\Delta K_{III})^2} \qquad [2.2]$$

where γ, γ_1, and γ_2 are parameters to be defined. Using ΔK_{eq} and assuming that there is no crack closure effect, the crack growth rate can be determined using Eq 1.5. That is, the authors opted to maintain the same crack growth rate throughout the experiment.

For the next experiment, the 30° loading case, pre-cracking was performed according to the loads originally predicted. However after the specimen was rotated, the new method of determining the loading was performed. From the previous test data, it was determined that a crack growth rate of ≈ 6 x 10^{-5} mm/cycle was a safe rate to run the experiments and maintain nominally linear elastic conditions.. A loading ratio R = 0.4 was chosen for the experiment. This crack growth rate was maintained by allowing the crack to grow until the rate increased to ≈ 8 x 10^{-5} mm/cycle. The load was then dropped by approximately 5%, resulting in a crack growth rate of ≈ 4 x 10^{-5} mm/cycle. This process was repeated to maintain an average crack growth rate of ≈ 6 x 10^{-5} mm/cycle and therefore maintain a constant average ΔK_{eq} during the experiment.

For loading angles 45°, 60°, 75°, and 90°, the new pre-cracking loads and method of load shedding to control crack growth rate were recomputed to maintain an approximately constant crack growth rate. In all the remaining experiments, R = 0.4. Cycle count, crack growth, and load data for each experiment are provided in Appendix A. Recall for experiments for Φ = 15°, 30°, and 45° only the one degree of freedom horizontal uni-slide was used to visually track the crack so the recorded value in the appendix is only the x position as shown in Figure 2.5. For Φ = 60°, x' and y' positions are recorded and reported in the appendix. Recorded data for Φ = 75° is not reported since the crack did not propagate after applying hundreds of thousands of load cycles using the same loads as applied in the Φ = 60° experiment.

2.5 DETERMINATION OF EXPERIMENTAL CRACK PATHS

In order to obtain the experimental crack path for each loading case, images of the front and back of each specimen were necessary after the fatigue tests were conducted. The surfaces of each of the specimens had to be prepared so that when images were obtained, the crack would be visible and there would be no reflection on the surface. First, the surface was sanded with 600 grit sand paper to roughen the surface and remove the mirror finish. Then dry pigment was rubbed into the crack. The surface was sanded again to remove excess pigment on the surface, leaving the remaining pigment in the crack.

A 2.5 Megapixel Point Grey CCD camera was positioned on a tripod to ensure that images were taken perpendicular to the surface of the specimen. The specimen was positioned, and two rulers were placed on the surface of the specimen – one vertically and the other horizontally-- to provide a scale when the images were digitized. Images were taken of the front and back surfaces, and loaded into GetData Graph Digitizer software [24]. First, using the ruler, 5 points were created at position (X,Y) and 5 more points were created at (X+1", Y+1") as shown in Figure 2.8.

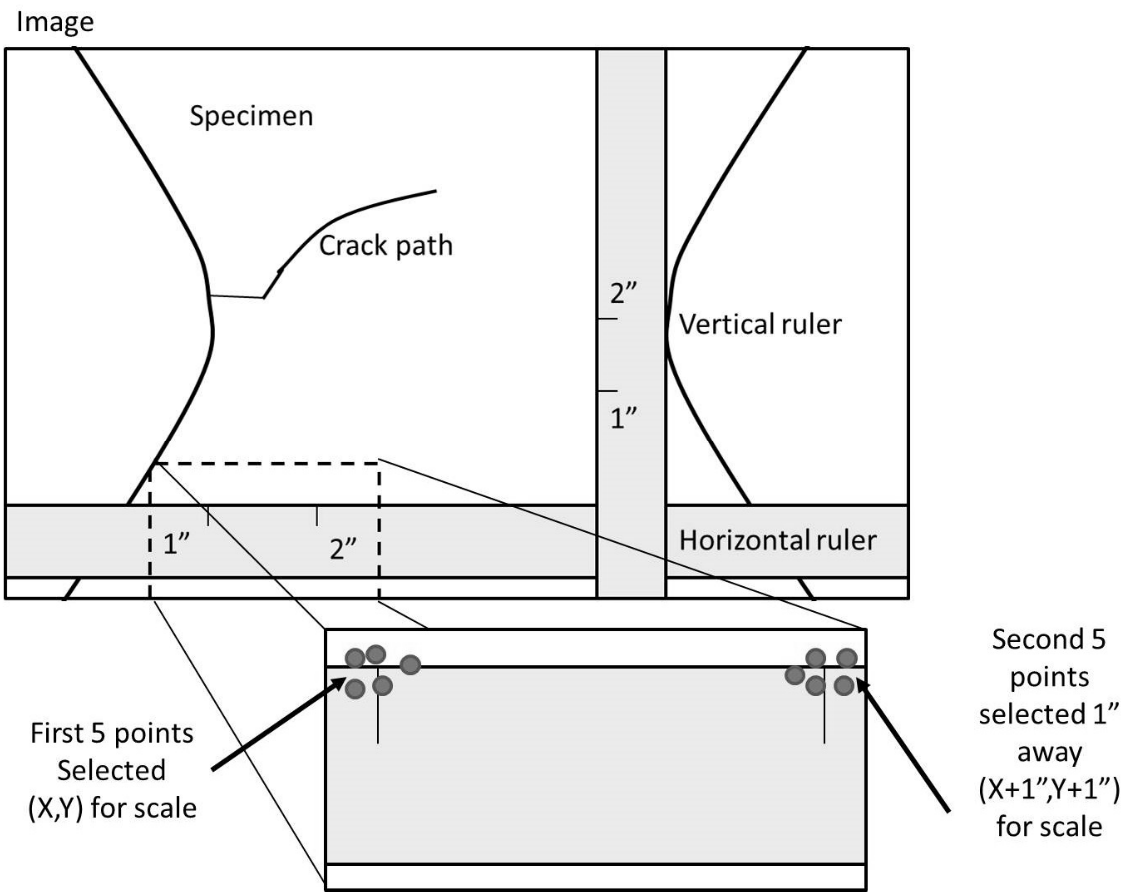

Figure 2.8. Schematic of the images digitized and an exaggerated view of how the points were selected for determining the scale factor from pixels to meters.

The distance between each set of points for the front (*f)* and back (*b)* of specimens for each loading case, Φ, were determined in pixels and averaged to be used for a scale factor. For each specimen, the average value and the standard deviation of the vertical and horizontal scale factors for each case for the front (back) , $s_{v,f}^{\Phi} \pm \Delta s_{v,f}^{\Phi}$ $(s_{v,b}^{\Phi} \pm \Delta s_{v,b}^{\Phi})$ and $s_{h,f}^{\Phi} \pm \Delta s_{h,f}^{\Phi}(s_{v,b}^{\Phi} \pm \Delta s_{v,b}^{\Phi})$ respectively, are given in Table 2.1. Then *i* points were selected along the front and back crack paths for each loading case, $(x_i^{\Phi}, y_i^{\Phi})_f$ and $(x_i^{\Phi}, y_i^{\Phi})_b$, and exported to Microsoft Excel. It was assumed that the error associated with selecting the points along the crack path was Δx_i^{Φ}, $\Delta y_i^{\Phi} \approx \pm 1$ pixel. Points along the path were converted from pixels to meters using the scale factor, to give metric positions $(X_i^{\Phi}, Y_i^{\Phi})_f$ and $(X_i^{\Phi}, Y_i^{\Phi})_b$.

$$X_i^{\Phi} = s_h^{\Phi} * x_i^{\Phi}, Y_i^{\Phi} = s_v^{\Phi} * y_i^{\Phi} \quad [2.3]$$

The standard deviation for the front and back of each specimen associated with the crack path position, $(X_i^{\Phi}, Y_i^{\Phi})_f$ and $(X_i^{\Phi}, Y_i^{\Phi})_b$, was determined using error propagation for multiplication [25]:

$$\Delta X_{i,f}^{\Phi} = X_{i,f}^{\Phi} * \sqrt{\left(\frac{\Delta s_{h,f}^{\Phi}}{s_{h,f}^{\Phi}}\right)^2 + \left(\frac{\Delta x_i^{\Phi}}{x_{i,f}^{\Phi}}\right)^2}, \Delta Y_{i,f}^{\Phi} = Y_{i,f}^{\Phi} * \sqrt{\left(\frac{\Delta s_{v,f}^{\Phi}}{s_{v,f}^{\Phi}}\right)^2 + \left(\frac{\Delta y_i^{\Phi}}{y_{i,f}^{\Phi}}\right)^2}$$

$$\Delta X_{i,b}^{\Phi} = X_{i,b}^{\Phi} * \sqrt{\left(\frac{\Delta s_{h,b}^{\Phi}}{s_{h,b}^{\Phi}}\right)^2 + \left(\frac{\Delta x_i^{\Phi}}{x_{i,b}^{\Phi}}\right)^2}, \Delta Y_{i,b}^{\Phi} = Y_{i,b}^{\Phi} * \sqrt{\left(\frac{\Delta s_{v,b}^{\Phi}}{s_{v,b}^{\Phi}}\right)^2 + \left(\frac{\Delta y_i^{\Phi}}{y_{i,b}^{\Phi}}\right)^2} \quad [2.4]$$

The percent error in the crack path for each loading case, Φ, is defined as the maximum percent error of the X_i^{Φ} and Y_i^{Φ} points on the front and back of the specimen and is as follows:

$$Percent\ Error^{\Phi} = 2 * \langle \frac{\Delta X_{i,f}^{\Phi}}{X_{i,f}^{\Phi}}, \frac{\Delta X_{i,b}^{\Phi}}{X_{i,b}^{\Phi}}, \frac{\Delta Y_{i,f}^{\Phi}}{Y_{i,f}^{\Phi}}, \frac{\Delta Y_{i,b}^{\Phi}}{Y_{i,b}^{\Phi}} \rangle_{max} * 100 \quad [2.5]$$

and are reported in Table 2.2. As shown in Table 2.2, the estimated errors are small and assumed to be negligible. From this point forward only the average crack path points will be considered in analysis.

Using Microsoft PowerPoint, the images for the front and back of each specimen were set to ≈ 50% transparency and layered on top of each other. It was observed that the specimen was slightly rotated in a couple of those images. The images were rotated such that the edges of the specimen in both images were aligned. Using the angle of rotation used in Power Point to align the images, the crack paths corresponding to those images were rotated by the same angle. Then, the average points for each specimen were translated to the coordinate system shown in Figure 2.9. The X and Y points along the crack for the front and back of each specimen were plotted, and a second order polynomial was fitted to the data using least squares. To verify that the digitized crack path was accurate, a plot of the polynomial fit was layered on top of the image of the specimen.

Table 2.1. Scale factors used to convert digitized points from pixels to meters.

Loading Case	Front Image Scale Factor (m/pixel x 10^{-5})		Back Image Scale Factor (m/pixel x 10^{-5})	
	Vertical Scale	Horizontal Scale	Vertical Scale	Horizontal Scale
15°	6.44 ± 0.03	6.41 ± 0.02	6.43 ± 0.02	6.39 ± 0.01
30°	7.14 ± 0.05	7.09 ± 0.04	7.14 ± 0.06	7.13 ± 0.03
45°	6.50 ± 0.07	6.48 ± 0.02	6.56 ± 0.02	6.52 ± 0.02
60°	6.48 ± 0.02	6.51 ± 0.00	6.55 ± 0.01	6.52 ± 0.03

Table 2.2. Percent error in crack path position.

Loading Case	Percent Error
15°	1.0%
30°	1.3%
45°	2.2%
60°	0.8%

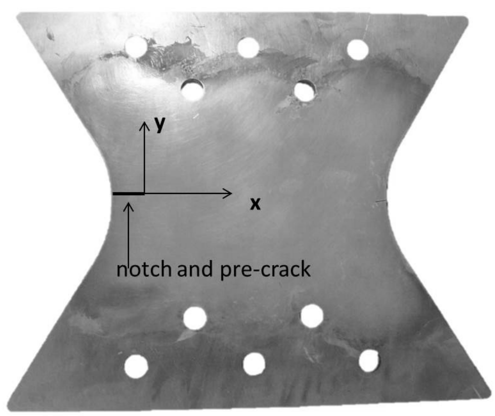

Figure 2.9. Coordinate system used to define crack paths from the tip of the pre-crack.

For the cases where the two degree of freedom slide apparatus was used, the x and y data points recorded during the experiment in the coordinate system shown in Figure 2.5 were rotated and translated into the coordinate system in Figure 2.9, in addition to digitizing the crack path.

2.6 EXPERIMENTAL RESULTS

For the experiments performed using the modified load prediction method of controlling the crack growth rate, the discrete crack growth rate $\Delta a/\Delta N$ was plotted along the crack length a in Figures 2.10-2.12.

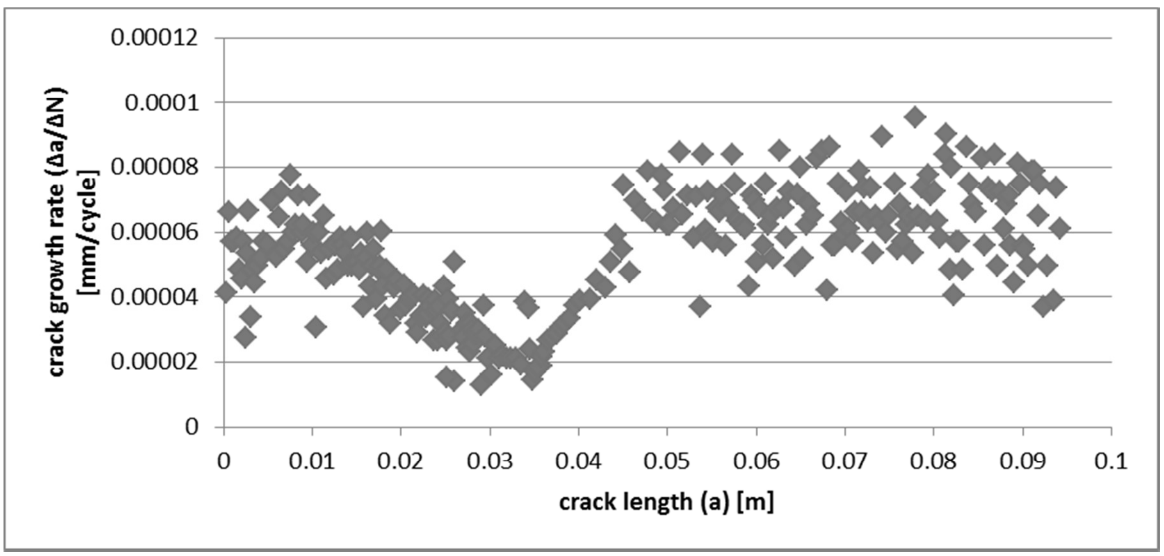

Figure 2.10. Crack growth rate along crack path for 30° loading case.

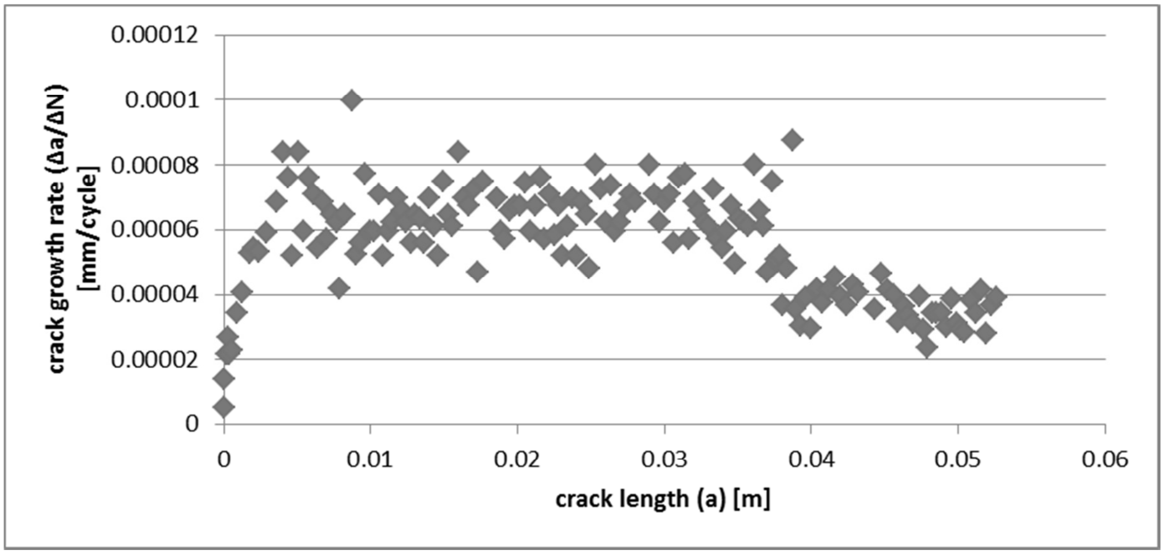

Figure 2.11. Crack growth rate along crack path for 45° loading case.

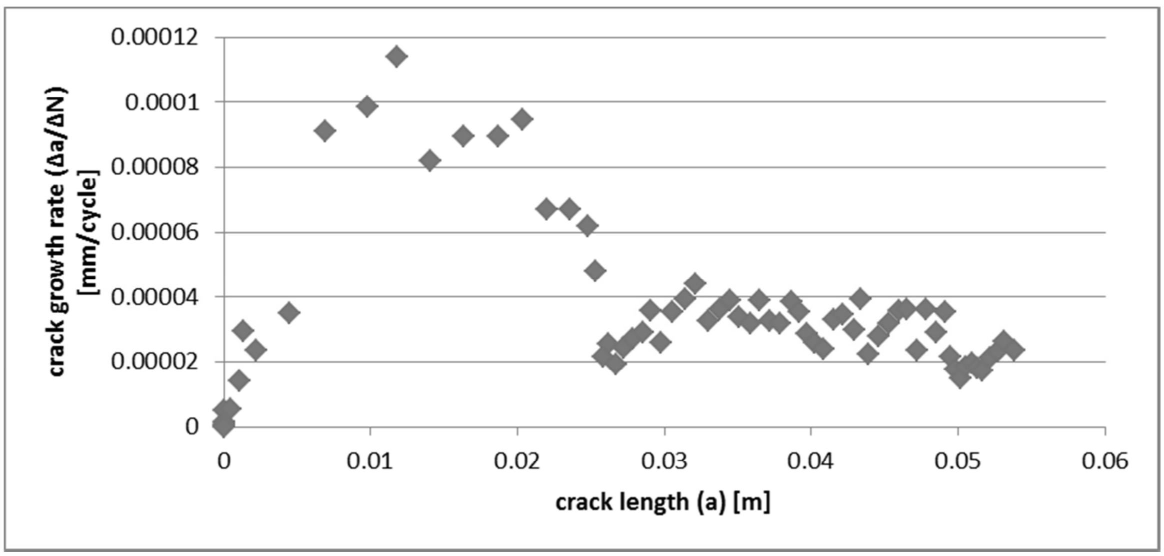

Figure 2.12. Crack growth rate along crack path for 60° loading case.

For loading cases 15°, 30°, 45°, and 60°, fatigue crack propagation occurred, and for loading cases 75° and 90°, no crack propagation occurred. Figure 2.13 shows the originally digitized crack path for the 15° loading case. Figure 2.14 shows the data for the 15° loading case crack path before crack slanting occurred along with the polynomial fit for the data. Figures 2.15-2.17 show the digitized crack path data for the front and back of the specimens for the 30°, 45°, and 60° loading cases respectively along with the polynomial fit for each data set.

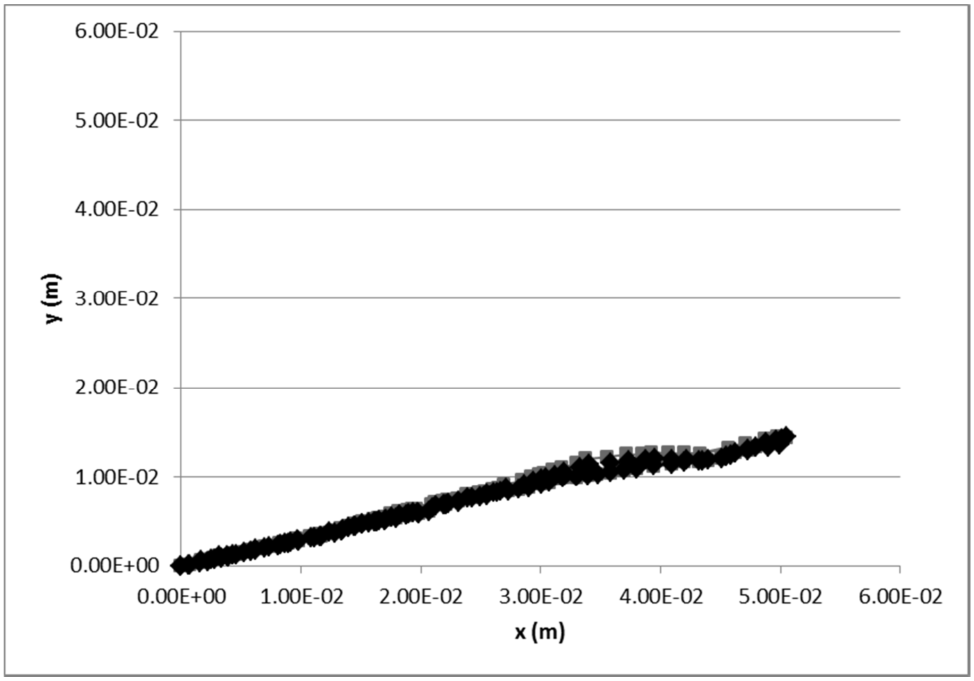

Figure 2.13. Originally digitized crack path data for 15° loading case.

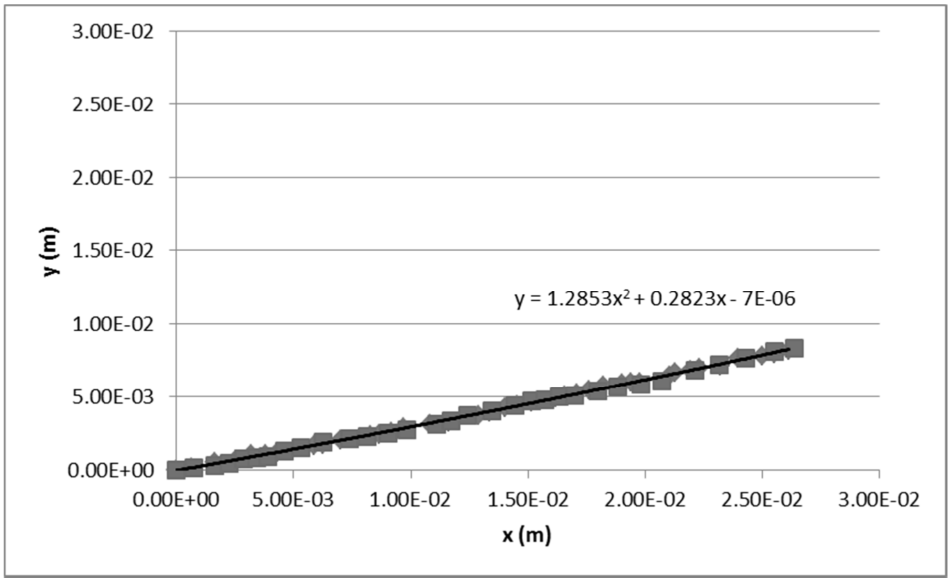

Figure 2.14. Digitized crack path and polynomial fit for 15° loading case.

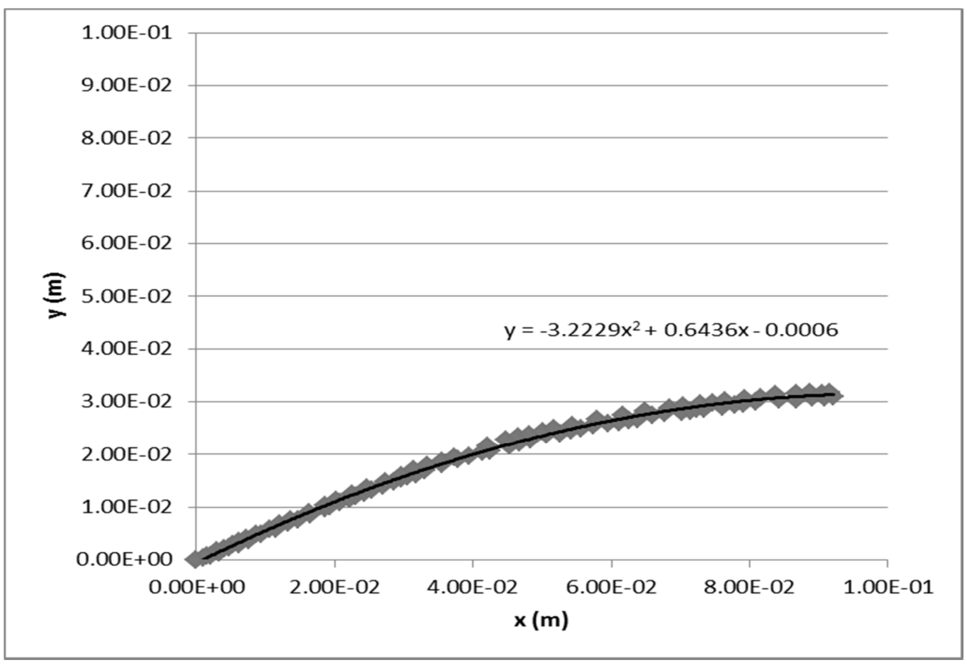

Figure 2.15. Digitized crack path and polynomial fit for 30° loading case.

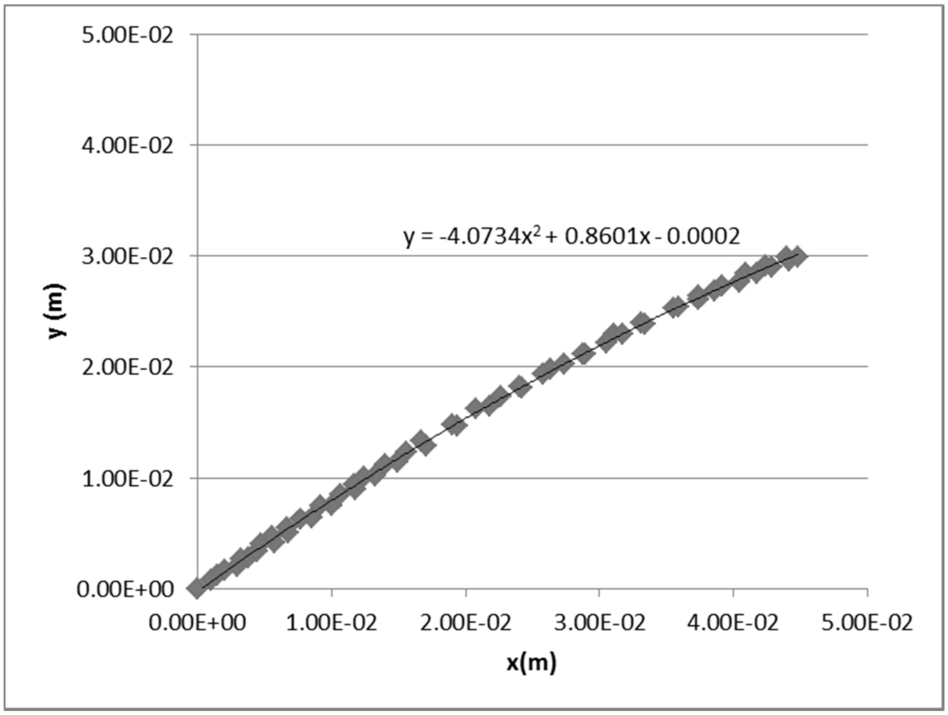

Figure 2.16. Digitized crack path and polynomial fit for 45° loading case.

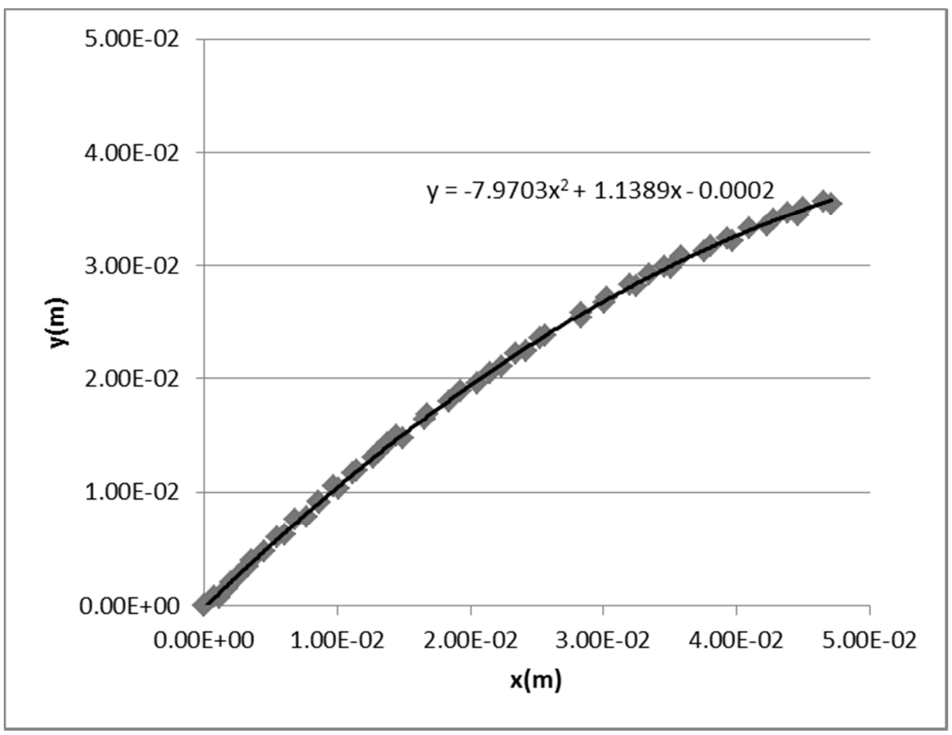

Figure 2.17. Digitized crack path and polynomial fit for 60° loading case.

The rotated and translated crack path determined experimentally using the two degree of freedom slide apparatus and the digitized crack path for $\Phi = 60°$ were plotted in Figure 2.18 to verify the accuracy of the digitization process. The following plot shows that the two methods of obtaining the experimental crack path are in good agreement with each other. The calipers used for measuring the amount of travel of the slide and microscope objective have an accuracy of 0.00127mm which results in less than 0.01% error in the measuring process. Even though the digitized crack path for $\Phi = 60°$ had 0.8% error (Table 2.2), the digitization process has more opportunity to induce error through obtaining, aligning, digitizing, and scaling the images. While error in either path is negligible, the process of directly measuring the crack tip location using the dual caliper apparatus during the experiment is accurate, efficient, and has less opportunity for inducing error.

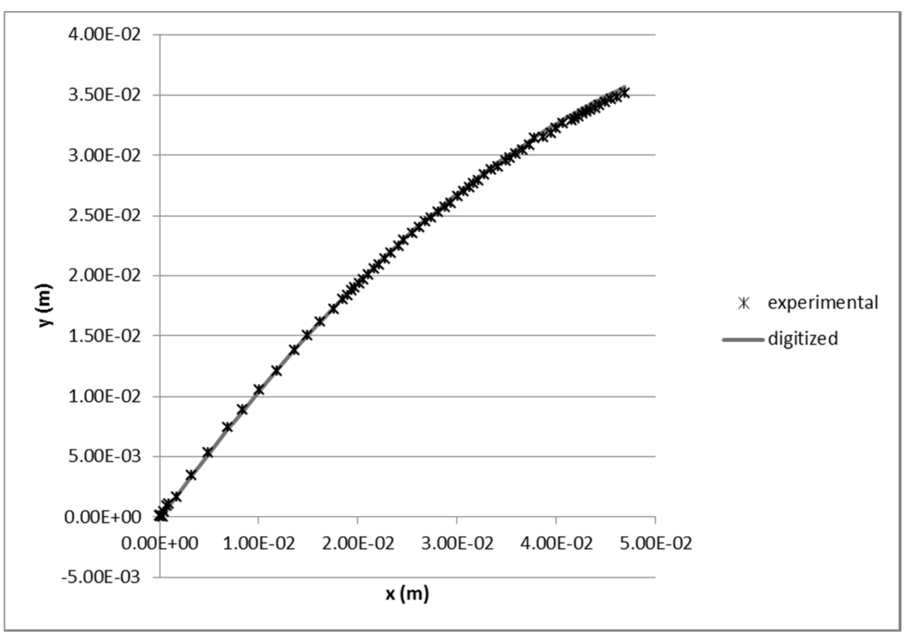

Figure 2.18. Crack path for $\Phi = 60°$ determined by slide apparatus experimentally versus the crack path determined by digitization.

CHAPTER 3

THEORETICAL WORK

3.1 CRACK3D

CRACK3D is a three-dimensional finite element code first developed by the University of South Carolina and later jointly by the University of South Carolina and Correlated Solutions, Inc.. It is capable of simulating elastic-plastic stable tearing crack extension and linear-elastic fatigue crack propagation, both with curved crack fronts and curvilinear crack paths for mixed-mode conditions. Two methods of crack growth simulations are available: nodal release and local re-meshing. Nodal release assumes that the crack path is known prior to running the simulation and is useful in evaluating crack growth events with known crack paths from experimental measurements or for what-if design scenarios. In the case that the crack path is to be predicted, local re-meshing is used to extend the crack [1] [2] [3]. For the case of fatigue crack propagation, there are three steps to crack growth predictions: (1) will the crack grow? (2) in what direction will it grow? (3) how far will it extend for a certain number of loading cycles or how many loading cycles will be required to extend the crack by a certain amount?

For determining if the crack will propagate, $\Delta K > \Delta K_{TH}$ must be true as discussed in Section 1.2. CRACK3D can be used to evaluate ΔK, which can be used to check if $\Delta K > \Delta K_{TH}$ is satisfied. Once this crack growth criterion is met, CRACK3D can be used to simulate the crack growth process and predict (a) the direction of crack growth and (b) the variations of stress intensity factors with the amount of crack growth, which can be used to predict the number of loading cycles as a function of the amount of crack growth.

In CRACK3D the determination of stress intensity factors is done using the method of three-dimensional virtual crack closure technique (3D-VCCT) [3] [1] [2] [4] [5], which is based on the approach of the strain energy release rate [6], which is the amount of energy released per unit thickness per unit crack extension when new crack surfaces are created during crack extension. The 3D-VCCT can be used in finite element simulations to calculate accurately and efficiently the mixed-mode strain energy release rates, G_I, G_{II}, and G_{III}, which are related to the mixed-mode stress intensity factors K_I, K_{II}, and K_{III}. Since fatigue crack propagation often occurs under nominally linearly elastic conditions, it is assumed that the amount of energy required to extend the crack a small increment is the same as the amount of energy required to close the crack. In Mode I, the work required to close the crack per unit thickness is equivalent to one half the nodal force multiplied with the opening displacement. In VCCT, this product between the nodal force and opening displacement is approximated by using the nodal force at nodes immediately ahead of the crack front and the crack opening displacement at corresponding nodes immediately behind the crack front from the same finite element solution. Okada et al. [4] applied VCCT to three-dimensional analysis using tetrahedral elements. Deng et al. [3] [1] [2] later adopted Okada's 3D-VCCT for general crack growth simulations by proposing a locally structured re-meshing approach.

To illustrate the 3D-VCCT, consider crack growth simulations using the nodal release option. The extended crack is created by separating the crack front and mid- nodes attached to the element just ahead of the crack front into coincident nodal pairs. It is assumed that these nodal pairs are connected with a stiff spring with length zero as shown in Figure 3.1.

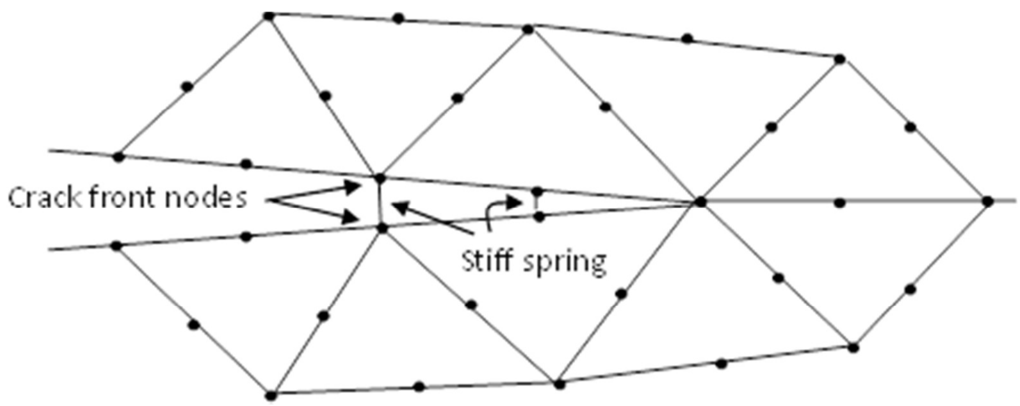

Figure 3.1. An exaggerated local 2D view of a crack-front finite element mesh on the plane normal to the crack front, where the rigid springs between the node pairs have zero length.

Stiff spring constants, K_x, K_y, and K_z, which are large but otherwise arbitrary values set in the nodal release option, and the displacements, u_x, u_y, and u_z, of the upper (+) and lower (-) nodes are used to compute the forces, F_x, F_y, and F_z (Eq 3.1) for each node, where the coordinate system is such that x is along the direction of crack extension, y is perpendicular to crack extension, and z is through the thickness and tangent to the crack front.

$$F_x = K_x({u_x}^+ - {u_x}^-), F_y = K_y({u_y}^+ - {u_y}^-), F_z = K_z({u_z}^+ - {u_z}^-) \quad [3.1]$$

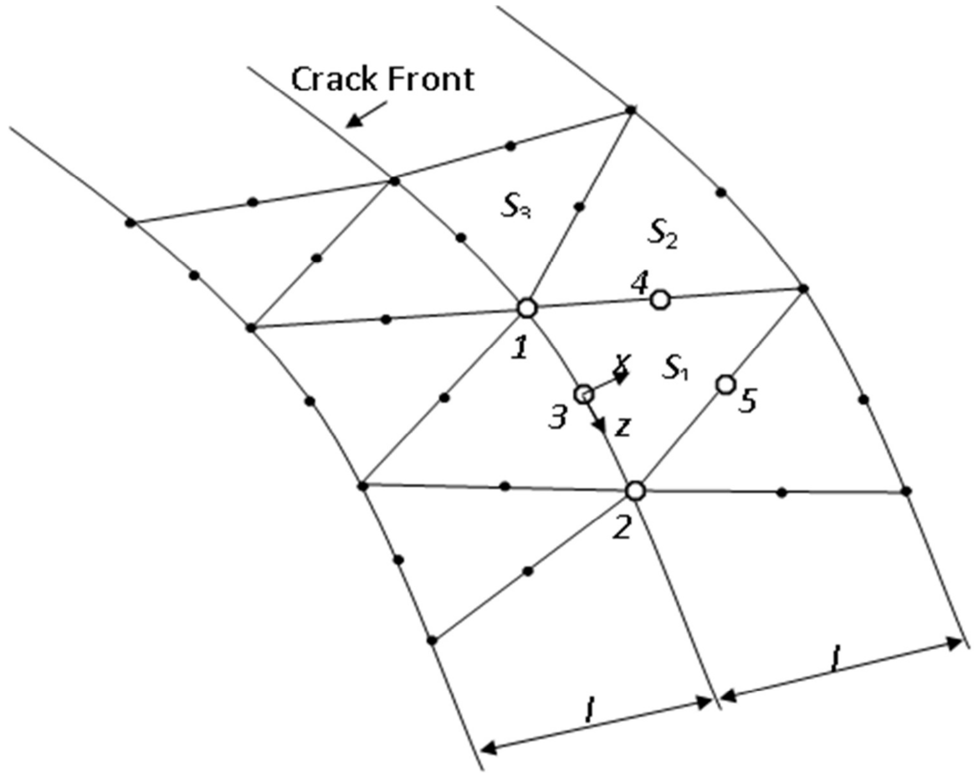

Figure 3.2. A local view of a crack front mesh on the extended crack surface, where the local coordinate system for a mid-node on the crack front has its origin at the node.

Figure 3.2 shows the view of the crack front through the thickness where l is one elements length and elements 1, 2, and 3 only. S_1, S_2, and S_3 are the areas of the sides of the tetrahedral elements on the extended crack surface for elements 1, 2, and 3 respectively. Nodes 1, 2, and 3 are nodes located on the crack front where node 1 is attached to elements 1, 2, and 3 and node 2 is only attached to element 1.

Some nodes, such as 1 in Fig. 3.2, share element surfaces therefore the resultant forces, F_x, F_y, *and* F_z for node 1, must be divided among the surfaces S_1, S_2, and S_3. For element surface 1,

$$F_{x1} = \frac{S_1 F_x}{S_1+S_2+S_3}, F_{y1} = \frac{S_1 F_y}{S_1+S_2+S_3}, F_{z1} = \frac{S_1 F_z}{S_1+S_2+S_3} \quad [3.2]$$

Then for element surface 1, the 3-D strain energy release rates, G_I, G_{II}, *and* G_{III}, are estimated by summing up the work required to close the nodal pairs on the element surface and are expressed as [4]

$$G_I \approx \frac{1}{3S_1}\sum_i F_{yi}u_{yi},\ G_{II} \approx \frac{1}{3S_1}\sum_i F_{xi}u_{xi},\ G_{III} \approx \frac{1}{3S_1}\sum_i F_{zi}u_{zi} \qquad [3.3]$$

where u_{xi}, u_{yi}, and u_{zi} are the relative displacements between the top and bottom crack surfaces at nodes behind the crack front that correspond to nodal forces F_{xi}, F_{yi}, and F_{zi} for i nodes attached to the element surface ahead of the crack front. Finally, the SIFs for plane strain are related to strain energy release rates by

$$K_I = \sqrt{\frac{G_I E}{1-\nu^2}},\ K_{II} = \pm\sqrt{\frac{G_{II} E}{1-\nu^2}},\ K_{III} = \pm\sqrt{\frac{2G_{III} E}{2(1+\nu)}} \qquad [3.4]$$

where E is Young's modulus and ν is Poisson's ratio. It is noted that the signs for K_{II} and K_{III} are the same as the signs of the relative displacements behind the crack front along the x and z axes, respectively.

It is noted that the SIF values described above correspond to the maximum loading value applied during a loading cycle. Once the SIFs for the maximum applied load are predicted using the VCCT, the direction in which the crack will propagate is predicted using MCS criterion [5]. The MCS criterion assumes that a crack will grow in the direction, θ_c, that maximizes the local circumferential stress, $\sigma_{\theta\theta}$, at a specified location ahead of the crack tip. The local stress around the crack tip can be expressed as a function of SIF and position with respect to the crack tip in polar coordinates (r,θ) (see Figure 3.3).

$$\sigma_{\theta\theta} = \frac{1}{\sqrt{2\pi r}}\cos\left(\frac{\theta}{2}\right)\left(K_I\,(\cos\left(\frac{\theta}{2}\right))^2 - \frac{3}{2}K_{II}\sin\theta\right)$$

$$\sigma_{r\theta} = \frac{1}{2\sqrt{2\pi r}}\cos\left(\frac{\theta}{2}\right)\left(K_I\sin\theta + K_{II}(3\cos\theta - 1)\right) \qquad [3.5]$$

Where $\sigma_{\theta\theta}$ is the circumferential normal stress near the crack tip and $\sigma_{r\theta}$ is the shear stress.

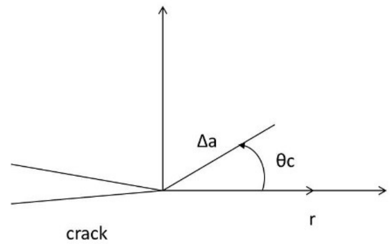

Figure 3.3. Diagram of crack growth direction according to the MCS criterion.

It can be shown that that $\sigma_{\theta\theta}$ is maximum or minimum when the shear stress $\sigma_{r\theta}$ is zero. So setting $\sigma_{r\theta}$ from Eq 3.5 to zero

$$0 = \left(K_I \sin\theta + K_{II}(3\cos\theta - 1)\right) \qquad [3.6]$$

and solving for θ,

$$\theta_c = 2\tan^{-1}\left(\frac{\frac{K_I}{K_{II}} \pm \sqrt{\left(\frac{K_I}{K_{II}}\right)^2 + 8}}{4}\right) \qquad [3.7]$$

The root that maximizes $\sigma_{\theta\theta}$ gives θ_c as the direction in which the crack will extend [5].

To apply the VCCT in crack growth simulations using the local re-meshing option (instead of the nodal release option), the local mesh immediately ahead and behind the crack front must be properly structured, so that the local mesh immediately behind the crack front can be viewed as being shifted by one element size from the local mesh immediately ahead of the crack front, Therefore, once crack growth is determined to occur along a certain direction with a certain increment, the new mesh around the new crack front is generated such that there is a structured mesh (within a local re-meshing zone around the new crack front) with equal number of elements behind the crack front and ahead of the crack front. [3] [1] [2]

A fatigue crack growth rate model, such as the Paris' Law, is used to determine how many cycles it will take for the crack to grow the amount of crack extension chosen by the user [7]. However, since mixed-mode conditions are considered, ΔK as presented in Chapter 1 is no longer Mode I. After K_I, K_{II}, and K_{III} are predicted, ΔK_I, ΔK_{II}, and ΔK_{III} can be computed using Eq 1.2, and ΔK_{eq} from Eq 2.2. Again, assuming that there is no crack closure effect, the crack growth rate can be determined using a Paris-type Law as in Eq 1.5.

3.2 GEOMETRY, MESH GENERATION, AND BOUNDARY CONDITIONS

The Arcan fixture and specimen were modeled as shown in Figure 3.4. The fixture and specimen are connected by bolts. For simplicity, this fixture-specimen connection is approximated by a continuous bond at the fixture-specimen boundary. To this end, the bolts are not modeled and the fixture and specimen are treated as three solid regions with different thicknesses. Also, the outside radius of the fixture in the model corresponds to the radius of the center of the pin holes on the actual fixture.

An idealized through-thickness edge notch and pre-crack exactly 12.7mm long was modeled as the initial crack in the exact geometric vertical center of the specimen and is perfectly horizontal into the width of the specimen. Material properties for the fixture and specimen are Young's modulus = 2.07 x 10^{11} Pa and 7.11 x 10^{10} Pa and Poisson's ratio = 0.30 and 0.33 respectively. Both materials are modeled as being elastic-plastic through the use of their actual stress-strain curves.

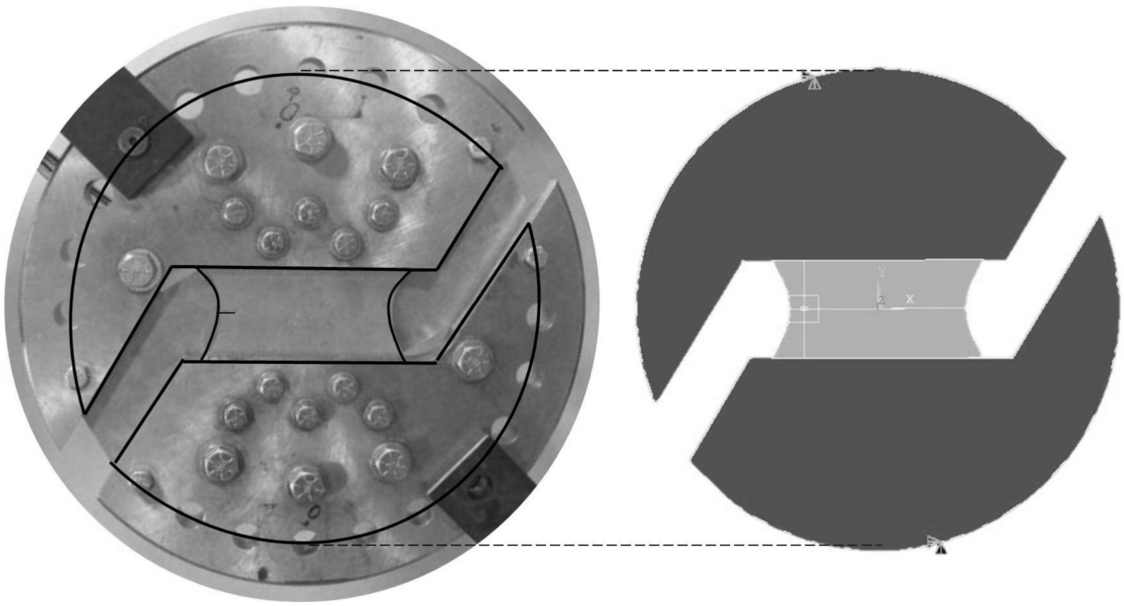

Figure 3.4. Diagram of a picture of actual Arcan fixture and specimen (left) and image of finite element model geometry (right).

The volumes were then meshed with 10 noded tetrahedral elements. Figure 3.5 shows the initial mesh generated, and Figure 3.6 shows the initial three zones of the mesh. As discussed in Section 3.1 for local re-meshing, structured elements were created one element ahead and one element behind the crack front. Then a transition zone was created from the structured element to the far field mesh. Elements in this zone should transition from the local minimum element size to a maximum element size at the boundary of the local re-meshing zone. The far-field mesh away from the local region can be coarse, provided it can adequately transfer loading information to the crack front local region.

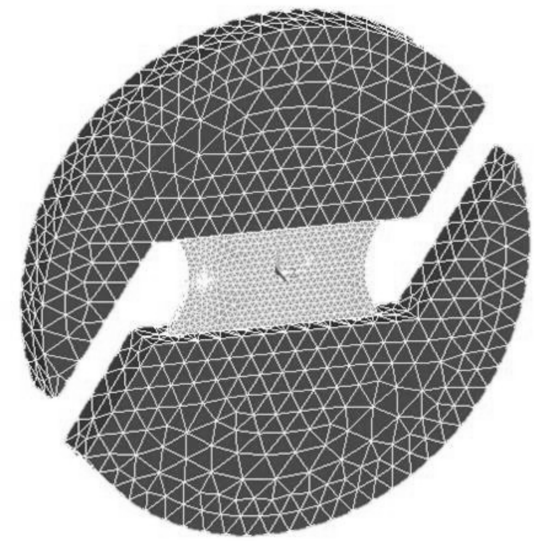

Figure 3.5. Image of the 3D mesh.

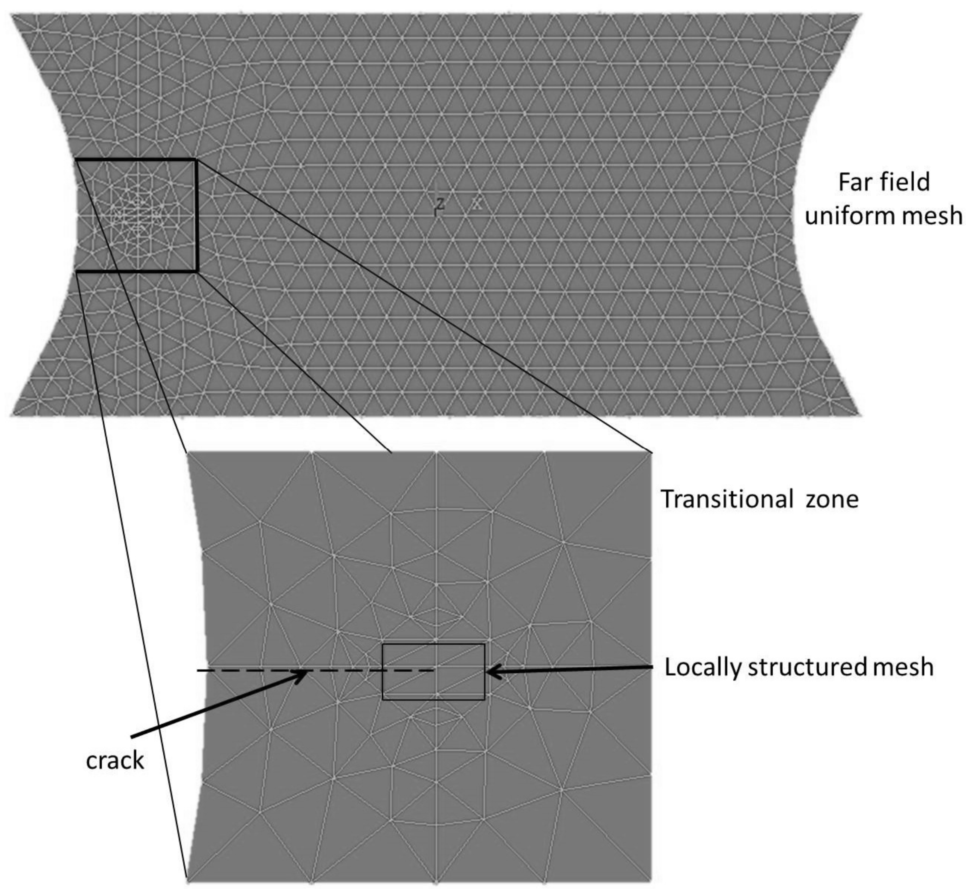

Figure 3.6. A 2D view of the initial 3D finite element mesh in the specimen region.

The first mesh shown in Figure 3.6 has two elements through the thickness. A second refined mesh was generated with 4 elements through the thickness in the structured area to check for convergence of the mesh.

For each loading angle, Φ, a set of lines (one on the top fixture and the other on the bottom fixture) corresponding to the center of the pins were created on the surface of the fixture model in the through-thickness direction. The boundary conditions were such that the displacement of the bottom line was set to zero in the x and y directions (u_x & $u_y = 0$) and only the z displacement specified was of the center point on the bottom line ($u_z=0$). The displacement of the corresponding top line had a magnitude of 1 x 10^{-3}mm along the direction of loading, Φ, as shown in Figure 3.7, which was decomposed into x and y components (see Table 3.1).

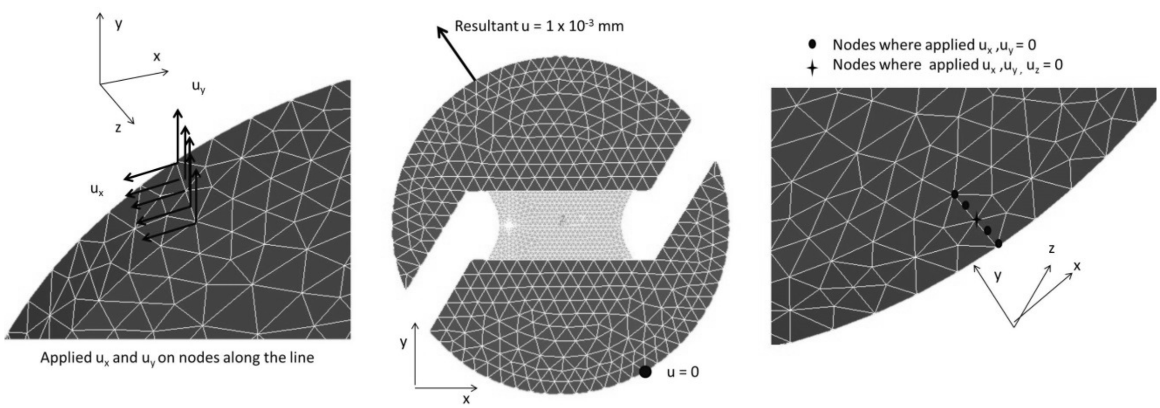

Figure 3.7. Boundary conditions at Φ = 30°.

Table 3.1. Table of applied displacements for line on top fixture.

Loading Case	Displacement in x direction (u_x) [1 x 10^{-3} mm]	Displacement in y direction (u_y) [1 x 10^{-3} mm]
15°	-0.259	0.966
30°	-0.500	0.866
45°	-0.707	0.707
60°	-0.866	0.500

3.3 SIMULATION PROCEDURE

The initial finite element meshes were created using ANSYS 14 [9]. Mesh data for both the initial and initial refined meshes was exported from ANSYS using the "NWRITE" and "EWRITE" commands, and the files were named NODES.DAT and ELEMS.DAT respectively according to the CRACK3D manual.

There are 3 input files for CRACK3D for simulations using the local re-meshing option. The first file, CRACK3D.MSH, contains the mesh information. The second file, CRACK3D.DAT, is used to define the analysis type, parameters for analysis, and boundary conditions. The last file used only for local re-meshing, CRACK3D.GEO, defines the boundary lines and surfaces in which the crack and re-meshing are contained.

Two CRACK3D.MSH and CRACK3D.GEO files were created. One set of files was for the initial mesh with 2 elements through the thickness at the crack front, and the second file was for the initial mesh with 4 elements through the thickness. MESH3D, a preprocessor for CRACK3D, was used to generate the CRACK3D.MSH file from the NODES.DAT and ELEMS.DAT files. CRACK3D.GEO was created with the help of ANSYS macros created by Dr. Weiming Lan. Output from the macros was compiled in Microsoft's Notepad to create the CRACK3D.GEO file.

The CRACK3D.DAT file was created in Microsoft's Notepad following the CRACK3D manual. A different CRACK3D.DAT file was created for each of the loading cases. The crack growth simulation was performed using local re-meshing for fatigue crack growth with VCCT and the MCS criterion for crack growth direction prediction. Parameters for ΔK_{eq} defined in Eq 2.2 were chosen as follows: $\gamma=0$, $\gamma_1=1$, $\gamma_2=1$. Paris Law data from CRACK3D was not used for life prediction because the parameters for the specific material and loading ratio being simulated were not currently available so that parameters for a different *R*-ratio were input. Also, the minimum element size, maximum element size, radius for the local re-meshing region, and increment for crack growth were defined. Boundary conditions were input for the specific loading case as described above in Section 3.2. As an example, the input files for the simulation for loading case $\Phi = 45°$ are contained in Appendix C.

The first simulations were performed to check for convergence of the crack path. For the 15° loading case, simulations were performed using the first initial mesh with 2 elements through the thickness and with the initial refined mesh containing 4 elements through the thickness. The minimum element sizes equivalent to 1 /2 the thickness, 1 /4 the thickness, and 1/8 the thickness were used, and crack growth increments for 0.001m and 0.002m were used. The maximum element size and re-meshing zone size remained constant at 0.006m and 0.012m respectively. Table 3.2 shows all the combinations of simulations performed to check convergence.

Table 3.2. All combinations of simulations performed to verify convergence of solution

Number of elements through thickness of initial mesh	Minimum element size [m]	Crack growth increment [m]
2	.003	0.001
		0.002
	.0015	0.001
		0.002
4	.0015	0.001
		0.002
	.00075	0.001
		0.002

Simulations were performed for loading cases $\Phi = 15°$, 30°, 45°, and 60°. In some cases the local re-meshing operation in CRACK3D had numerical difficulties and could not continue when the crack growth amount reached a specific value. In such cases, the local re-meshing parameters such as the minimum element size, the maximum element size, or re-meshing region size were adjusted slightly in a trial and error fashion. Also, sometimes the first initial mesh with 2 elements through the thickness was used while other times the refined mesh was used. After simulations were performed using CRACK3D, POST3D was run which converted results from CRACK3D into result files compatible with ANSYS for further post-processing.

3.4 POST PROCESSING OF SIMULATION RESULTS

CRACK3D.SIF is an output file from CRACK3D which contained x, y, z, G_I, G_{II}, G_{III}, K_I, K_{II}, and K_{III} for each node along the crack front at each crack growth increment. CRACK3D.CXT contains the total reaction load for each crack growth increment. The total reaction load was summed over the nodes along the top line which the displacements were specified and was defined in the CRACK3D.DAT file. The data from these two files was imported to Microsoft Excel for post-processing of each simulation.

The reaction load from the prediction and the maximum load applied in the experiment were used to create a scale factor for the SIFs, since for nominally linear elastic conditions the load and SIF remain proportional. The SIF values were scaled to the experimental values for the maximum load. Then, ΔK_I and ΔK_{II} were calculated using Eq 1.4.

3.5 THEORETICAL RESULTS

The crack path for each of the simulations run for convergence check were plotted. No crack propagation occurred for the simulations with minimum element size of 1 /8 of the thickness (0.00075 m).

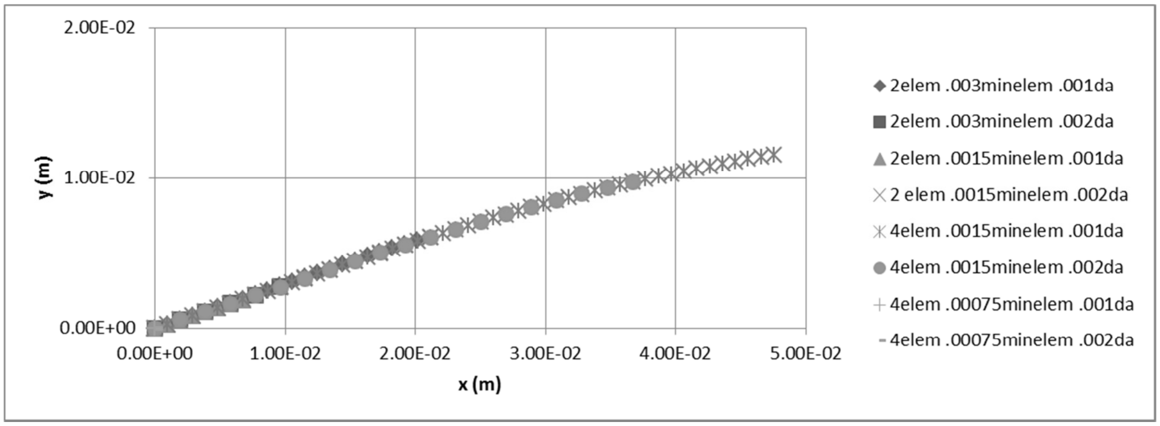

Figure 3.8. Crack path for Φ = 15° with various initial meshes, minimum element sizes, and crack increments.

Figure 3.9 shows the deformed mesh for loading case Φ = 45° for *a* = 0.03 m with a close up of the crack and re-meshing zone.

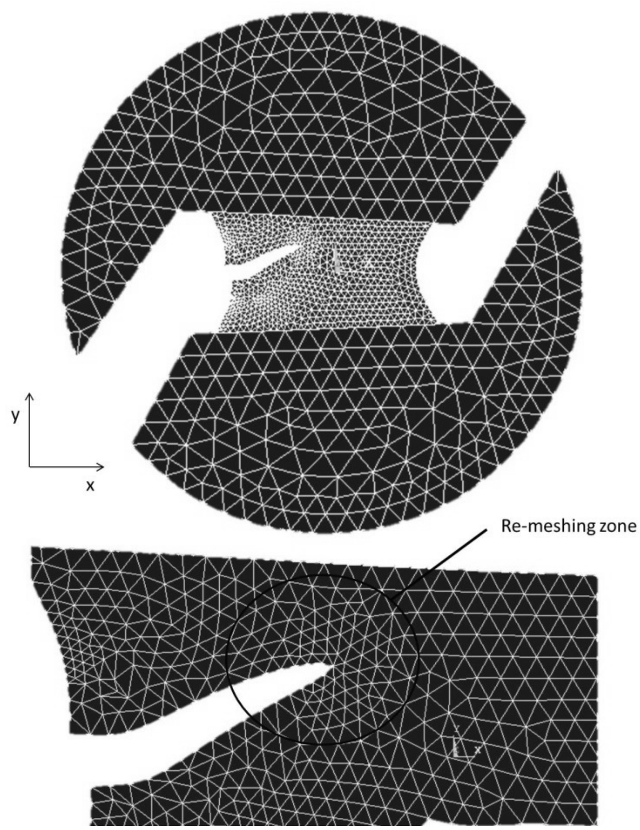

Figure 3.9. 2D view of the 3D deformed mesh for Φ = 45° (top) and a close up of the crack path and re-meshing zone around the crack front.

For loading cases Φ = 15°, 30°, 45°, and 60°, Figures 3.10-3.13 show the comparison between the experimental crack paths and the predicted crack paths.

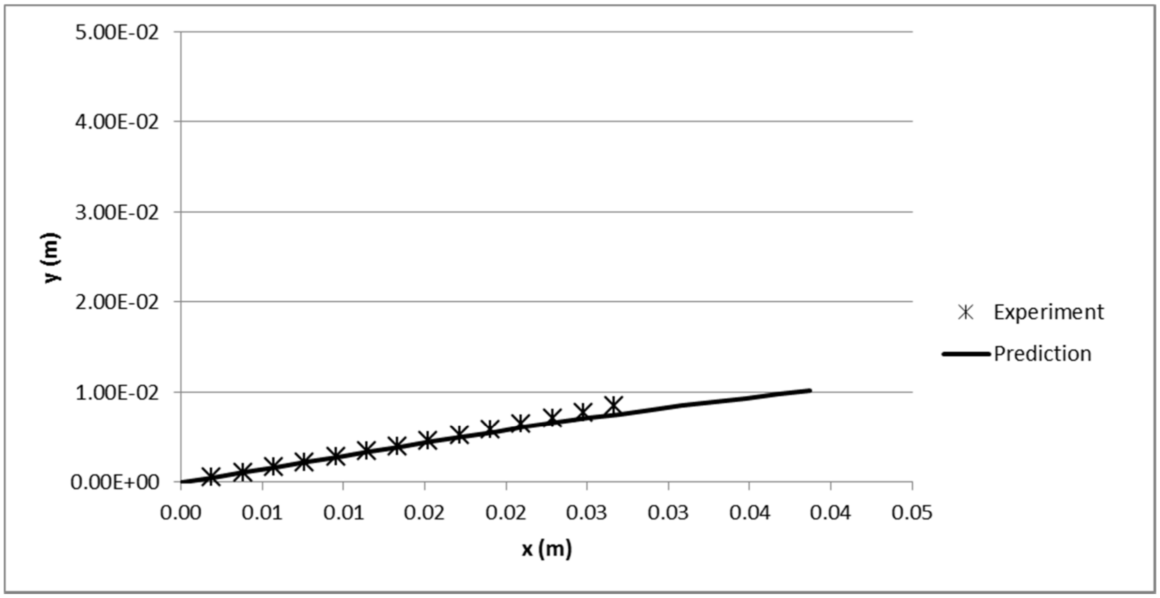

Figure 3.10. The experimental and predicted crack path for the 15° loading case.

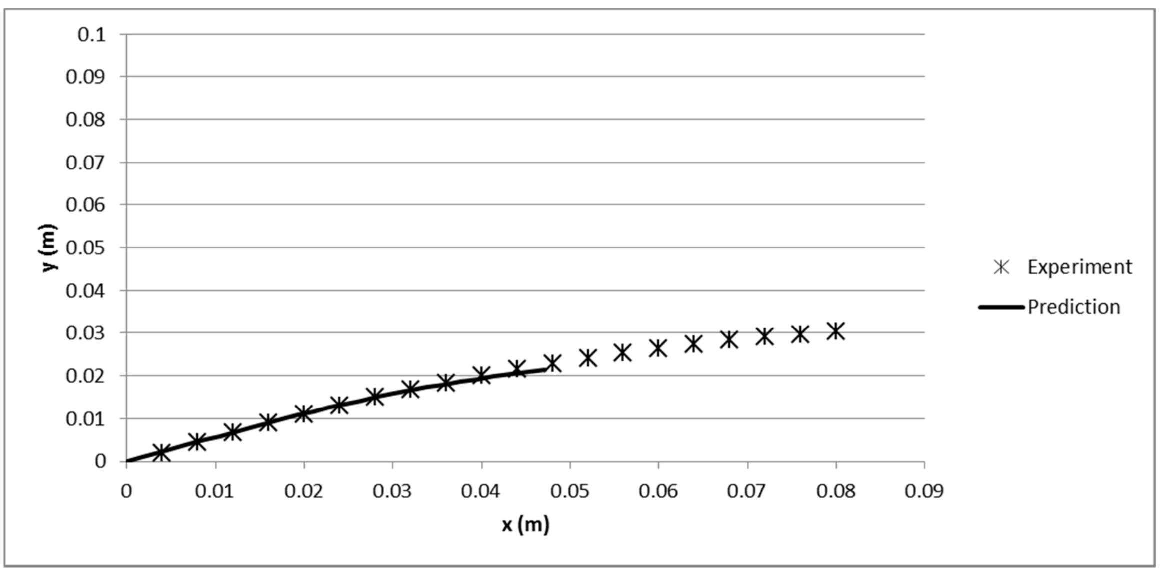

Figure 3.11. The experimental and predicted crack path for the 30° loading case.

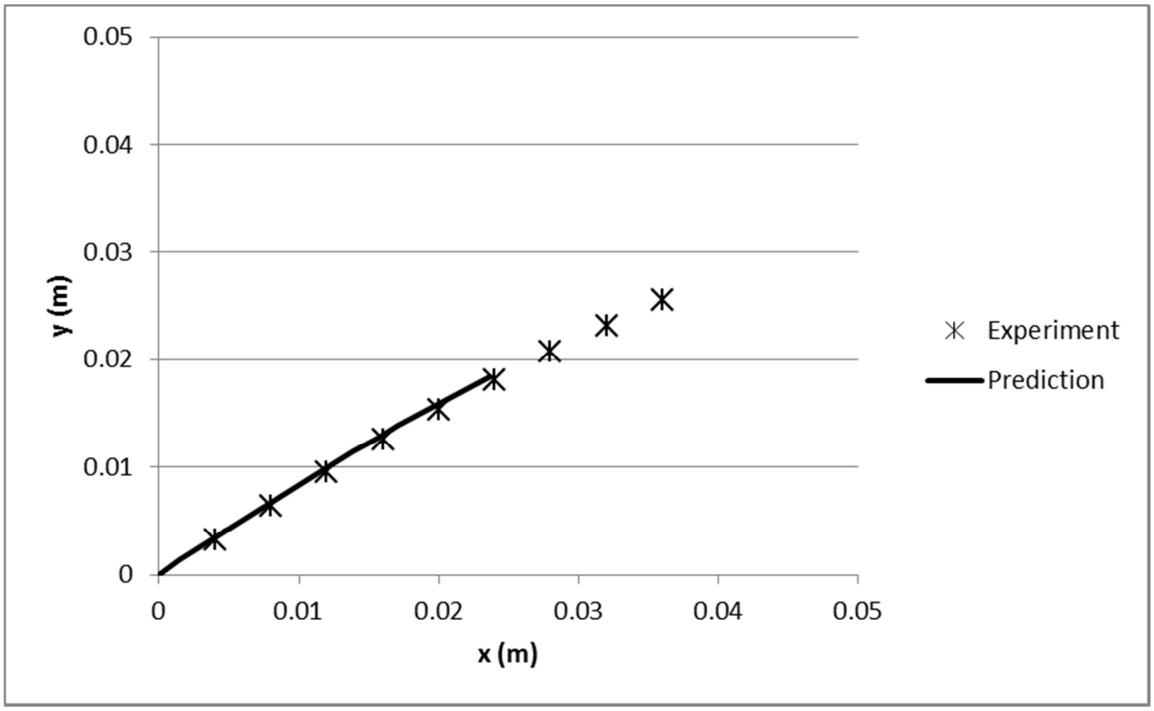

Figure 3.12. The experimental and predicted crack path for the 45° loading case.

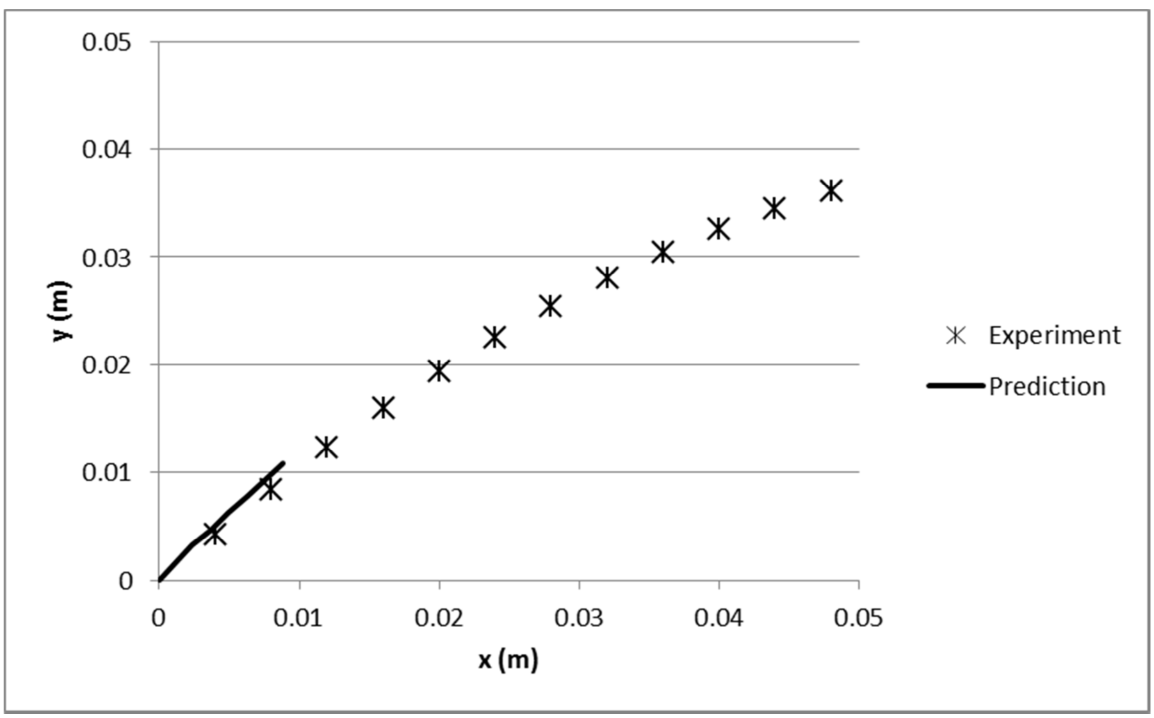

Figure 3.13. The experimental and predicted crack path for the 60° loading case.

The ΔK_I and ΔK_{II} for each loading cases Φ = 15°, 30°, 45°, and 60° are plotted along the crack length *a* in Figures 3.14-3.17.

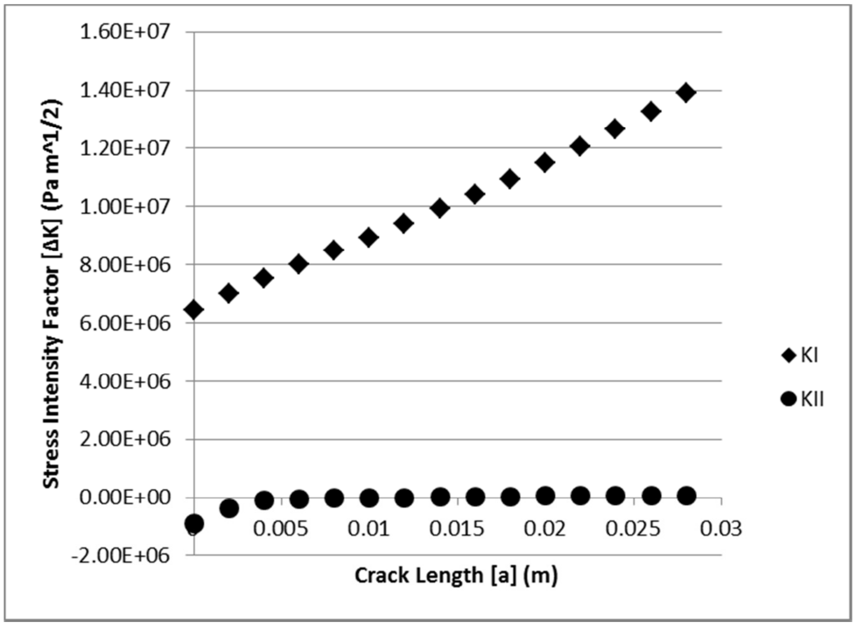

Figure 3.14. Plot of ΔK_I and ΔK_{II} along the crack path for the 15° loading case.

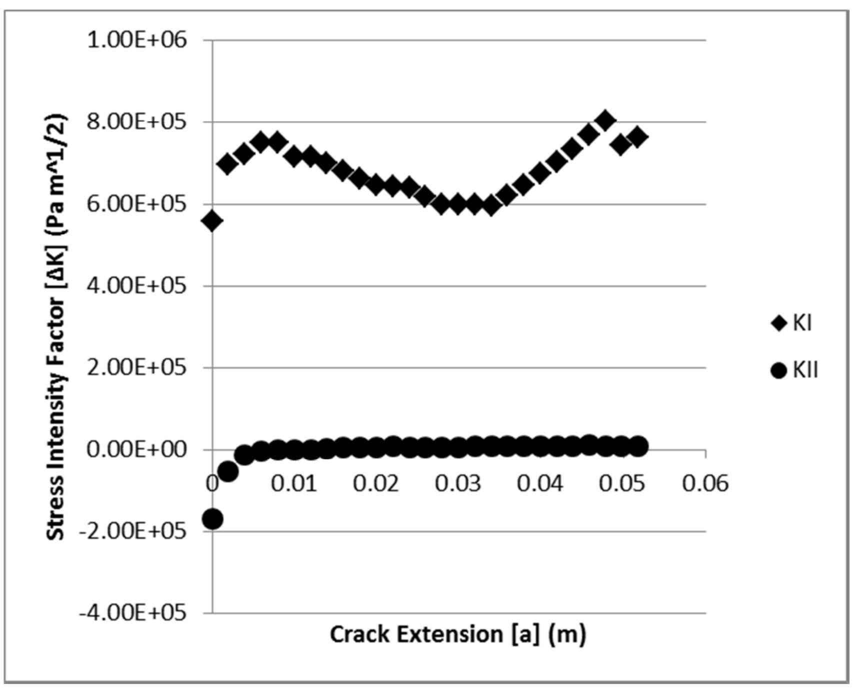

Figure 3.15. Plot of ΔK_I and ΔK_{II} along the crack path for the 30° loading case.

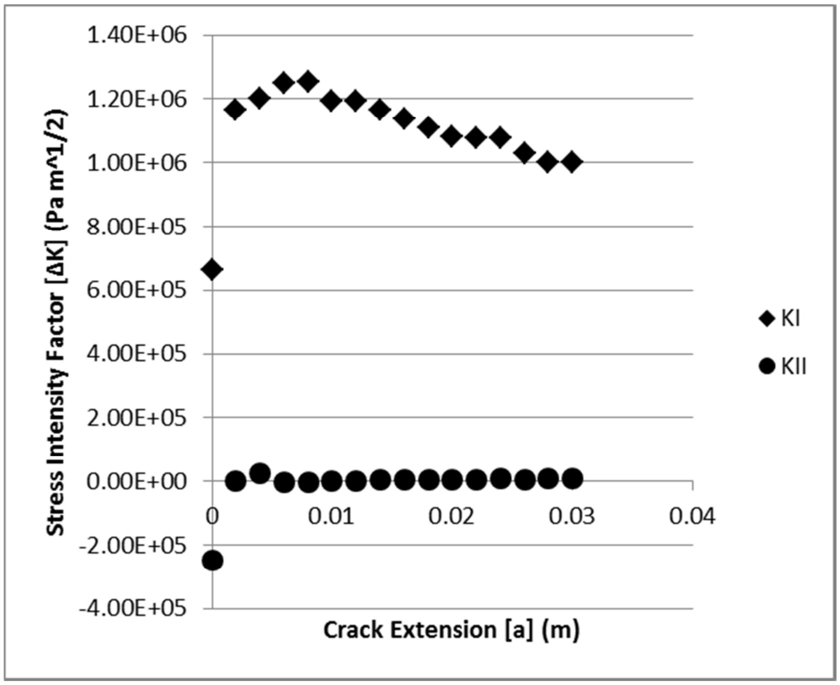

Figure 3.16. Plot of ΔK_I and ΔK_{II} along the crack path for the 45° loading case.

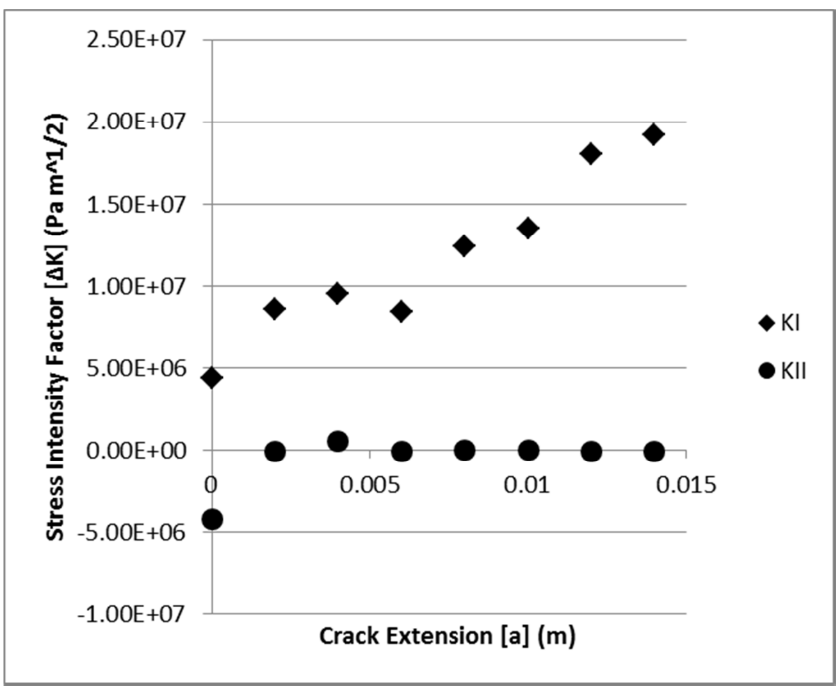

Figure 3.17. Plot of ΔK_I and ΔK_{II} along the crack path for the 60° loading case.

CHAPTER 4

DISCUSSION

4.1 DISCUSSION OF EXPERIMENTAL RESULTS

There are several issues that require discussion. First, as noted in Section 2.5, the experimental crack paths were determined through an imaging-digitization-scaling process, where imaging was performed on the fatigue specimen after completion of the crack growth process. Results from this process gave consistent results for all loading angles, Φ, and hence the resulting crack paths are used for direct comparison to the simulation predictions.

Secondly, regarding the crack growth process, as shown in Figures 3.10 to 3.13, there is excellent agreement between the measured and predicted crack growth paths. Furthermore, as shown in Figures 3.14 to 3.17, the simulation data shows that the crack growth process is occurring under nominally Mode I conditions, with $\Delta K_{II} = 0$, confirming that the fatigue crack tended to propagate under locally tensile conditions. For small loading angles, the crack growth direction is approximately perpendicular to the loading direction. However, as loading angle increases, the crack deviates from the perpendicular direction, implying that the local Mode I direction is no longer perpendicular to the loading angle. In fact, the curvilinear trend of the crack path which begins around x = 0.03m is the result of the influence of the loading process via the Arcan fixture on the stress field in the specimen. For $\Phi = 30^o$, Figure 4.1 shows a plot of the crack path, with an additional line indicating the edge of the top fixture. Clearly, the Arcan fixture is sufficiently close to the crack path to have an influence on the local crack tip stress field in the specimen. In fact, the data for all loading angles show that as the crack approaches the steel fixture, it begins to turn and follow the edge of the upper fixture. Since the thickness of the Arcan fixture is much greater than the specimen and is manufactured from stainless steel, the crack turns to follow the "path of least resistance". That is, it would require more energy to create new surfaces inside the fixture, so the crack turns to continue propagating in the aluminum specimen.

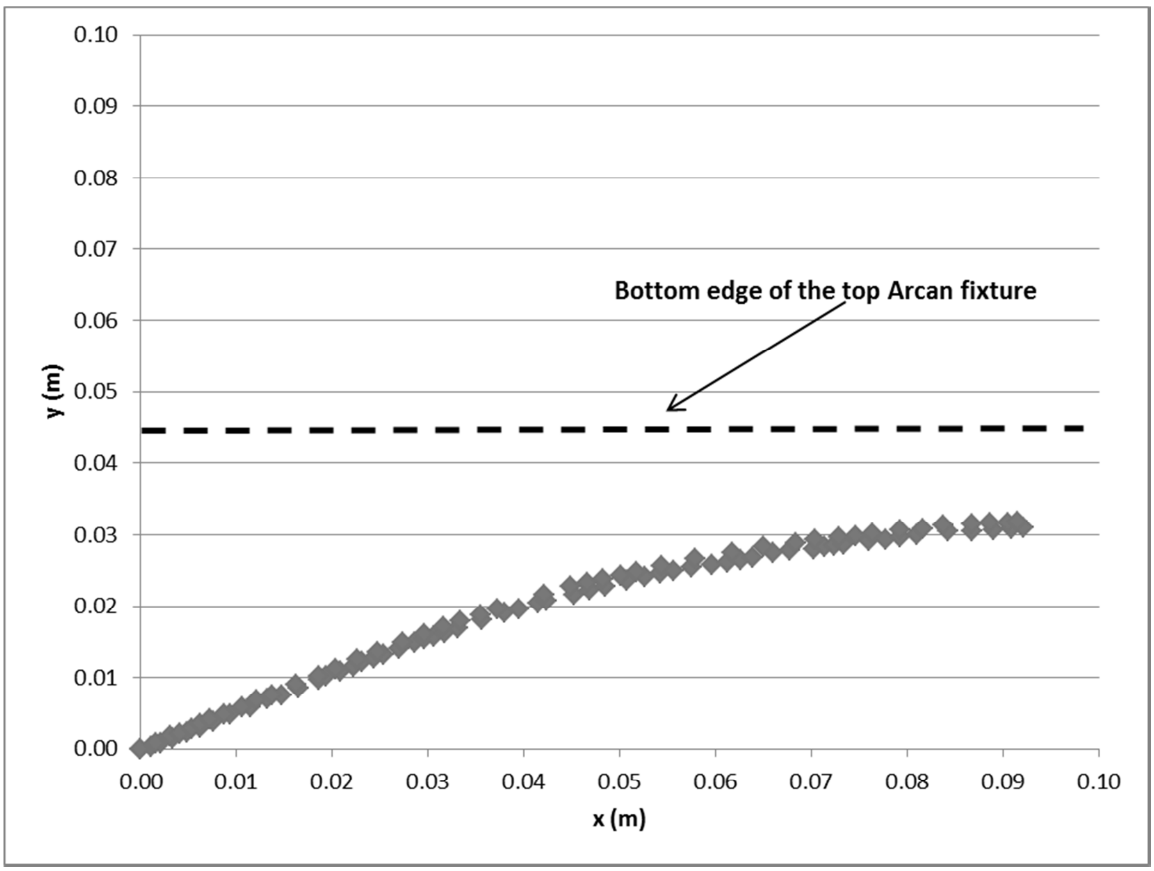

Figure 4.1. Plot of the crack path for Φ = 30° and edge of top fixture.

Thirdly, we were unable to observe crack growth for $\Phi = 75°$ and $\Phi = 90°$. There are two plausible reasons why the crack did not grow in these cases. Firstly, other studies have shown that the stress distribution for the Arcan fixture is not uniform, with the largest gradients occurring in the 75° orientation [1]. The relatively short initial notch and initial pre-crack used in the experiment may have positioned the crack tip in an area of negative or low stress. This may have put the crack into compression or kept ΔK_{eq} below ΔK_{TH}, the threshold value required to initiate crack growth in the material. Preliminary FEA by the author was consistent with this observation. Another possibility for both Φ = 75° and 90° is that the Mode II component of the far field loading is larger than the Mode I component. In such cases, there may not be sufficient Mode I loading to open the crack tip and overcome friction and local plastic deformation along the contacting crack surfaces to allow the fatigue crack to propagate.

4.2 DISCUSSION OF THEORETICAL RESULTS

Prior to discussing the results for the Arcan fatigue studies, it is important to note that benchmark studies have been performed, and it has been verified that CRACK3D is able to accurately predict the crack path for elastic plastic stable tearing using the Arcan fixture to achieve mixed-mode loading conditions using local re-meshing [2] [3] [4] [5] [6]. The direction of crack extension for stable tearing is predicted with a different criteria, crack opening displacement [2] [3] [4] [5] [6], while as discussed here, VCCT and MCS criterion are used in predicting the direction of fatigue crack propagation.

An important aspect of the simulations studies is to confirm consistency in the predicted crack path for each loading angle. The convergence of the predicted crack path for $\Phi = 15°$ was checked, and the plot in Figure 3.8 shows there is good agreement in the predicted crack path for all combinations of initial meshes, crack growth increments, and minimum element sizes, with the lone exception of simulations where minimum element size was 0.00075m. It was observed that the various combinations did not provide the same amount of crack growth, though the results from all combinations gave generally consistent trends in crack growth path across all converged simulations.

It is worth noting that, for each simulation, at a certain point CRACK3D was unable to re-mesh the volume according to the re-meshing criteria provided in the code. Thus, the program was terminated at this point. Though the precise reason for the inability to continue propagating the fatigue crack is not fully understood, it must be stated that there is no theoretical reason why there should be an issue in the ability to predict the direction of crack propagation for longer amounts of crack extension using MCS criterion. Since other fatigue studies were performed with CRACK3D where the crack grew all the way across a different specimen geometry, the most likely reason for the limited amount of crack extension is that CRACK3D could not arrange elements in an acceptable manner inside the size of the re-meshing region for this specimen geometry to "match" the surrounding, un-meshed region. The effect of overall geometry is most clearly evident in Figure 4.1. Here, as the crack propagated, the re-meshing region approached the interface of the specimen and the fixture (see Fig 4.1). Since the code currently does not have the ability to define internal boundaries to control the re-meshing near material boundaries, as the re-meshing region approached the fixture boundary, the program could not re-mesh the region satisfactorily, resulting in termination of the crack growth process. Even with these issues, our convergence analysis does show that any of these combinations of re-meshing parameters will give similar results when re-meshing is possible.

As shown in Figures 3.10 – 3.13, the predicted and experimental crack paths are in good agreement with each other in the region where re-meshing was achievable. As commented above regarding the robustness of CRACK3D, the simulations with the longest predicted crack path for each loading case were reported.

As noted previously, Figures 3.14 – 3.17 show that ΔK_{II} quickly goes to zero along the predicted crack path, conditions that are consistent with the use of MCS criterion for predicting the direction of crack growth. For the first case, $\Phi = 15°$, for the segment of crack path considered, the load was held constant, and so it is expected that ΔK_I increases as shown in Fig. 3.14. However after crack slanting occurred for $\Phi = 15°$, ΔK_I for the remaining experiments was held approximately constant (see Figure 3.15 – 3.17) via a modified method of load shedding to control the crack growth rate and maintain crack tip conditions that were nominally consistent with elasticity assumptions (e.g., small plastic zone relative to specimen dimensions). This was necessary so that crack growth occurred under conditions that reflected local stress intensity factor control. Figures 2.10 and 2.11 show that, for most crack lengths, the crack growth rate, *da/dN*, was maintained between the range of 4×10^{-5} mm/cycle and 8×10^{-5} mm/cycle, while also ensuring that the plastic zone size at the crack tip was small. For loading angle $\Phi=45°$, near the end of the experiment the crack growth range was below these limits for *da/dN,* ranging from a minimum of 2×10^{-5} mm/cycle to a maximum of 4×10^{-5} (see Figures 2.11 and 2.12), which increased the time required to complete the experiment but did not alter the nominally elastic conditions required for these studies.

There are several comments to be made in regards to the efficiency and effectiveness of this modified method for controlling the change in SIF during the experiment. First, during one of the experiments the crack measurement system (microscope objectives, calipers) had to be re-zeroed. Since the crack lengths were re-measured and were slightly different (shorter) afterwards, one negative value for *da/dN* was obtained immediately after the re-zeroing process. This data point is not shown in Figure 2.10. Causes for other outliers in the data not shown in Figures 2.10 – 2.12 include (a) slight errors in the measured crack lengths while the experiment was being performed, (b) local variations in material (e.g., inclusions) or (c) other defects introduced in the manufacturing process. The effects identified in (a-c) were somewhat magnified in this study since crack growth was measured over very short cycle counts Thus, changes in crack growth for any of the reasons noted above will appear as steep gradients in the $\Delta a/\Delta N$ data. If crack growth had been averaged in over a much larger time frame (more cycles), then these effects would be more muted.

Secondly, the goal of this modified load shedding technique was to maintain an average constant *da/dN*, and so far it has been discussed that in general that goal was achieved with only a few outliers in the data. However for short segments of crack growth increasing or decreasing trends in *da/dN* exist (Figures 2.10- 2.12). These trends in the data can be seen in Figure 2.10 between 40 and 60 mm of crack length and in Figure 2.11 and 2.12 at the beginning of the experiment around 10 mm of crack length. However for the experiment with $\Phi=60°$, in an effort to maintain the specified range of crack growth rates, the loads were increased too much and the crack growth rate jumped beyond the set limits. In this case, over short cycle counts the load was decreased until *da/dN* was back in the appropriate range. It is noted that these trends are the result of the difficulty in the practical application of this modified load shedding approach. The inability to precisely control *da/dN* means that ΔK_{eq} does not actually remain constant during the experiment and could potentially result in ΔK_{eq} becoming too large and the nominally elastic conditions may not be present.

Thirdly, this modified method is based on the premise that, according to Paris' Law (Eq 1.5), *da/dN* and ΔK_{eq} are proportional. Thus, trends in the measured crack growth rate and the computed ΔK_{eq} at the crack tip should be consistent throughout the crack growth process. To determine whether this approach gave consistent results, predicted values for K_I and K_{II} were scaled to the experimental values using the resultant load from the simulations and the maximum load applied during the experiment. ΔK_I and ΔK_{II} were then calculated using Eq 1.4 and ΔK_{eq} was calculated according to Eq. 2.2 with parameters $\gamma = 0$, $\gamma_1 = 1$, and $\gamma_2=1$ as discussed in Section 3.3. Figures 4.2-4.4 show a direct comparison of the scaled ΔK_{eq} and the discrete crack growth rate recorded during the experiment, $\Delta a/\Delta N$, as a function of crack length, *a*.

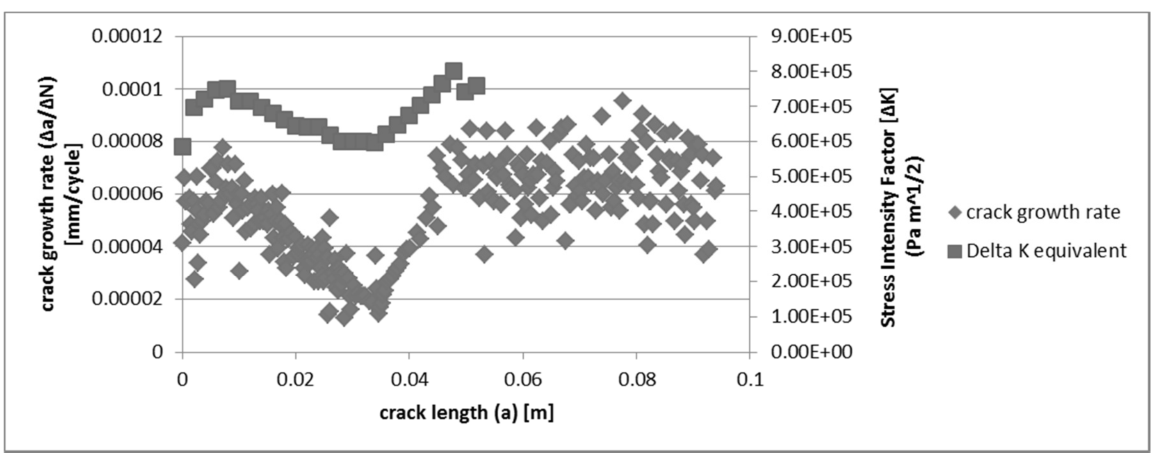

Figure 4.2. Plot of ΔK_{eq} and *da/dN* along crack length for 30° loading case.

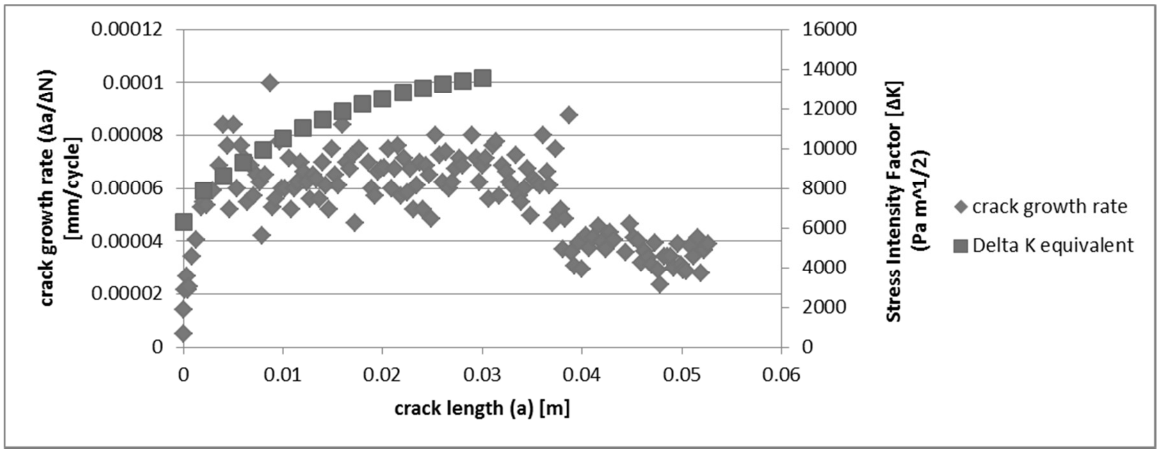

Figure 4.3. Plot of ΔK_{eq} and *da/dN* along crack length for 45° loading case.

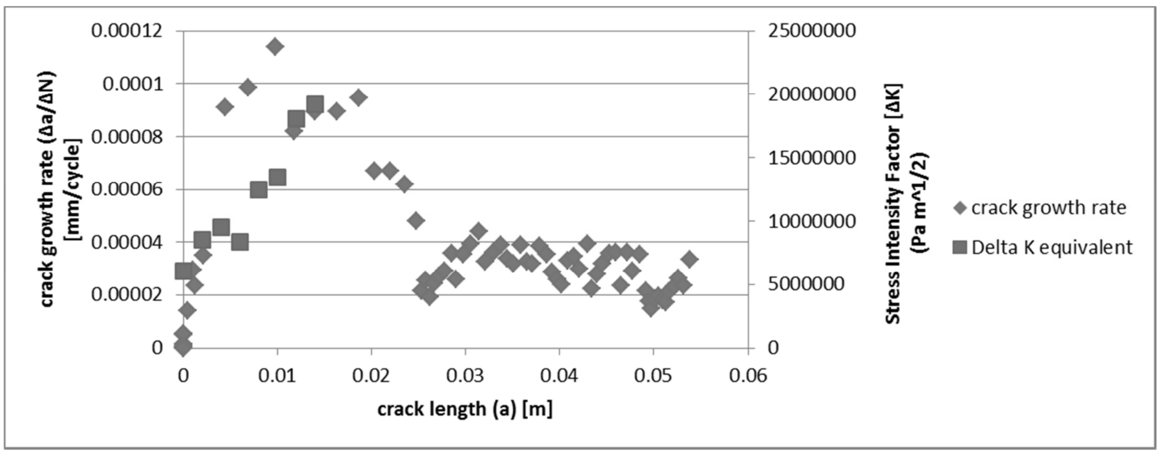

Figure 4.4. Plot of ΔK_{eq} and *da/dN* along crack length for 60° loading case.

Figures 4.2 - 4.4 show that the trend in ΔK_{eq} follows the trend in *da/dN* as expected from Paris' Law (Eq 1.5).

Fourthly, load control was used to determine the crack growth rate since it directly alters ΔK_{eq} (instead of using crude empirical expressions). Even though Figs 4.2-4.4 show that ΔK_{eq} is a viable approach, there are some challenges associated with controlling the crack growth rate in experiments. First, some previous knowledge of loading and crack growth rates must be known to have a starting point to ensure that the experiments are within the nominally linear elastic range. Secondly, the procedure is quite time consuming since the crack must be measured approximately every 5,000 cycles until the rate is established (see the first 20mm of crack growth for $\Phi = 45°$ and $\Phi = 60°$ in Figures 4.3 and 4.4 respectively). After the rate was established, it was determined that the load had to be decreased ≈ every 25,000 cycles. Thus, unless an automated approach is developed to perform the crack growth rate estimations, the experimentalist must be near the test stand through the duration of the experiment to take the crack growth measurements for these cycle count intervals. Thirdly, the loads should be adjusted in small increments to minimize changes that might cause crack closure or other unwanted effects. This slow adjustment can take 10 to 20 mm of crack growth, and thus the ΔK_{eq} is not held constant for the whole experiment. In this regard, it is noted that a more accurate way of predicting loads for the experiment is to use ΔK_{eq} values obtained by performing FEA before the experiment to determine the maximum loads which can be applied and the maximum crack length the loads can be used before the plastic zone at the crack tip becomes too large. However, this would require a priori knowledge of the crack path, which is generally not the case. Fourthly, though simply changing loads slightly to maintain modest crack growth rates is effective for the experimentalist, changing the loads during the experiment also makes the simulations more time consuming. Multiple models and simulations have to be performed for each load step if load boundary conditions are used. This avoids more post- processing on the back end. However, it is very time consuming to build multiple models. A more efficient way is to use one simulation in displacement control. The reaction load can be scaled at each crack growth increment with the loads for the corresponding crack growth increment from the experiment. This requires more post- processing and accurate records for the experiment. Also, if the *R*-ratio is not held constant through the experiment, the life prediction using Paris' Law (Eq. 1.5) can become more difficult since the constants *C* and *m* may depend on *R* and the rate data must be known for the whole range of loading ratios used.

Finally, it is noted that standards for fatigue testing suggest that they be run using constant amplitude (constant load levels) [31]. This method is most efficient experimentally and in simulations. However with ΔK increasing, not as much crack growth can be obtained before large plasticity occurs at the crack tip or stable tearing initiates. As discussed earlier, the method of load shedding selected in this study was chosen to obtain the maximum amount of crack extension under nominally elastic conditions.

CHAPTER 5

CONCLUSIONS

Fatigue crack growth experiments have been performed successfully on an edge-cracked Arcan specimen manufactured from 2024-T351 aluminum and subjected to far-field mixed mode I/II loading with loading angles Φ = 15°, 30°, 45°, and 60°. Experimental results from these experiments included (a) crack paths, (b) crack extension vs. fatigue cycles and (c) the minimum and maximum loads applied during each cycle. Results show that (a) the two degree of freedom slide apparatus developed especially for these experiments is an effective and efficient method of determining experimental crack paths, eliminating the cumbersome post-processing requirements for digitizing and scaling images of the specimen after crack extension had occurred, (b) crack extension occurs along different curvilinear paths for each loading angle, extending from the original crack tip towards the upper Arcan grip, (c) initial kinking angle of the fatigue crack indicates that the local Mode I direction deviates the direction perpendicular to the loading angle as the Mode II component of loading increases, (d) the load shedding process used to maintain crack growth rates in a specific range that was used for Φ = 30°, 45°, and 60° is consistent with controlling ΔK_{eq}, as shown through direct comparison of experimental crack growth rates and predicted ΔK_{eq} values at points along the measured crack paths, and (e) further study is required for loading angles Φ = 75° and 90° where fatigue crack growth was not observed experimentally.

Simulations of the fatigue crack growth process for the Arcan fixture-specimen combination have been performed using a custom-finite element code for fracture analysis, CRACK3D. In this code, VCCT is used to quantify the local stress intensity factors and the MCSC is used to determine the direction of current crack extension. Results from the simulations show that (a) CRACK3D is an effective simulation platform for fatigue crack growth in many cases, (b) the re-meshing algorithms in CRACK3D are not readily adaptable for crack growth near material junctures where there are significant differences in element size; the ability to handle such cases is currently being developed, but not yet available, (c) direct comparison of the experimental results and predictions indicate that the measured and CRACK3D predicted crack paths using local re-meshing to maintain accuracy in the local fields are in excellent agreement over the range of crack growth where the simulations were convergent, (d) predictions using an idealized notch and pre-crack yield little error between the predicted and experimental crack paths, and(e) indicate that the direction of crack propagation corresponds to the direction which maximizes Mode I and minimized Mode II, which is consistent with results from previous studies [1] [2]

CHAPTER 6

Recommendations for Future Work

It is recommended that for the current study, a life prediction be completed using the predicted values of ΔK_{eq} and Paris' Law (Eq 1.5) to compare predicted *da/dN* to the experimental crack growth rate ($\Delta a/\Delta N$). Currently the rate data for R = 0.4 is not available, and the Paris' Law constants for R = 0.4 are unknown for Al-2024-T351. The data may be available through the last version of AFGROW [1] available to the public [2], though this has not yet been verified.

While the current study only compared the predicted crack path to the experimental crack path, it is recommended that further experiments be conducted to obtain the experimental values of ΔK_I and ΔK_{II} for comparison. It has been shown that DIC is an accurate method of obtaining SIFs around the crack tip [3] [4]. Currently, a script in MATLAB [5] has been created to use the displacement field around the crack tip, accounting for rigid body translation and rotation, in William's solution [6] to iteratively solve for values of K_I and K_{II} until the solution has reached convergence using a Levenberg-Marquardt least squares [7] to solve the over-determined system of non-linear equations. To implement this experimentally, it is suggested that for various crack lengths, the specimen be statically loaded to zero, maximum, and minimum force with images of the crack tip being obtained at each load level. Then DIC can be conducted for the maximum and minimum loads with the image at zero force being the reference image. From those displacement fields corresponding to the maximum and minimum loads and the method of determining the SIFs discussed above, ΔK_I and ΔK_{II} can then be determined using Eq 1.2.

It has been suggested that further experiments be conducted to experimentally determine SIFs, and as discussed in the Chapter 4, the current method of load prediction is not efficient while performing the experiment or for the simulation post-processing. Since the crack paths have now been determined, it is recommended that for this second set of experiments FEA be used to predict the loads for the experiment. It would be optimal to keep constant amplitude for as long a crack path as possible before having to perform load shedding to keep the number of load shedding steps at a minimum.

The current work did not provide sufficient information for $\Phi = 75°$ and 90°, and further work is necessary to understand fatigue crack propagation when Mode II is dominant. It is recommended that a finite element model of the fixture and specimen with the fatigue pre-crack should be built. The stress fields at the crack tip should be evaluated. To perform experiments at these loading angles, it may be necessary to grow the fatigue pre-crack further, into a region of higher stress or to keep the pre-crack in the same location but apply higher loads.

If previous studies show that fatigue cracks always propagate in Mode I, it may be because the local Mode I direction is the only direction providing enough opening without friction of the surfaces caused by the shear and cyclic loading. Stable tearing cracks propagate in the Mode II direction for $\Phi = 75°$ and 90°, but for that case, there is no cyclic loading and the loads are increased to overcome the friction between the surfaces. It is recommended that a tensile bar should be used to apply a constant K_I to the Arcan specimen while cyclic loading is applied at either $\Phi = 75°$ and 90°, as shown in Figure 6.1. That tension may provide enough opening of the crack tip to allow the fatigue crack to propagate in the Mode II direction . The tension bar should be manufactured carefully such that it does not interfere with the ability to visibly track the crack growth. It should also not apply a moment to the specimen if possible, and the tensile load applied should be able to be held constant and be able to be adjusted. The load should also be recorded, and it is suggested that a strain gage to be used to do so.

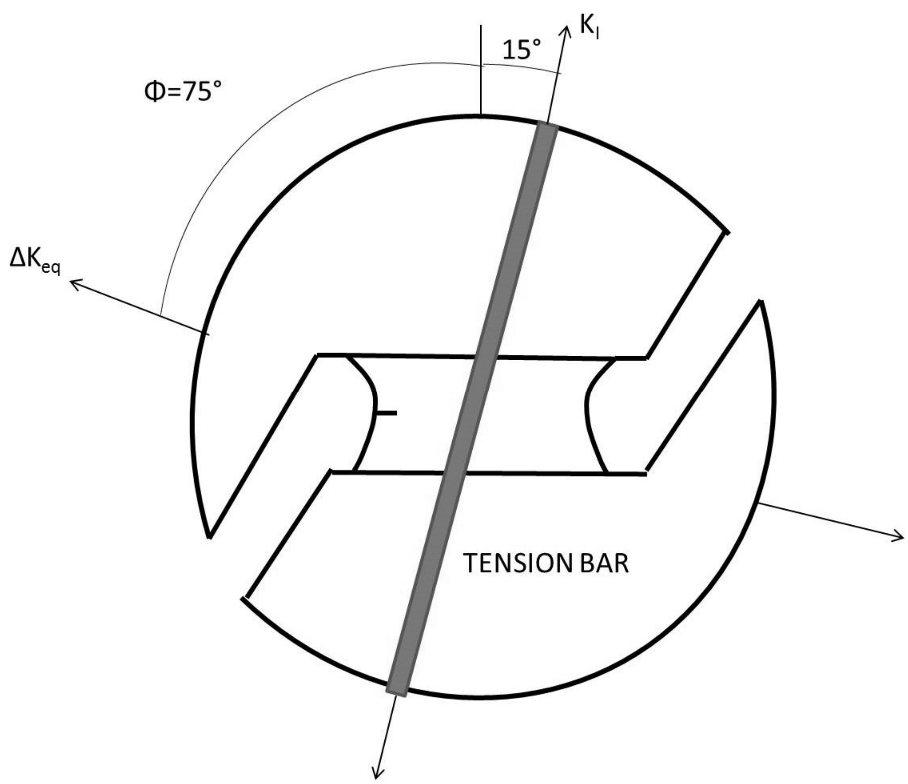

Figure 6.1. Schematic of Arcan fixture with proposed tension bar for $\Phi = 75°$.

REFERENCES

[1] National Transportation Safety Board, "Aloha Airlines, Flight 243, Boeing 737-200, N73711," 1988.

[2] R. Witkin, "Cracks are Found on Aging Jetliner," *The New York Times,* 18 October 1988.

[3] Federal Aviation Administration, "FAA to order Inspections for Fatigue Crack on Boeing 737's," 1998.

[4] "Southwest Checks Fleet after Hole forces Landing: Hole in fuselage causes pressure-loss scare on Boeing 737," *Associated Press,* 14 July 2009.

[5] L. Stark, M. Hosford and M. S. James, "Southwest Air Emergency: Inspection Program Missed Crack in Plane," 3 April 2011. [Online]. Available: http://abcnews.go.com/US/southwest-air-emergency-inspection-program-missed-cracks-plane/story?id=13286094#.UbtcfpXD_IU. [Accessed June 2013].

[6] S. Trimble, "Fatigue Cracks Raise Questions about Key Decision in F-35 Redesign," *Flight,* November 2010.

[7] H. L. Ewalds and R. J. Wanhill, Fracture Mechanics, London: Edward Arnold Ltd, 1984.

[8] F. Erdogan and G. C. Sih, "On the crack extension in plates under plane loading and transverse shear," *Journal of Basic Engineering,* no. 85D, pp. 519-527, 1963.

[9] P. Paris and F. Erdogan, "A critical analysis of crack propagation laws," *Journal of Basic Engineering,* pp. 528-534, 1963.

[10] R. Zhang and L. He, "Measurement of mixed-mode stress intensity factors using digital image correlation," *Optics and Lasers in Engineering,* pp. 1001-1007, 2012.

[11] P. Lopez-Crespo, A. Sherenlikht, E. A. Patterson, J. R. Yates and P. J. Withers, "The stress intensity of mixed mode cracks determined by digital image correlation," *Journal of Strain Analysis,* pp. 769-780, 2008.

[12] Y. Murakami, Stress Intensity Factors Handbook, vol. 1, Oxford: Pergamon Press, 1987.

[13] S. A. Fawaz, "Personal Conversation," 2009.

[14] J. ,. S. G. D. M. H. J.M Greer, "Some comments on the Arcan mixed-mode (I/II) test specimen," *Engineering Fracture Mechanics,* pp. 2088-2094, 2011.

[15] S. Liu, Y. J. Chao and R. R. Gaddam, "Fracture Type Transition under Mixed Mode I/II Quasi-static and Fatigue Loading Conditions," in *Society for Experimental Mechanics*, 2004.

[16] B. E. Amstutz, M. A. Sutton and D. S. Dawicke, "Experimental Study of Mixed Mode I/II Stable Crack Growth in Thin 2024-T3 Aluminum," *Fatigue and Fracture, ASTM STP 1256,* vol. 26, pp. 256-273, 1995.

[17] B. E. Amstutz, M. A. Sutton, D. S. Dawicke and M. L. Boone, "Effects of Mixed Mode I/II Loading and Grain Orientation on Crack Initiation and Stable Tearing in 2024-T3 Aluminum," *ASTM STP 1296,* vol. 27, pp. 105-125, 1997.

[18] S. Boljanovic and S. Maksimovic, "Analysis of the crack growth propagation process under mixed-mode loading," *Engineering Fracture Mechanics,* no. 78, pp. 1565-1576, 2011.

[19] "MSC Software," [Online]. Available: www.mscsoftware.com/product/msc-nastran.

[20] "ASTM International," [Online]. Available: http://www.astm.org/Standards/E399.htm.

[21] D. D. S. Dawicke, Interviewee, *Personal communication, NASA Langley Research Center.* [Interview]. 2011.

[22] H. Tada, P. C. Paris and G. R. Irwin, The Stress Analysis of Cracks Handbook, 3rd ed.

[23] Richard, Buchholz, Kullmer and Schollmann, "2D- and 3D-mixed mode fracutre criteria," *Key Engineering Materials,* pp. 251-260, 2003.

[24] "GetData Graph Digitizer," [Online]. Available: http://www.getdata-graph-digitizer.com/.

[25] V. Lindberg, "Uncertainties and Error Propagation Part I of a manual on Uncertainties, Graphing, and the Vernier Caliper," 1 July 2000. [Online]. Available: www.rit.edu/~w~uphysi/uncertainties/Uncertaintiespart2.html#muldiv. [Accessed July 2013].

[26] X. Deng, X. Ke, M. A. Sutton, E. E. Miller and H. W. Schreier, "3D VCCT wiht locally structured re-meshing for evaluation mixed-mode stress intensity factors in crack grwoth simulations along curved crack paths," in *presentation at the Society of Engineering Science 49th Annual Technical Meeting*, Georgia Tech, GA, USA, Oct 10-12,2012.

[27] X. Deng, X. Ke, M. A. Sutton, E. E. Miller and H. W. Schreier, "Locally structured re-meshing to enable accurate determination of stress intensity factors using 3D VCCT for crack growth simulations with curved crack paths," in *presentation at the International Symposium on Solid Mechanics in Honor of Professor Xing Zhang*, Beijing University of Aeronautics and Astronautics, China, Nov.3,2012.

[28] X. Den, X. Ke, M. A. Sutton, E. E. Miller and H. W. Schreier, "FEM for 3D SIF determination for fatigue crack growth simulations iwth curved crack fronts and paths," in *to be presented at the ASME 2013 International Mechanical Engineering Congress & Exposition*, San Diego, CA, USA, Nov. 15-21,2013.

[29] H. Okada, H. Kawai and K. Araki, "A virtual crack closure-integral method (VCCM) to compute the energy release rates and stress intensity factors based on quadratic tetrahedral finite elements," *Engineering Fracture Mechanics,* pp. 4466-4485, 2008.

[30] "ANSYS," [Online]. Available: www.ansys.com/products.

[31] "ASTM E468 - 11 Standar Practice for Presentation of Constant Amplitude Fatigue Test Results for Metallic Materials," [Online]. Available: www.astm.org/Standards/E468.htm.

[32] "AFGROW," [Online]. Available: www.afgrow.net.

[33] U. S. A. F. Rob Reuter, Interviewee, *Personal Conversation.* [Interview].

[34] "MATLAB," [Online]. Available: www.mathworks.com/products/matlab/.

[35] G. R. Irwin, "Analysis of stresses and strains near the end of a crack traveling a plate.," *Transaction of ASME, Journal of Applied Mechanics,* vol. 24, pp. 361-364, 1957.

[36] K. Levenberg, "A method for the solution of certain non-linear problems in least squares," *Quarterly of Applied Mathematics,* vol. 2, 164-168.

APPENDIX A – EXPERIMENTAL DATA RECORDED

Table A.1. Experimental data recorded data for Φ = 15°.

Cycles(N)	X-position of crack tip [m]	Maximum Load (Pmax) [N]	Minimum Load (Pmin) [N]
Pre-cracking			
50,000	0.0067	48308	7962
100,000	0.0073		
130,000	0.0081	45630	7558
150,000	0.0092	43392	7166
170,000	0.0100	38277	6592
177,000	0.0105	36867	6183
187,000	0.0110		
197,000	0.0115	35532	5907
202,000	0.0116	34153	5725
212,000	0.0121		
217,000	0.0123	32650	5542
221,000	0.0124		
225,400	0.0126		
225,400	0.0126		
Marking Crack Front			
231,000	0.0127	28384	14203
240,000	0.0127		
260,000	0.0128		
275,000	0.0129		
290,000	0.0129		
Test			
290,000	0.0124		
300,000	0.0127	31756	5396
315,000	0.0132		
330,000	0.0137		
345,000	0.0143		
360,000	0.0149		
375,000	0.0157		
390,000	0.0165		

405,000	0.0173		
420,000	0.0183		
430,000	0.0190		
440,000	0.0198		
450,000	0.0206		
460,000	0.0215		
470,000	0.0225		
480,000	0.0236		
487,500	0.0243		
495,000	0.0254		
500,000	0.0260		
505,000	0.0267		
510,000	0.0274		
515,000	0.0282		
520,000	0.0290		
525,000	0.0299		
530,000	0.0308		
535,000	0.0318		
540,000	0.0329		
545,000	0.0340		
550,000	0.0351		
555,000	0.0364		
560,000	0.0378		
565,000	0.0394		
570,000	0.0413		
573,000	0.0423		
576,000	0.0434		
579,000	0.0448		
582,000	0.0461		
585,000	0.0477		
588,000	0.0490		
591,000	0.0507		
594,000	0.0526		
597,000	0.0551		
598,000	0.0560		
598,300	0.0561	29109	4568
598,600	0.0562		
598,800	0.0563		
599,000	0.0566		
599,300	0.0567	27116	4528
599,600	0.0568		

599,900	0.0568		
600,200	0.0570		
600,400	0.0571		
600,600	0.0571		
600,800	0.0573		
601,000	0.0573	25261	4551
601,400	0.0574		
601,800	0.0575		
602,200	0.0577		
602,600	0.0578		
603,000	0.0578	23335	4551
603,600	0.0581		
604,200	0.0582		
604,800	0.0583		
605,400	0.0585		
606,000	0.0586	20982	4551
606,600	0.0586		
607,600	0.0588		
608,600	0.0590		
608,800	0.0590		
609,600	0.0591	19172	4546
610,800	0.0593		
612,000	0.0594		
613,800	0.0596		
615,600	0.0602		
617,400	0.0604	17433	4519
618,200	0.0604	15760	4515
620,600	0.0605		
623,000	0.0607		
623,400	0.0609		
630,000	0.0618	14234	4453
638,000	0.0620	12677	4453
640,000	0.0621		
662,000	0.0626	11468	4462
676,000	0.0628		
696,000	0.0630	9791	4444
726,000	0.0630		
761,000	0.0632		
781,000	0.0633		
801,000	0.0634		
821,000	0.0634	7580	6076

861,000	0.0634		
925,000	0.0634		
1,005,000	0.0634	8447	6761
1,030,000	0.0634	8447	5916
1,045,000	0.0634	19990	16005
1,057,000	0.0636	.	
1,067,000	0.0637		
1,081,000	0.0638		
1,093,000	0.0639	8332	4728
1,123,000	0.0640		
1,195,000	0.0640		
1,270,000	0.0640		
1,320,000	0.0640	9070	4453

Table A.2. Experimental data recorded data for Φ = 30°.

Cycles(N)	X- position of crack tip [m]	Maximum Load (Pmax) [N]	Minimum Load (Pmin) [N]
Pre-cracking			
50,000	0.0060	45012	4897
100,000	0.0063		
150,000	0.0095		
160,000	0.0098	36386	4813
170,000	0.0103		
175,000	0.0105	35279	4622
180,000	0.0107		
185,000	0.0109	34100	4599
190,000	0.0111		
197,000	0.0114		
202,000	0.0116	32948	4613
210,000	0.0119		
215,000	0.0122		
220,000	0.0124	31662	4546
225,000	0.0127		
Marking Crack Front			
240,000	0.0128	30768	15391
250,000	0.0129		
285,000	0.0130		
315,000	0.0131		
340,000	0.0133		
Testing			
345,000	0.0113	29945	4791
346,000	0.0115	51155	45416
348,000	0.0117		
350,000	0.0118	49108	19648
355,000	0.0121	47334	18949
360,000	0.0124		
365,000	0.0127		
370,000	0.0130	45461	18304
375,000	0.0132		
380,000	0.0134	43899	17691
385,000	0.0137		
387,000	0.0139		
390,000	0.0140	42765	17183

395,000	0.0142		
397,000	0.0144		
400,000	0.0145	41453	16610
405,000	0.0147		
410,000	0.0149		
416,000	0.0152		
422,000	0.0156		
428,000	0.0159		
434,000	0.0162		
440,000	0.0166		
445,000	0.0170		
450,000	0.0173	40087	16085
455,000	0.0176		
460,000	0.0179	38886	15578
465,000	0.0182		
470,000	0.0185		
475,000	0.0189	37561	15071
480,000	0.0192		
485,000	0.0195	36493	16859
490,000	0.0199		
495,000	0.0202	35501	14221
500,000	0.0205		
505,000	0.0207	34536	13852
510,000	0.0211		
515,000	0.0214		
520,000	0.0217	33642	13460
525,000	0.0218		
530,000	0.0221		
535,000	0.0224	32752	13118
540,000	0.0227		
545,000	0.0229	31876	12784
550,000	0.0232		
555,000	0.0236		
560,000	0.0238	31071	12464
565,000	0.0241		
570,000	0.0243	30301	12144
575,000	0.0246		
580,000	0.0249		
585,000	0.0252	29545	11850

590,000	0.0254		
595,000	0.0257		
600,000	0.0260	28824	11561
605,000	0.0262		
610,000	0.0265	28104	11298
615,000	0.0267		
620,000	0.0270		
625,000	0.0272	27437	11032
630,000	0.0274		
635,000	0.0277		
640,000	0.0279	26778	10760
645,000	0.0282		
650,000	0.0285		
655,000	0.0287	26133	10533
660,000	0.0289		
665,000	0.0291		
667,000	0.0293	25515	10315
672,000	0.0295		
677,000	0.0296		
682,000	0.0299		
685,000	0.0300		
695,000	0.0304	24923	10080
705,000	0.0309		
715,000	0.0312	24341	9835
725,000	0.0317		
735,000	0.0320	23789	9626
740,000	0.0322		
750,000	0.0326	23229	9399
755,000	0.0328		
765,000	0.0332	22708	9199
770,000	0.0333		
775,000	0.0335		
780,000	0.0337		
785,000	0.0339	22210	8981
795,000	0.0342		
802,500	0.0345		
807,500	0.0347	21712	8790
812,500	0.0348		
817,500	0.0350		

827,500	0.0354		
832,500	0.0355	21205	8585
837,500	0.0357		
842,500	0.0359		
847,500	0.0360	20782	8363
852,500	0.0362		
857,500	0.0364		
862,500	0.0365		
867,500	0.0367		
872,500	0.0369	20346	8162
877,500	0.0370		
882,500	0.0372		
887,500	0.0374		
892,500	0.0374	19924	7962
897,500	0.0377		
902,500	0.0378		
908,500	0.0369		
914,500	0.0382	19439	7802
920,500	0.0383		
926,500	0.0385		
932,500	0.0387		
938,500	0.0389	19021	7651
944,500	0.0391		
950,500	0.0392		
956,500	0.0394		
962,500	0.0396	18598	7464
968,500	0.0397		
974,500	0.0399		
980,500	0.0401		
986,500	0.0402		
995,500	0.0404	18207	7313
1,005,500	0.0407		
1,015,500	0.0410		
1,025,500	0.0412	17811	7144
1,035,500	0.0414		
1,055,500	0.0419		
1,075,500	0.0423	17415	6984
1,095,500	0.0427		
1,115,500	0.0432	17050	6828

1,135,500	0.0436	16676	6681
1,155,500	0.0440		
1,185,500	0.0446	16307	6543
1,215,500	0.0452		
1,230,500	0.0475		
	0.0000		
1,245,500	0.0457		
1,260,000	0.0460		
1,275,000	0.0462		
1,290,000	0.0465		
1,305,000	0.0468		
1,320,000	0.0471		
1,335,000	0.0474		
1,350,000	0.0478		
1,365,000	0.0483		
1,380,000	0.0487		
1,395,000	0.0491		
1,410,000	0.0496		
1,425,000	0.0501		
1,440,000	0.0507		
1,455,000	0.0513		
1,470,000	0.0519		
1,495,000	0.0530		
1,510,000	0.0536		
1,530,000	0.0546		
1,540,000	0.0552		
1,550,000	0.0558		
1,560,000	0.0565		
1,564,000	0.0567		
1,574,000	0.0574		
1,584,000	0.0581		
1,594,000	0.0589		
1,604,000	0.0595		
1,614,000	0.0603		
1,624,000	0.0610	14973	5978
1,629,000	0.0613	14572	5907
1,634,000	0.0616		
1,639,000	0.0620		
1,644,000	0.0624		

1,654,000	0.0630	14265	5769
1,659,000	0.0634		
1,669,000	0.0640	13959	5627
1,679,000	0.0647		
1,684,000	0.0649	13727	5480
1,689,000	0.0653		
1,694,000	0.0656	13425	5342
1,699,000	0.0660		
1,704,000	0.0663	13118	5236
1,709,000	0.0665		
1,714,000	0.0669		
1,719,000	0.0672		
1,724,000	0.0676		
1,729,000	0.0678	12838	5120
1,734,000	0.0682		
1,739,000	0.0686		
1,744,000	0.0690	12544	5004
1,749,000	0.0693	12277	4915
1,754,000	0.0696		
1,759,000	0.0699	12010	4804
1,764,000	0.0702		
1,769,000	0.0704		
1,774,000	0.0708		
1,779,000	0.0711		
1,784,000	0.0714	11752	4706
1,789,000	0.0717		
1,794,000	0.0720		
1,799,000	0.0724		
1,804,000	0.0727	11499	4599
1,809,000	0.0730		
1,814,000	0.0733		
1,819,000	0.0736		
1,824,000	0.0740		
1,829,000	0.0744	11223	4506
1,834,000	0.0747	10983	4390
1,839,000	0.0750		
1,844,000	0.0753	10787	4297
1,854,000	0.0760		
1,859,000	0.0764		

1,864,000	0.0767	10556	4186
1,869,000	0.0770		
1,874,000	0.0773		
1,879,000	0.0776		
1,884,000	0.0780		
1,889,000	0.0785	10289	4110
1,894,000	0.0790	10066	4026
1,899,000	0.0792	9622	3852
1,904,000	0.0796		
1,909,000	0.0799	9408	3763
1,914,000	0.0802		
1,919,000	0.0806		
1,924,000	0.0809	9194	3679
1,929,000	0.0812	8994	3603
1,934,000	0.0815		
1,939,000	0.0819	8785	3510
1,944,000	0.0821		
1,949,000	0.0825		
1,954,000	0.0829		
1,959,000	0.0832	8585	3438
1,964,000	0.0836		
1,969,000	0.0839	8385	3363
1,974,000	0.0842		
1,979,000	0.0845	8198	3292
1,984,000	0.0848		
1,989,000	0.0852		
1,994,000	0.0856	8016	3216
1,999,000	0.0859		
2,004,000	0.0862		
2,009,000	0.0866		
2,014,000	0.0870	7642	3003
2,019,000	0.0872	7464	2936
2,024,000	0.0876		
2,029,000	0.0879	7295	2874
2,034,000	0.0882		
2,039,000	0.0885		
2,044,000	0.0888		
2,049,000	0.0893		
2,054,000	0.0896	7122	2874

2,059,000	0.0899		
2,064,000	0.0903	6966	2811
2,069,000	0.0907		
2,074,000	0.0910	6806	2749
2,079,000	0.0914	6637	2682
2,084,000	0.0917		
2,089,000	0.0920	6486	2620
2,094,000	0.0924		
2,099,000	0.0928	6352	2549
2,104,000	0.0931	6205	2487
2,109,000	0.0935		
2,114,000	0.0937	6058	2433
2,119,000	0.0940		
2,124,000	0.0943		
2,129,000	0.0945		
2,134,000	0.0949		
2,139,000	0.0953	5907	2220
2,144,000	0.0957		
2,149,000	0.0960	5765	2313
2,154,000	0.0964		
2,159,000	0.0968	5765	2313
2,164,000	0.0971	5636	2260
2,169,000	0.0974		
2,174,000	0.0978	5494	2060
2,179,000	0.0982	5356	1993
2,184,000	0.0985	5231	2100
2,189,000	0.0988		
2,194,000	0.0991	5098	2046
2,199,000	0.0995		
2,204,000	0.0998	4982	1828
2,209,000	0.1001		
2,214,000	0.1003	4849	1953
2,219,000	0.1007		
2,224,000	0.1011	4728	1899
2,229,000	0.1014	4613	1855
2,234,000	0.1017		
2,239,000	0.1019		
2,244,000	0.1023	4515	1646
2,249,000	0.1027	4390	1761

2,254,000	0.1030	4284	1721
2,259,000	0.1034	4177	1486
2,264,000	0.1036		
2,274,000	0.1041		
2,284,000	0.1045		
2,294,000	0.1052		
2,299,000	0.1055	4075	1624
2,304,000	0.1058		

Table A.3. Experimental data recorded data for Φ = 45°.

Cycles(N)	X-Position of Crack Tip [m]	Maximum Load (Pmax) [N]	Minimum Load (Pmin) [N]
Pre-cracking			
25,000	0.0064	68356	26961
40,000	0.0073		
55,000	0.0082	61025	24278
70,000	0.0092	57871	23353
80,000	0.0097	55469	22157
90,000	0.0103	53005	21280
100,000	0.0108	51528	20440
110,000	0.0113		
120,000	0.0116	47124	18981
130,000	0.0121		
140,000	0.0125	45372	18264
Marking Crack Front			
145,000	0.0094	43851	26338
150,000	0.0094	47787	28722
160,000	0.0095		
170,000	0.0096		
185,000	0.0098		
Testing			
195,000	0.0094	42458	17081
200,000	0.0094	47089	18273
205,000	0.0095		
210,000	0.0096	48930	19661
215,000	0.0098		
220,000	0.0099		
225,000	0.0100		
235,000	0.0103		
245,000	0.0107		
255,000	0.0113		
260,000	0.0115		
265,000	0.0118		
275,000	0.0124		
285,000	0.0131		
290,000	0.0135		
295,000	0.0139	47823	18949
300,000	0.0141	46511	18313

305,000	0.0146		
310,000	0.0149	44927	17691
315,000	0.0152		
320,000	0.0156	43014	17148
325,000	0.0159	41497	16605
330,000	0.0162		
335,000	0.0165		
340,000	0.0168	40163	16107
345,000	0.0171		
350,000	0.0173		
355,000	0.0177	38700	15622
360,000	0.0182		
365,000	0.0184	37441	15168
370,000	0.0187		
375,000	0.0191		
380,000	0.0194	36391	14750
385,000	0.0197		
390,000	0.0200		
395,000	0.0203	35363	14337
400,000	0.0206		
405,000	0.0209		
410,000	0.0213		
415,000	0.0216	34429	13950
420,000	0.0219		
425,000	0.0222		
430,000	0.0225	33504	13598
435,000	0.0228		
440,000	0.0231		
445,000	0.0235		
450,000	0.0238	32708	13269
455,000	0.0240		
460,000	0.0244		
465,000	0.0247	31778	12882
470,000	0.0250		
475,000	0.0254		
480,000	0.0258	30986	12557
485,000	0.0261		
490,000	0.0265		
495,000	0.0267	30190	12242

500,000	0.0271		
505,000	0.0270	29461	11943
510,000	0.0277		
515,000	0.0280		
520,000	0.0283	28740	11650
525,000	0.0286		
530,000	0.0289		
535,000	0.0293		
540,000	0.0296		
545,000	0.0300		
550,000	0.0303	28042	11370
555,000	0.0306		
560,000	0.0310		
565,000	0.0313	27361	11107
570,000	0.0316		
575,000	0.0319	26694	10823
580,000	0.0323		
585,000	0.0325		
590,000	0.0328		
595,000	0.0332		
600,000	0.0335	26089	10578
605,000	0.0338		
610,000	0.0341		
615,000	0.0344		
620,000	0.0348		
625,000	0.0351		
630,000	0.0354	25484	10324
635,000	0.0358		
640,000	0.0361	24892	10080
645,000	0.0364		
650,000	0.0367		
655,000	0.0371		
660,000	0.0374	24318	9857
665,000	0.0437		
670,000	0.0380		
675,000	0.0384		
680,000	0.0388	23856	9626
685,000	0.0391		
690,000	0.0395		

695,000	0.0398		
700,000	0.0401	23220	9399
705,000	0.0405		
710,000	0.0409		
715,000	0.0411	22708	9190
720,000	0.0415		
725,000	0.0418		
730,000	0.0421	22192	8990
735,000	0.0424		
740,000	0.0428		
745,000	0.0431	21205	6361
750,000	0.0434		
755,000	0.0437		
760,000	0.0440		
765,000	0.0442		
770,000	0.0446		
775,000	0.0449		
780,000	0.0452		
785,000	0.0456		
790,000	0.0459	20742	8394
795,000	0.0462	20275	8207
800,000	0.0464		
805,000	0.0468		
810,000	0.0471	19505	7847
815,000	0.0473	18972	7678
820,000	0.0475	18554	7504
825,000	0.0478		
830,000	0.0482		
835,000	0.0482	18162	7344
840,000	0.0484	17762	7188
850,000	0.0487	17379	7037
860,000	0.0491		
870,000	0.0494		
880,000	0.0498		
890,000	0.0502		
900,000	0.0506		
910,000	0.0511		
920,000	0.0514	16997	6877
930,000	0.0518		

940,000	0.0522		
950,000	0.0527	16997	6739
960,000	0.0601		
970,000	0.0534	16267	7473
980,000	0.0538		
990,000	0.0542	15929	6445
1,000,000	0.0547		
1,010,000	0.0551	15920	6285
1,020,000	0.0554	15244	6170
1,030,000	0.0557		
1,040,000	0.0561		
1,050,000	0.0564	14910	6023
1,060,000	0.0568		
1,070,000	0.0571	14586	6170
1,080,000	0.0573		
1,090,000	0.0577		
1,100,000	0.0580	14265	5769
1,110,000	0.0583		
1,120,000	0.0586		
1,130,000	0.0590		
1,140,000	0.0593	13959	5640
1,150,000	0.0596		
1,160,000	0.0599		
1,170,000	0.0603		
1,180,000	0.0606		
1,190,000	0.0610		
1,200,000	0.0613	13660	5525
1,210,000	0.0617		
1,220,000	0.0621		

Table A.4. Experimental data recorded data for Φ = 60°.

Cycles(N)	X-Position of Crack Tip [m]	Y-Position of Crack Tip [m]	Maximum Load (Pmax) [N]	Minimum Load (Pmin) [N]
Pre-cracking				
30,000	0.0072	0.0006	67346	26769
45,000	0.0081	0.0006		
60,000	0.0090	0.0006	60451	24350
75,000	0.0097	0.0006	55798	23282
90,000	0.0104	0.0005		
105,000	0.0109	0.0005	50292	21182
120,000	0.0114	0.0006		
135,000	0.0119	0.0007	46177	19688
150,000	0.0124	0.0007	46270	19221
165,000	0.0129	0.0007		
Marking Crack Front				
175,000	0.0131	0.0006	54646	33984
185,000	0.0133	0.0007		
240,000	0.0133	0.0007	42859	11908
Testing				
240,000	0.0070	0.0113		
250,000	0.0071	0.0113	43370	18789
260,000	0.0071	0.0113	47565	19763
270,000	0.0071	0.0114	51292	21182
280,000	0.0071	0.0114		
290,000	0.0071	0.0114	53739	20377
300,000	0.0071	0.0116	61817	20156
330,000	0.0076	0.0115		
350,000	0.0081	0.0115		
360,000	0.0084	0.0116		
385,000	0.0093	0.0120		
410,000	0.0115	0.0123		
435,000	0.0140	0.0129	55149	22188
460,000	0.0168	0.0135	50999	20426
485,000	0.0189	0.0141		
510,000	0.0211	0.0148	41609	16605
535,000	0.0234	0.0155	39415	15625
560,000	0.0257	0.0162	36617	14759
585,000	0.0274	0.0167	32630	13225

610,000	0.0291	0.0173	30977	12562
635,000	0.0306	0.0179	29469	11943
660,000	0.0318	0.0183	26716	10814
685,000	0.0324	0.0186	23224	9399
705,000	0.0329	0.0187		
725,000	0.0333	0.0189		
745,000	0.0338	0.0191		
765,000	0.0343	0.0193		
785,000	0.0349	0.0195		
805,000	0.0356	0.0198		
825,000	0.0361	0.0200		
845,000	0.0368	0.0203		
865,000	0.0376	0.0206		
885,000	0.0385	0.0210		
905,000	0.0391	0.0212	22192	8990
930,000	0.0400	0.0217		
950,000	0.0408	0.0220		
970,000	0.0415	0.0223	21205	8585
990,000	0.0421	0.0227		
1,010,000	0.0429	0.0230		
1,030,000	0.0436	0.0234	20271	8661
1,050,000	0.0442	0.0237		
1,070,000	0.0450	0.0241		
1,090,000	0.0457	0.0243	19403	7856
1,110,000	0.0462	0.0247		
1,130,000	0.0468	0.0249		
1,150,000	0.0472	0.0252	18585	7486
1,170,000	0.0479	0.0255		
1,190,000	0.0486	0.0259		
1,210,000	0.0492	0.0263	17771	7188
1,230,000	0.0500	0.0268		
1,250,000	0.0504	0.0270	17001	7313
1,270,000	0.0510	0.0274		
1,290,000	0.0516	0.0278		
1,310,000	0.0523	0.0282		
1,330,000	0.0531	0.0283	16276	6868
1,350,000	0.0535	0.0291		
1,370,000	0.0543	0.0296		
1,390,000	0.0548	0.0299	15578	6592

1,410,000	0.0555	0.0303		
1,440,000	0.0562	0.0308	14906	5863
1,460,000	0.0565	0.0311	14270	5760
1,480,000	0.0568	0.0313		
1,500,000	0.0572	0.0315		
1,520,000	0.0576	0.0318		
1,540,000	0.0580	0.0321		
1,560,000	0.0583	0.0324		
1,580,000	0.0587	0.0327		
1,600,000	0.0592	0.0330		
1,620,000	0.0597	0.0334		
1,640,000	0.0602	0.0339		
1,660,000	0.0609	0.0343		

Table A.5. Experimental data recorded data for Φ = 90°.

Cycles(N)	X-Position of Crack Tip [m]	Y-Position of Crack Tip [m]	Maximum Load (Pmax) [N]	Minimum Load (Pmin) [N]
Pre-cracking				
0	0.0065	0.0000	67128	26961
5,000	0.0065	0.0000		
15,000	0.0066	0.0002		
25,000	0.0071	0.0003		
35,000	0.0078	0.0002		
45,000	0.0082	0.0001	60207	24341
55,000	0.0088	0.0001		
65,000	0.0092	0.0001	54855	22148
75,000	0.0095	0.0000		
85,000	0.0101	0.0000		
95,000	0.0104	0.0001	50470	20453
105,000	0.0109	0.0001		
120,000	0.0116	0.0001	46849	18972
130,000	0.0110	0.0001		
140,000	0.0124	0.0001		
150,000	0.0128	0.0001		
Testing				
150,000	0.00024	0.01259	44206.4	17677.2
155,000	0.00024	0.01262		
165,000	0.00024	0.01262		
175,000	0.00024	0.01262		
185,000	0.00024	0.01273		
195,000	0.00024	0.01273		
205,000	0.00024	0.01273		
225,000	0.00024	0.01273		
235,000	0.00024	0.01273		

APPENDIX B –DETAILS AND TIPS FOR CRACK3D INPUT FILES GENERATION

First, the geometry has to be created to accommodate the crack and the three zones in the mesh, and steps for building the geometry will now be discussed. The volume for the top fixture was created by creating keypoints at the position where the end of each of the two diagonal lines and the straight line segment for the bottom edge of the fixture are located. Then keypoints were created at a radius of 0.14 m and in approximately 7° intervals being sure that keypoints were positioned at the same location where the center of the pin holes are on the fixture. A spline through the keypoints was used to create the arc of the top edge of the fixture. The front area was created by selecting the lines. The volume was created by extruding the area along the normal direction in an amount equivalent to the thickness of the grip. To create the bottom fixture, the top fixture volume was then reflected about the x-axis then again about the y-axis. The volume, areas, lines, and keypoints remaining from the first reflection was deleted. Material properties for the fixture were assigned to the two volumes.

The initial geometry was created using multiple volumes in order to create a crack and volumes for the three zones of the mesh: a locally structured finer mesh immediately around the crack front to facilitate 3D VCCT, a far-field coarser mesh away from the crack front region, and a graded mesh in a transitional zone between the far-field coarser mesh and the locally structured finer mesh, as shown in Figure B.1. Specifically, volumes 1, 2, 3, and 4 are for the locally structured mesh, volumes 5, 6, 7, and 8 are for the transitional zone with a graded mesh, and volumes 9, 10, 11, and 12 are for the far-field mesh. The crack is created in ANSYS by creating the bottom surfaces (seen as lines in the 2D view in Fig. B.1) of volumes 5 and 1 in the same position as the top surfaces (seen as lines in Fig. B.1) of volumes 8 and 4. The lines do not share the same end point at the edge of the specimen however they share the same keypoints at the crack front (i.e. the coincident vertices and edge of volumes 1, 2, 3, and 4 share the same keypoints and line).

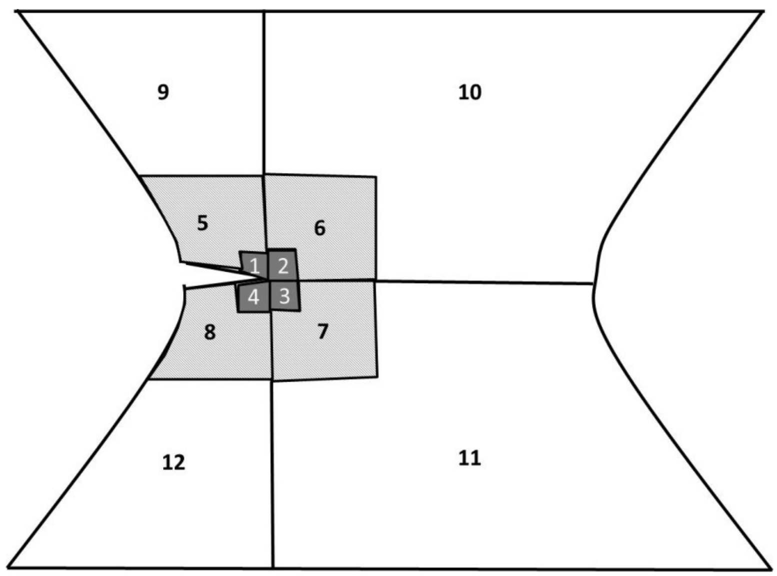

Figure B.1. A 2D schematic diagram of volumes in the specimen region used to create the initial finite element mesh.

The volumes were created in the same way the fixture volumes were created: by creating keypoints, then lines, areas, and extruding the areas along the normal to create volumes. Material properties were assigned to all the volumes of the specimen geometry. To create connectivity, all the volumes for the fixture and specimen were glued together with the exceptions of volumes attached to the areas which are the top and bottom crack surfaces: volume 5 was not glued to 8 and volume 1 was not glued to 4.

Secondly, A structured mesh was created in volumes 1, 2, 3, and 4 by first meshing the surface areas with mapped triangular element. Size division for the elements was set such that each edge of the volume was one element length so that the minimum element size is one half of the thickness. The volume was then freely meshed using 10 noded tetrahedral elements, and the area elements were deleted. The element and node numbers were compressed. Then the size division for each of the remaining lines for the remaining volumes of the specimen was set to be maximum element size. The remaining volumes for the specimen and fixture were freely meshed using 10 noded tetrahedral elements.

Thirdly, The CRACK3D.GEO file was created. The CRACK3D.GEO file defines the surface boundary of the geometry by listing nodes attached to areas and lines on the outside of the geometry. That is, areas or lines, contained within the geometry do not need to be included. In defining surface areas for CRACK3D, surface areas may be comprised of multiple areas in ANSYS. In defining surface lines, lines may also be comprised of multiple lines, however, lines can old boarder two surface areas. Take for example, in Figure B.1, all areas 1, 2, 3, 4, 5, 6, 7, 8, 9, 10, 11, and 12 are considered one area, and boundary lines do not include the lines such as the line separating areas 4 from 6. It is also only necessary to include the boundaries in which the crack propagation is contained. Since the crack will not grow into the fixture, only specimen boundaries were included in the .GEO file. In listing the lines, the nodes must be listed along boundary lines in order along the line, and in listing the elements on the boundary surfaces, this file requires that area normals in ANSYS be pointing away from the geometry listing the nodes attached to the elements on the boundary surfaces in a counter clockwise manner. The area normals were plotted, and it was verified that for each surface area of the specimen and fixture, the area normal was pointing outwards. If a normal was not pointing outwards, the area normal was reversed.

Fourthly, for the re-meshing parameters in the CRACK3D.DAT file, based on benchmark studies, it is sufficient to have a minimum structured element size of one half of the specimen thickness. It is suggested that the local re-meshing zone be 6 to 10 times larger than the minimum element size. The maximum element size may be coarse but sufficient for transferring the load data to the crack front and equivalent to the element size in the far field mesh. It is also suggested that the far field mesh be uniform so that during crack extension the maximum element size in the re-meshing zone is constant and consistent with far field mesh elements. In CRACK3D the amount of crack extension (crack increment) at a crack growth step is chosen by the user as an input.

Appendix C – Files Associated with CRACK3D for $\Phi = 45°$

This appendix contains the input and output files for CRACK3D for the 45° loading case simulation. However CRACK3D.MSH is not included since that file was generated via ANSYS and MESH3D software while CRACK.GEO and CRACK.DAT are included since those files are user generated according to the CRACK3D user manual. The only output files reported where those used for post-processing: CRACK3D.SIF and CRACK3D.CXT.

CRACK3D.DAT

```
Arcan 4 elem through thickness

3 1 0 2 1 -100
1 1 2 2 1 1 10

1 361

1 1001
2 1001
1 7.11e10 0.33
2 2.07e11 0.30

2 6 45 1

0 1 1
0.5 1.8131e-24 -1 0 0 5.3366 0 1

5 2 -1 3 0 0.0520 -1 -1

0.0015 0.006 0.012 0.002

1       16649   16664   2
2       16780   16759   2
3       16781   16760   2
4       16782   16761   2
5       16783   16762   2
6       16784   16763   2
7       16785   16764   2
8       16786   16765   2
```

9	16612	16597	2

10	16650	16665	2
11	16770	16749	2
12	16787	16766	2
13	16772	16751	2
14	16788	16767	2
15	16774	16753	2
16	16789	16768	2
17	16776	16755	2
18	16611	16596	2

19	16647	16647	-1
20	16705	16705	-1
21	16704	16704	-1
22	16703	16703	-1
23	16702	16702	-1
24	16701	16701	-1
25	16700	16700	-1
26	16699	16699	-1
27	16595	16595	-1

28	16678	16678	-2
29	16791	16791	-2
30	16808	16808	-2
31	16793	16793	-2
32	16809	16809	-2
33	16795	16795	-2
34	16810	16810	-2
35	16797	16797	-2
36	16626	16626	-2

37	16679	16679	-2
38	16801	16801	-2
39	16802	16802	-2
40	16803	16803	-2
41	16804	16804	-2
42	16805	16805	-2
43	16806	16806	-2
44	16807	16807	-2
45	16627	16627	-2

2 -1 -1
Loading for 45 deg case
1 1 1 10 0 0 0

12196 110 -0.0000000707 0.0000000707 0
13255 110 -0.0000000707 0.0000000707 0
13254 110 -0.0000000707 0.0000000707 0
13253 110 -0.0000000707 0.0000000707 0
11546 110 -0.0000000707 0.0000000707 0
1233 110 0 0 0
2499 110 0 0 0
2498 111 0 0 0
2497 110 0 0 0
583 110 0 0 0

5

1233 2499 2498 2497 583

100 0.5 0 0 0

CRACK3D.GEO

9 21 0 6

76 78 96 50 52 58 58 1078 1080

1

```
141 30 139 345 344 140
34 14 347 35 334 333
34 135 137 340 136 341
30 32 139 31 343 344
346 141 126 335 142 329
346 26 28 338 27 336
34 137 32 341 342 33
347 303 133 332 304 330
347 133 135 330 134 331
137 139 32 138 343 342
28 30 141 29 345 339
347 135 34 331 340 333
347 14 303 334 302 332
327 346 126 337 329 328
26 346 327 338 337 326
28 141 346 339 335 336
7697 5864 7699 7645 7636 7637
6721 5896 5898 7665 5897 7664
5857 5864 7697 5863 7645 7647
5912 7698 6705 7643 7641 7649
5880 5882 6737 5881 7680 7681
6713 5904 5906 7657 5905 7656
5876 6743 5874 7686 7687 5875
14 303 7698 302 7642 7644
6735 5882 5884 7679 5883 7678
6715 5902 5904 7659 5903 7658
5902 6715 6717 7659 6716 7660
5886 6733 5884 7676 7677 5885
6733 6735 5884 6734 7678 7677
6737 6739 5880 6738 7682 7681
5872 6745 6747 7689 6746 7690
5902 6717 5900 7660 7661 5901
6719 5900 6717 7662 7661 6718
7699 6698 7565 7640 7566 7638
6711 5906 5908 7655 5907 7654
7699 6753 6698 7639 6754 7640
7699 5864 6753 7636 7648 7639
7565 5857 7697 7564 7647 7646
7565 7697 7699 7646 7637 7638
5878 6739 6741 7683 6740 7684
6745 5874 6743 7688 7687 6744
14 7698 5912 7644 7643 5913
133 7698 303 7635 7642 304
5888 6729 6731 7673 6730 7674
6707 5910 5912 7651 5911 7650
6707 5912 6705 7650 7649 6706
6739 5878 5880 7683 5879 7682
6715 5904 6713 7658 7657 6714
```

5874 6745 5872 7688 7689 5873
5906 6711 6713 7655 6712 7656
6731 6733 5886 6732 7676 7675
6721 5898 6719 7664 7663 6720
5878 6741 5876 7684 7685 5877
5876 6741 6743 7685 6742 7686
6719 5898 5900 7663 5899 7662
6705 7698 133 7641 7635 6704
6753 5864 5866 7648 5865 7696
5896 6723 5894 7666 7667 5895
5866 6751 6753 7695 6752 7696
6737 5882 6735 7680 7679 6736
6731 5886 5888 7675 5887 7674
6725 5894 6723 7668 7667 6724
6727 5892 6725 7670 7669 6726
5870 6749 5868 7692 7693 5869
5870 5872 6747 5871 7690 7691
6721 6723 5896 6722 7666 7665
6725 5892 5894 7669 5893 7668
6751 5868 6749 7694 7693 6750
5870 6747 6749 7691 6748 7692
5892 6727 5890 7670 7671 5891
6751 5866 5868 7695 5867 7694
6729 5890 6727 7672 7671 6728
5908 6709 6711 7653 6710 7654
5890 6729 5888 7672 7673 5889
6709 5908 5910 7653 5909 7652
6707 6709 5910 6708 7652 7651

2

1990 2269 2292 2270 2278 2280
2013 2292 2291 2272 2277 2281
2269 2291 2292 2282 2277 2278
1993 2292 2013 2279 2272 2285
2005 2013 2291 2014 2281 2283
2013 2011 1993 2012 2286 2285
1995 2011 1997 2288 2287 1996
2293 2007 2001 2273 2006 2271
1993 1990 2292 1992 2280 2279
2293 2003 1991 2275 2004 2276
2005 2291 2269 2283 2282 2268
2007 1999 2009 2284 2289 2008
2009 1999 1997 2289 1998 2290
2011 2009 1997 2010 2290 2287
2007 2293 1999 2273 2274 2284
2001 2003 2293 2002 2275 2271
1993 2011 1995 2286 2288 1994
2293 1991 1999 2276 2000 2274
2114 2116 2023 2115 2351 2350
2112 2027 2110 2347 2346 2111
2358 2069 2356 2297 2305 2296
2017 2358 2356 2295 2296 2304
2019 2120 2017 2355 2307 2018
2057 2080 2082 2316 2081 2317
2053 2086 2051 2321 2322 2052

2067	2358	2120	2299	2298	2121
2061	2063	2076	2062	2311	2312
2017	2120	2358	2307	2298	2295
2065	2357	2072	2302	2300	2308
2049	2088	2090	2324	2089	2325
2356	2069	2015	2305	2068	2306
2088	2051	2086	2323	2322	2087
2053	2055	2084	2054	2319	2320
2049	2051	2088	2050	2323	2324
2047	2090	2092	2326	2091	2327
2055	2082	2084	2318	2083	2319
2031	2108	2029	2343	2344	2030
2033	2035	2104	2034	2339	2340
2114	2023	2025	2350	2024	2349
2047	2049	2090	2048	2325	2326
2059	2061	2078	2060	2313	2314
2080	2057	2059	2316	2058	2315
2031	2033	2106	2032	2341	2342
2029	2110	2027	2345	2346	2028
2358	2067	2069	2299	2070	2297
2118	2021	2116	2353	2352	2117
2094	2045	2092	2329	2328	2093
2045	2047	2092	2046	2327	2328
2015	2017	2356	2016	2304	2306
2106	2108	2031	2107	2343	2342
2094	2096	2043	2095	2331	2330
2108	2110	2029	2109	2345	2344
2106	2033	2104	2341	2340	2105
2269	1990	2357	2270	2294	2301
2096	2098	2041	2097	2333	2332
2072	2074	2065	2073	2309	2308
2082	2055	2057	2318	2056	2317
2039	2041	2098	2040	2333	2334
2063	2065	2074	2064	2309	2310
2086	2053	2084	2321	2320	2085
2116	2021	2023	2352	2022	2351
2357	2005	2269	2303	2268	2301
2005	2357	2065	2303	2302	2066
2102	2104	2035	2103	2339	2338
2078	2080	2059	2079	2315	2314
2094	2043	2045	2330	2044	2329
2076	2078	2061	2077	2313	2312
2072	2357	1990	2300	2294	2071
2120	2019	2118	2355	2354	2119
2074	2076	2063	2075	2311	2310
2118	2019	2021	2354	2020	2353
2041	2043	2096	2042	2331	2332
2112	2114	2025	2113	2349	2348
2037	2102	2035	2337	2338	2036
2100	2039	2098	2335	2334	2099
2112	2025	2027	2348	2026	2347
2100	2037	2039	2336	2038	2335
2102	2037	2100	2337	2336	2101

3

7506 5801 7633 7505 7601 7600
6690 7631 6692 7612 7611 6691
7628 5847 5849 7617 5848 7618
7630 6692 7631 7614 7611 7603
6690 6688 7632 6689 7610 7609
7633 5801 5847 7601 5846 7599
7632 7631 6690 7602 7612 7609
7628 7631 7632 7584 7602 7606
7633 6688 6642 7598 6687 7590
7633 7632 6688 7583 7610 7598
7626 7627 5851 7593 7620 7621
6694 6692 7630 6693 7614 7613
7627 7626 7630 7593 7608 7585
7633 7628 7632 7582 7606 7583
7633 5847 7628 7599 7617 7582
5849 7627 7628 7619 7592 7618
5849 5851 7627 5850 7620 7619
7627 7631 7628 7607 7584 7592
7630 7631 7627 7603 7607 7585
6642 7506 7633 7507 7600 7590
6696 7634 6686 7595 7597 6697
5851 5853 7626 5852 7622 7621
5845 7634 5855 7589 7591 5856
7626 7629 7630 7586 7605 7608
6694 7629 6696 7616 7615 6695
6694 7630 7629 7613 7605 7616
5853 5855 7625 5854 7624 7623
7626 7625 7629 7594 7604 7586
7625 7634 7629 7588 7587 7604
7629 7634 6696 7587 7595 7615
7625 5855 7634 7624 7591 7588
5845 7562 7634 7561 7596 7589
7562 6686 7634 7563 7597 7596
7625 7626 5853 7594 7622 7623
5801 10450 7506 10418 10417 7505
10450 5801 8863 10418 8862 10416
8865 8867 10448 8866 10429 10428
8861 10376 10451 10375 10413 10415
10447 10446 10444 10397 10421 10422
8869 10447 8867 10431 10430 8868
10453 6642 7506 10408 7507 10406
10446 8869 8871 10432 8870 10433
9607 9609 10445 9608 10435 10434
9605 9607 10452 9606 10410 10412
10446 10447 8869 10397 10431 10432
9609 10444 10445 10436 10398 10435
10443 10448 10447 10424 10395 10423
9611 10444 9609 10437 10436 9610
8871 10451 10446 10414 10399 10433
10451 10445 10446 10404 10420 10399
10449 8863 8865 10426 8864 10427
10447 10444 10443 10422 10396 10423
7506 10450 10453 10417 10405 10406
10444 10446 10445 10421 10420 10398
6642 10453 9615 10408 10407 9616

8865 10448 10449 10428 10402 10427
10450 8863 10449 10416 10426 10403
9611 9613 10443 9612 10439 10438
9613 10442 10443 10440 10394 10439
10451 8871 8861 10414 8872 10415
10452 10376 9605 10411 10377 10412
10452 9607 10445 10410 10434 10400
10451 10376 10452 10413 10411 10409
10452 10445 10451 10400 10404 10409
10453 10450 10449 10405 10403 10393
10442 9613 9615 10440 9614 10441
10442 10448 10443 10425 10424 10394
10444 9611 10443 10437 10438 10396
10453 10449 10442 10393 10419 10401
9615 10453 10442 10407 10401 10441
10448 8867 10447 10429 10430 10395
10448 10442 10449 10425 10419 10402
10391 8861 8876 10387 8877 10385
8861 10391 10376 10387 10386 10375
10391 9605 10376 10378 10377 10386
9605 10391 9618 10378 10384 9617
10391 8876 9618 10385 10390 10384
2069 10392 2015 10382 10379 2068
9618 8876 9620 10390 10389 9619
2069 2067 10392 2070 10383 10382
9620 8876 8874 10389 8875 10388
8874 2015 10392 8873 10379 10380
10392 2067 9620 10383 9621 10381
9620 8874 10392 10388 10380 10381
5857 7580 5859 7568 7569 5858
6702 7581 5861 7570 7571 7579
7580 7565 6698 7575 7566 7576
6700 5861 5859 7578 5860 7577
7565 7580 5857 7575 7568 7564
6698 6700 7580 6699 7574 7576
7581 7562 5845 7572 7561 7573
6702 5861 6700 7579 7578 6701
7581 5845 5861 7573 5862 7571
6702 6686 7581 6703 7567 7570
7581 6686 7562 7567 7563 7572
7580 6700 5859 7574 7577 7569

4

5313 5608 5302 5597 5599 5314
5427 5607 1991 5600 5594 5428
5425 5311 5427 5606 5605 5426
5311 5607 5427 5602 5600 5605
5607 2003 1991 5601 2004 5594
5313 5425 5608 5604 5596 5597
5313 5311 5425 5312 5606 5604
5416 5608 5425 5595 5596 5424
5311 2001 5607 5310 5603 5602
5416 5559 5608 5560 5598 5595

5302 5608 5559 5599 5598 5558
2001 2003 5607 2002 5601 5603
5304 5298 5590 5303 5578 5576
5593 5588 5422 5561 5586 5566
5588 5593 5591 5561 5565 5564
5592 5418 5589 5571 5585 5562
5302 5308 5591 5309 5574 5575
5304 5590 5589 5576 5563 5580
5593 5422 5416 5566 5423 5568
5589 5418 5420 5585 5419 5584
5592 5412 5418 5572 5417 5571
5589 5420 5588 5584 5587 5579
5543 5412 5592 5544 5572 5570
5420 5422 5588 5421 5586 5587
5308 5306 5588 5307 5582 5583
5588 5306 5589 5582 5581 5579
5559 5591 5593 5573 5565 5567
5590 5298 5543 5578 5542 5577
5592 5589 5590 5562 5563 5569
5590 5543 5592 5577 5570 5569
5304 5589 5306 5580 5581 5305
5308 5588 5591 5583 5564 5574
5302 5591 5559 5575 5573 5558
5559 5593 5416 5567 5568 5560
17960 5298 18124 17961 18121 18123
18036 18125 5412 18119 18118 18039
18125 5543 5412 18116 5544 18118
18036 18113 18125 18114 18117 18119
18124 5543 18125 18120 18116 18115
18124 18125 18113 18115 18117 18122
17960 18124 18113 18123 18122 18112
18124 5298 5543 18121 5542 18120
18138 18127 17962 18136 18126 18137
18037 18127 18139 18128 18131 18133
17960 18138 17962 18135 18137 17974
18138 18139 18127 18129 18131 18136
18037 18139 18036 18133 18132 18038
18113 18139 18138 18130 18129 18134
18113 18036 18139 18114 18132 18130
18138 17960 18113 18135 18112 18134

5

280 8 6 275 7 274
251 2 283 250 267 265
4 1 282 3 270 268
160 162 281 161 276 277
280 164 285 278 258 253
162 164 280 163 278 279
282 1 248 270 247 269
282 281 4 255 272 268
284 160 281 263 277 254
284 127 160 264 159 263
248 127 284 249 264 262
283 8 280 266 275 256

281 280 6 271 274 273
164 155 285 165 260 258
283 2 8 267 9 266
283 280 285 256 253 257
281 6 4 273 5 272
281 162 280 276 279 271
248 284 282 262 261 269
282 284 281 261 254 255
155 251 285 252 259 260
285 251 283 259 265 257
365 1 39 356 40 354
39 131 365 361 348 354
366 131 127 352 132 353
37 26 364 36 360 359
126 129 364 128 357 349
248 1 365 247 356 355
366 127 248 353 249 351
364 327 126 358 328 349
364 26 327 360 326 358
129 37 364 362 359 357
365 131 366 348 352 350
366 248 365 351 355 350
39 37 131 38 363 361
37 129 131 362 130 363
18767 18778 18779 18776 18769 18771
18778 18614 2 18777 18615 18775
18767 18614 18778 18766 18777 18776
18779 155 18702 18772 18704 18773
18767 18779 18702 18771 18773 18768
251 18779 18778 18770 18769 18774
155 18779 251 18772 18770 252
18778 2 251 18775 250 18774
18793 18792 18767 18783 18789 18786
18793 18702 18690 18787 18703 18785
18767 18702 18793 18768 18787 18786
18792 18614 18767 18791 18766 18789
18781 18793 18690 18784 18785 18782
18793 18781 18792 18784 18788 18783
18616 18792 18781 18790 18788 18780
18792 18616 18614 18790 18628 18791

6

16762 16702 16700 16767 16701 16753
16762 16700 16764 16753 16768 16763
16764 16700 16595 16768 16699 16755
16764 16597 16529 16765 16754 16758
16647 16704 16664 16705 16749 16665
16760 16527 16664 16748 16663 16759
16760 16533 16527 16756 16534 16748
16597 16523 16529 16598 16528 16754
16531 16764 16529 16752 16758 16530
16760 16664 16704 16759 16749 16766
16531 16533 16762 16532 16750 16757
16762 16764 16531 16763 16752 16757

16595 16597 16764 16596 16765 16755
16760 16702 16762 16751 16767 16761
16702 16760 16704 16751 16766 16703
16762 16533 16760 16750 16756 16761
18622 18620 18853 18621 18824 18833
18853 18857 18858 18818 18813 18812
18698 18700 18848 18699 18847 18846
18694 18856 18692 18820 18815 18693
18694 18852 18856 18825 18821 18820
18849 18626 18624 18844 18625 18845
18626 18849 16523 18844 18797 18627
16531 16529 18855 16530 18827 18826
18700 16527 18848 18701 18798 18847
18696 18698 18850 18697 18843 18842
18859 18692 18856 18810 18815 18811
18859 18781 18690 18799 18782 18803
18694 18696 18852 18695 18834 18825
18851 18624 18622 18840 18623 18841
18856 18858 18857 18816 18813 18804
18854 16533 16531 18796 16532 18822
18848 16533 18854 18839 18796 18831
18852 18696 18850 18834 18842 18835
18781 18859 18860 18799 18801 18800
18860 18616 18781 18802 18780 18800
18857 18860 18856 18808 18795 18804
18856 18860 18859 18795 18801 18811
18848 16527 16533 18798 16534 18839
18850 18698 18848 18843 18846 18838
18857 18853 18620 18818 18824 18819
18853 18855 18851 18823 18829 18832
18849 16529 16523 18836 16528 18797
18855 18854 16531 18807 18822 18826
18851 18849 18624 18837 18845 18840
18690 18692 18859 18691 18810 18803
18855 16529 18849 18827 18836 18828
18618 18860 18857 18809 18808 18814
18860 18618 18616 18809 18617 18802
18851 18622 18853 18841 18833 18832
18853 18858 18855 18812 18806 18823
18858 18854 18855 18805 18807 18806
18854 18858 18852 18805 18817 18794
18618 18857 18620 18814 18819 18619
18855 18849 18851 18828 18837 18829
18856 18852 18858 18821 18817 18816
18850 18854 18852 18830 18794 18835
18850 18848 18854 18838 18831 18830

7

16702 16783 16781 16788 16782 16772
16704 16702 16781 16703 16772 16787
16595 16612 16785 16611 16786 16776
16785 16700 16595 16789 16699 16776
16781 16569 16563 16777 16570 16769
16781 16563 16649 16769 16648 16780

16700	16783	16702	16774	16788	16701
16647	16704	16649	16705	16770	16650
16783	16569	16781	16771	16777	16782
16781	16649	16704	16780	16770	16787
16783	16567	16569	16778	16568	16771
16783	16785	16567	16784	16773	16778
16700	16785	16783	16789	16784	16774
16785	16612	16565	16786	16775	16779
16785	16565	16567	16779	16566	16773
16565	16612	16559	16775	16613	16564
16563	18194	16569	18143	18184	16570
18127	17962	18206	18126	18147	18145
18195	17970	17972	18190	17971	18191
17970	18195	18197	18190	18182	18187
18201	18204	18199	18151	18160	18169
18200	16567	16569	18172	16568	18175
18197	17968	17970	18186	17969	18187
18049	18202	18047	18163	18167	18048
18198	18045	18047	18181	18046	18171
18205	18049	18037	18157	18050	18149
18205	18037	18127	18149	18128	18146
18043	18045	18196	18044	18189	18188
18199	17968	18197	18178	18186	18179
17966	18203	17964	18164	18158	17965
17966	17968	18199	17967	18178	18170
18196	18198	18200	18180	18140	18177
18194	18196	18200	18185	18177	18176
18201	16565	16567	18142	16566	18168
18204	18200	18198	18152	18140	18161
18194	18200	16569	18176	18175	18184
18204	18202	18203	18162	18150	18159
18041	18043	18194	18042	18193	18192
18196	18045	18198	18189	18181	18180
17962	17964	18206	17963	18154	18147
18202	18205	18206	18156	18148	18141
18199	18203	17966	18165	18164	18170
18206	18203	18202	18155	18150	18141
18203	18199	18204	18165	18160	18159
18195	16565	18201	18183	18142	18174
18201	16567	18200	18168	18172	18153
16559	16565	18195	16564	18183	18144
17972	16559	18195	17973	18144	18191
16563	18041	18194	18040	18192	18143
18194	18043	18196	18193	18188	18185
18205	18127	18206	18146	18145	18148
18201	18200	18204	18153	18152	18151
17964	18203	18206	18158	18155	18154
18204	18198	18202	18161	18166	18162
18205	18202	18049	18156	18163	18157
18047	18202	18198	18167	18166	18171
18201	18199	18197	18169	18179	18173
18195	18201	18197	18174	18173	18182

8

119 111 120 73 79 71
115 116 22 76 91 92
121 117 116 62 75 63
120 111 109 79 102 80
113 121 122 68 60 67
115 119 122 43 42 65
122 119 120 42 71 61
116 117 20 75 89 90
115 24 124 93 54 52
119 115 124 43 52 46
110 109 111 104 102 101
109 1 114 108 94 81
118 125 16 48 49 86
123 125 118 45 48 47
121 112 118 69 70 41
8 112 6 99 98 7
118 112 123 70 56 47
24 115 22 93 92 23
124 24 14 54 25 55
39 1 109 40 108 107
125 12 10 50 13 51
123 2 12 59 11 57
113 122 114 67 66 77
114 1 4 94 3 95
120 114 122 72 66 61
16 18 118 17 87 86
121 113 112 68 78 69
34 124 14 53 55 35
32 111 119 82 73 85
111 32 30 82 31 83
110 26 37 44 36 105
118 18 117 87 88 74
118 117 121 74 62 41
116 122 121 64 60 63
16 125 10 49 51 15
4 113 114 96 77 95
123 12 125 57 50 45
109 114 120 81 72 80
122 116 115 64 76 65
30 110 111 100 101 83
119 124 34 46 53 84
32 119 34 85 84 33
117 18 20 88 19 89
116 20 22 90 21 91
113 6 112 97 98 78
8 2 123 9 59 58
4 6 113 5 97 96
39 109 110 107 104 106
112 8 123 99 58 56
26 110 28 44 103 27
110 30 28 100 29 103
37 39 110 38 106 105
5288 5393 5398 5356 5326 5327
5391 5294 5390 5361 5362 5346
5396 5397 5388 5337 5336 5338
5390 5399 5395 5322 5320 5333

5290 5393 5288 5357 5356 5289
5387 5396 5388 5341 5338 5351
5396 5393 5392 5339 5344 5330
5386 5396 5394 5316 5342 5340
5386 5394 5385 5340 5354 5352
2013 5398 5386 5328 5321 5373
5392 5393 5290 5344 5357 5358
5386 5393 5396 5317 5339 5316
2001 5384 5311 5319 5380 5310
5384 2007 2009 5378 2008 5376
5399 5296 5286 5324 5297 5325
5304 5395 5298 5348 5318 5303
5394 5396 5387 5342 5341 5343
5313 5383 5302 5382 5381 5314
5392 5292 5391 5359 5360 5345
5302 5383 5387 5381 5355 5369
5383 5384 5385 5377 5375 5374
5391 5292 5294 5360 5293 5361
5385 5384 2009 5375 5376 5370
2009 2011 5385 2010 5371 5370
2013 2005 5398 2014 5329 5328
5384 2001 2007 5319 2006 5378
5397 5392 5391 5331 5345 5332
5397 5390 5389 5315 5334 5335
5398 5393 5386 5326 5317 5321
5385 5394 5383 5354 5353 5374
5296 5399 5390 5324 5322 5363
5389 5306 5388 5365 5366 5350
5390 5395 5389 5333 5349 5334
2013 5386 2011 5373 5372 2012
5399 5300 5395 5323 5347 5320
5388 5397 5389 5336 5335 5350
5397 5391 5390 5332 5346 5315
5390 5294 5296 5362 5295 5363
5383 5313 5384 5382 5379 5377
2011 5386 5385 5372 5352 5371
5389 5395 5304 5349 5348 5364
5300 5399 5286 5323 5325 5301
5388 5306 5308 5366 5307 5367
5387 5388 5308 5351 5367 5368
5394 5387 5383 5343 5355 5353
5398 2005 5288 5329 5287 5327
5304 5306 5389 5305 5365 5364
5392 5290 5292 5358 5291 5359
5384 5313 5311 5379 5312 5380
5392 5397 5396 5331 5337 5330
5302 5387 5308 5369 5368 5309
5298 5395 5300 5318 5347 5299
16523 16597 16608 16598 16609 16605
16345 16525 16608 16603 16610 16607
16608 16298 16345 16602 16346 16607
16345 16343 16525 16344 16526 16603
16608 16525 16523 16610 16524 16605
16600 16298 16608 16601 16602 16606
16608 16597 16600 16609 16604 16606
16600 16597 16595 16604 16596 16599

16615 16595 16623 16616 16620 16625
16623 16595 16612 16620 16611 16624
16561 16612 16559 16619 16613 16560
16426 16380 16615 16425 16614 16618
16615 16623 16426 16625 16622 16618
16424 16623 16561 16617 16621 16562
16612 16561 16623 16619 16621 16624
16623 16424 16426 16617 16427 16622
16298 16600 16301 16601 16630 16300
16462 16635 16627 16633 16636 16631
16460 16462 16627 16461 16631 16628
16635 16299 16301 16629 16302 16634
16299 16635 16462 16629 16633 16463
16635 16600 16595 16637 16599 16632
16635 16595 16627 16632 16626 16636
16301 16600 16635 16630 16637 16634
16615 16627 16595 16639 16626 16616
16644 16460 16627 16638 16628 16643
16380 16644 16615 16641 16646 16614
16382 16379 16497 16381 16496 16640
16627 16615 16644 16639 16646 16643
16382 16644 16380 16645 16641 16383
16497 16460 16644 16498 16638 16642
16382 16497 16644 16640 16642 16645
16981 5797 5799 16939 5800 16937
16976 16301 16299 16929 16302 16957
16909 16978 16972 16930 16954 16969
16980 16977 16979 16940 16946 16934
16974 16973 16976 16960 16959 16958
16976 16299 16975 16957 16962 16952
16920 16977 16922 16928 16949 16921
16973 16298 16301 16933 16300 16961
16972 16462 16460 16971 16461 16932
16907 16909 16972 16908 16969 16968
5799 5796 16979 5798 16931 16945
16460 16907 16972 16906 16968 16932
16980 16979 5915 16934 16944 16942
16977 16924 16922 16948 16923 16949
5797 16981 16913 16939 16938 16914
5799 16979 16981 16945 16935 16937
10 16924 16980 16925 16941 16943
5915 10 16980 5914 16943 16942
16920 16974 16977 16964 16955 16928
16298 16973 16916 16933 16967 16915
16973 16974 16918 16960 16965 16966
16913 16981 16978 16938 16936 16951
16972 16299 16462 16970 16463 16971
16972 16975 16299 16963 16962 16970
16977 16974 16976 16955 16958 16956
16918 16916 16973 16917 16967 16966
16920 16918 16974 16919 16965 16964
16980 16924 16977 16941 16948 16940
16975 16979 16977 16947 16946 16927
16979 5796 5915 16931 5916 16944
16911 16913 16978 16912 16951 16950
16976 16975 16977 16952 16927 16956

16981 16979 16978 16935 16926 16936
16975 16978 16979 16953 16926 16947
16975 16972 16978 16963 16954 16953
16911 16978 16909 16950 16930 16910
16976 16973 16301 16959 16961 16929
17480 17478 17543 17479 17516 17515
17542 17539 17544 17520 17488 17489
17544 8859 17547 17507 17501 17496
17543 17478 5286 17516 17477 17493
17544 8854 8859 17494 8860 17507
17547 17542 17544 17499 17489 17496
16909 17542 16911 17492 17518 16910
17480 17541 17482 17522 17521 17481
17541 17539 17540 17490 17525 17523
17541 17484 17482 17491 17483 17521
16379 17539 17537 17530 17529 17536
17544 17545 17543 17509 17511 17497
8856 17544 17543 17508 17497 17510
16907 16460 17537 16906 17495 17534
17541 17538 17484 17524 17532 17491
17538 17540 17546 17526 17498 17503
5797 16913 17547 16914 17500 17502
17546 16380 17486 17506 17487 17504
17484 17538 17486 17532 17531 17485
17539 16379 17540 17530 17527 17525
16497 16379 17537 16496 17536 17535
17544 17539 17545 17488 17513 17509
17543 17545 17541 17511 17514 17512
16909 17537 17542 17533 17519 17492
17538 17541 17540 17524 17523 17526
17538 17546 17486 17503 17504 17531
16380 17546 16382 17506 17505 16383
17540 16382 17546 17528 17505 17498
17540 16379 16382 17527 16381 17528
16460 16497 17537 16498 17535 17495
17547 16913 17542 17500 17517 17499
17541 17545 17539 17514 17513 17490
17547 8859 5797 17501 8858 17502
16911 17542 16913 17518 17517 16912
17537 16909 16907 17533 16908 17534
8854 17544 8856 17494 17508 8855
8856 17543 5286 17510 17493 8857
17537 17539 17542 17529 17520 17519
17541 17480 17543 17522 17515 17512
18034 17960 5298 17990 17961 17991
17484 18028 17482 18015 18014 17483
18030 17964 18033 18001 17993 17996
5300 5286 18035 5301 17987 17986
18027 18029 16424 18002 18007 18016
18031 18029 18027 18006 18002 17976
16380 18026 17486 17980 18022 17487
18026 16380 16426 17980 16425 18013
18026 16426 18029 18013 17978 18011
18025 17968 18030 18018 18008 18004
17972 17970 18025 17971 18020 18019
18032 18033 18034 17995 17988 17982

18033 17960 18034 17992 17990 17988
18034 5298 5300 17991 5299 17989
17482 18031 17480 17977 18000 17481
18035 17478 18031 17985 17999 17984
5286 17478 18035 17477 17985 17987
17962 18033 17964 17981 17993 17963
16561 16559 18025 16560 17979 18024
18028 18031 17482 18005 17977 18014
18026 18028 17484 18012 18015 18021
17968 18025 17970 18018 18020 17969
18031 17478 17480 17999 17479 18000
17486 18026 17484 18022 18021 17485
18028 18029 18031 18010 18006 18005
18028 18026 18029 18012 18011 18010
17966 18030 17968 18009 18008 17967
18025 18027 16424 18017 18016 18023
16424 18029 16426 18007 17978 16427
18025 16424 16561 18023 16562 18024
18033 18032 18030 17995 17975 17996
17964 18030 17966 18001 18009 17965
17962 17960 18033 17974 17992 17981
17972 18025 16559 18019 17979 17973
18032 18035 18031 17983 17984 17997
18032 18031 18027 17997 17976 17998
18034 5300 18032 17989 17994 17982
18035 18032 5300 17983 17994 17986
18032 18027 18030 17998 18003 17975
18025 18030 18027 18004 18003 18017
9586 9550 9585 8966 8967 8910
9590 9555 9554 8957 9010 8958
9539 9578 9540 8985 8984 9026
2037 9454 9455 9392 9299 9391
2029 2031 9458 2030 9385 9384
9470 9469 9518 9284 9201 9200
9552 9551 9587 9013 8964 8963
9494 9493 9540 9158 9108 9107
9530 9481 9529 9177 9178 9122
9480 9528 9529 9180 9123 9179
9549 9585 9550 8968 8967 9015
5294 5296 9464 5295 9371 9370
9541 9497 9496 9104 9156 9105
9496 9517 9537 9106 9067 9025
9439 9494 9440 9255 9254 9314
9491 9437 9436 9260 9317 9261
9440 9494 9468 9254 9203 9286
9595 9440 9468 8894 9286 8885
9508 9509 9455 9144 9224 9225
9552 9553 9508 9012 9081 9082
9455 9454 9508 9299 9226 9225
9445 9444 9498 9309 9246 9245
9442 9495 9496 9251 9157 9250
9442 9443 2061 9311 9415 9416
9443 9442 9496 9311 9250 9249
9574 9575 9533 8990 9035 9036
9532 9531 9573 9120 9039 9038
8854 9489 9536 9320 9162 8881

9463	9436	9434	8878	9318	9262
9519	9470	9518	9199	9200	9133
9475	5829	9474	9349	9350	9279
9520	9472	9471	9196	9282	9197
9450	2045	2047	9400	2046	9401
9438	9437	9492	9316	9259	9258
9515	9462	9461	9211	9292	9212
9538	9536	9576	9113	9030	9029
9517	9466	9465	9205	9288	9206
9466	9467	5290	9287	9365	9366
5825	9477	5823	9345	9344	5824
5292	9465	9466	9368	9288	9367
5294	9465	5292	9369	9368	5293
2039	9454	2037	9393	9392	2038
9584	9569	9585	8931	8932	8911
9447	2053	9446	9407	9408	9307
9542	9498	9497	9102	9155	9103
9489	8854	8859	9320	8860	9321
9561	9519	9560	9063	9064	9004
8867	9438	9439	9424	9315	9423
9519	9471	9470	9198	9283	9199
9558	9593	9578	8951	8902	8918
9577	9542	9541	8982	9023	8983
9594	2065	2005	8900	2066	8901
9442	2061	2063	9416	2062	9417
9560	9593	9561	8949	8948	9004
9476	9524	9525	9188	9127	9187
9507	9508	9454	9145	9226	9227
9508	9507	9552	9145	9083	9082
9587	9566	9588	8937	8938	8908
9572	9581	9573	8925	8924	8992
9586	9568	9567	8934	8997	8935
9532	9484	9483	9172	9270	9173
9484	5811	9483	9331	9332	9270
9544	9543	9579	9021	8980	8979
9580	9573	9581	8923	8924	8915
9579	9577	9575	8917	8919	8920
9579	9580	9544	8916	8978	8979
9539	9559	9578	9027	8879	8985
2039	9453	9454	9394	9300	9393
9591	9562	9592	8945	8946	8904
9561	9562	9520	9003	9061	9062
9590	9564	9563	8942	9001	8943
9480	5819	9479	9339	9340	9274
9571	9529	9570	9043	9044	8994
5801	8863	9595	8862	8895	8897
9572	9582	9581	8926	8914	8925
9504	9451	9450	9233	9303	9234
5811	9484	5809	9331	9330	5810
9518	9494	9540	9134	9107	9066
9560	9540	9578	9005	8984	8950
9493	9492	9539	9159	9110	9109
9572	9571	9582	8993	8927	8926
9585	9568	9586	8933	8934	8910
2021	9463	2019	9375	9374	2020
9449	9502	9503	9237	9150	9236

9543	9542	9577	9022	8982	8981
9552	9588	9553	8962	8961	9012
9463	2021	9462	9375	9376	9291
9510	9555	9511	9077	9076	9142
9562	9521	9520	9060	9131	9061
9532	9533	9484	9119	9171	9172
9531	9572	9573	9040	8992	9039
9549	9505	9504	9088	9148	9089
9506	9452	9505	9230	9231	9147
9463	9462	9491	9291	9210	9209
9491	9515	9492	9137	9111	9160
9472	5833	5835	9354	5834	9355
9522	9473	9521	9193	9194	9130
9519	9561	9520	9063	9062	9132
9524	9475	9523	9189	9190	9128
2063	2065	9441	2064	9419	9418
9566	9524	9565	9053	9054	8999
9496	9495	9517	9157	9135	9106
9508	9553	9509	9081	9080	9144
9461	9514	9515	9213	9138	9212
9436	9463	9491	8878	9209	9261
5831	5833	9473	5832	9353	9352
9532	9574	9533	9037	9036	9119
2051	9447	9448	9406	9306	9405
9449	9450	2047	9304	9401	9402
9462	2023	9461	9377	9378	9292
9558	9559	9514	9006	9069	9070
9527	9569	9528	9047	9046	9124
9471	5835	5837	9356	5836	9357
9469	5839	5841	9360	5840	9361
5837	5839	9470	5838	9359	9358
9471	5837	9470	9357	9358	9283
9483	9482	9531	9271	9175	9174
5811	5813	9483	5812	9333	9332
9480	9529	9481	9179	9178	9273
9482	9483	5813	9271	9333	9334
9447	2051	2053	9406	2052	9407
9459	2029	9458	9383	9384	9295
9458	2031	9457	9385	9386	9296
9466	5290	5292	9366	5291	9367
9538	9576	9577	9029	8987	8986
2057	2059	9444	2058	9413	9412
9507	9453	9506	9228	9229	9146
8861	8876	9434	8877	9433	9432
8867	9439	8865	9423	9422	8866
9465	9464	9516	9289	9208	9207
9589	9565	9564	8940	9000	8941
8854	9488	8856	9323	9322	8855
9464	9597	9488	8886	8883	9264
5817	5819	9480	5818	9339	9338
9472	9520	9521	9196	9131	9195
9563	9564	9522	9001	9057	9058
9552	9507	9551	9083	9084	9013
9438	9493	9439	9257	9256	9315
9438	8867	8869	9424	8868	9425
9513	9459	9512	9216	9217	9140

8876 9435 9434 9430 9319 9433
8876 8874 9435 8875 9431 9430
2015 2017 9435 2016 9372 8880
9450 9451 2045 9303 9399 9400
2029 9459 2027 9383 9382 2028
9467 9466 9495 9287 9204 9253
9553 9588 9589 8961 8907 8960
9563 9521 9562 9059 9060 9002
9551 9550 9586 9014 8966 8965
9550 9505 9549 9087 9088 9015
9541 9537 9538 9024 9031 8988
9496 9537 9541 9025 9024 9105
9479 9528 9480 9181 9180 9274
9488 8854 9490 9323 9266 9265
9524 9523 9565 9128 9055 9054
9523 9474 9522 9191 9192 9129
9481 9530 9482 9177 9176 9272
9482 5813 5815 9334 5814 9335
9530 9571 9572 9042 8993 9041
9483 9531 9532 9174 9120 9173
9503 9450 9449 9235 9304 9236
9560 9518 9540 9065 9066 9005
9518 9560 9519 9065 9064 9133
9461 9460 9514 9293 9214 9213
9537 9490 9538 9116 9112 9031
9505 9452 9451 9231 9302 9232
9504 9548 9549 9090 9016 9089
8869 8871 9437 8870 9427 9426
9527 9478 9526 9183 9184 9125
9507 9454 9453 9227 9300 9228
2041 9452 9453 9396 9301 9395
2039 2041 9453 2040 9395 9394
9446 9500 9447 9242 9241 9307
9543 9498 9542 9101 9102 9022
9545 9544 9580 9020 8978 8977
2057 9445 2055 9411 9410 2056
5827 9475 9476 9348 9278 9347
9526 9568 9527 9049 9048 9125
9465 5294 9464 9369 9370 9289
9488 9490 9516 9265 9165 9164
9449 2047 2049 9402 2048 9403
9576 9536 9535 9030 9114 9032
9467 9594 5288 8898 8899 9364
5288 5290 9467 5289 9365 9364
9530 9529 9571 9122 9043 9042
9503 9548 9504 9091 9090 9149
9446 2055 9445 9409 9410 9308
9580 9581 9545 8915 8976 8977
9460 2025 2027 9380 2026 9381
9457 9511 9458 9220 9219 9296
9554 9509 9553 9079 9080 9011
9521 9473 9472 9194 9281 9195
9522 9521 9563 9130 9059 9058
9574 9573 9580 8991 8923 8922
9505 9550 9506 9087 9086 9147
9453 9452 9506 9301 9230 9229

5825	9476	9477	9346	9277	9345
5827	9476	5825	9347	9346	5826
9566	9525	9524	9052	9127	9053
9477	9525	9526	9186	9126	9185
9443	2059	2061	9414	2060	9415
9567	9525	9566	9051	9052	8998
9497	9444	9443	9247	9310	9248
9455	2035	2037	9390	2036	9391
9516	9464	9488	9208	9264	9164
9517	9495	9466	9135	9204	9205
9516	9517	9465	9136	9206	9207
9537	9517	9516	9067	9136	9115
5833	9472	9473	9354	9281	9353
9441	9467	9495	9313	9253	9252
9479	5821	9478	9341	9342	9275
9479	5819	5821	9340	5820	9341
9444	2059	9443	9413	9414	9310
8861	9434	9436	9432	9318	9429
5841	9468	9469	9362	9285	9361
2033	9457	2031	9387	9386	2032
5288	9594	2005	8899	8901	5287
9559	9539	9492	9027	9110	9028
9491	9462	9515	9210	9211	9137
9513	9557	9558	9072	9007	9071
9563	9591	9590	8944	8905	8943
9591	9555	9590	8956	8957	8905
9562	9591	9563	8945	8944	9002
9562	9561	9592	9003	8947	8946
9585	9569	9568	8932	8996	8933
9576	9535	9534	9032	9117	9033
9489	9487	9535	9263	9166	9163
9564	9523	9522	9056	9129	9057
9549	9548	9584	9016	8970	8969
9569	9527	9568	9047	9048	8996
9477	9526	9478	9185	9184	9276
9504	9505	9451	9148	9232	9233
9502	9547	9503	9093	9092	9150
9471	9519	9520	9198	9132	9197
8859	5797	9596	8858	8893	8892
9535	9486	9534	9167	9168	9117
9535	9536	9489	9114	9162	9163
5815	5817	9481	5816	9337	9336
9518	9469	9494	9201	9202	9134
5803	5805	9487	5804	9325	9324
9476	9525	9477	9187	9186	9277
5827	5829	9475	5828	9349	9348
9587	9567	9566	8936	8998	8937
9434	9435	9463	9319	9290	9262
2017	2019	9435	2018	9373	9372
9463	9435	2019	9290	9373	9374
9435	8874	2015	9431	8873	8880
2041	2043	9452	2042	9397	9396
9442	2063	9441	9417	9418	9312
8863	8865	9440	8864	9421	9420
9576	9575	9577	8989	8919	8987
9575	9576	9534	8989	9033	9034

9529 9528 9570 9123 9045 9044
9527 9528 9479 9124 9181 9182
9500 9545 9501 9097 9096 9152
9459 9458 9512 9295 9218 9217
2057 9444 9445 9412 9309 9411
2033 9456 9457 9388 9297 9387
2035 9456 2033 9389 9388 2034
2043 9451 9452 9398 9302 9397
9506 9551 9507 9085 9084 9146
9487 5805 9486 9325 9326 9267
9487 9596 5803 8890 8891 9324
5807 5809 9485 5808 9329 9328
9596 9487 9489 8890 9263 8882
9436 9437 8871 9317 9427 9428
9559 9558 9578 9006 8918 8879
9547 9583 9548 8972 8971 9017
9561 9593 9592 8948 8903 8947
9592 9556 9591 8954 8955 8904
9571 9570 9583 8994 8929 8928
9549 9584 9585 8969 8911 8968
9533 9485 9484 9170 9269 9171
9584 9583 9570 8912 8929 8930
9537 9516 9490 9115 9165 9116
9441 9594 9467 8884 8898 9313
9536 9538 9490 9113 9112 9161
8854 9536 9490 8881 9161 9266
2025 9461 2023 9379 9378 2024
9460 9461 2025 9293 9379 9380
9559 9515 9514 9068 9138 9069
9514 9513 9558 9139 9071 9070
9497 9443 9496 9248 9249 9156
9494 9439 9493 9255 9256 9158
9484 9485 5809 9269 9329 9330
9486 5805 5807 9326 5806 9327
9487 9486 9535 9267 9167 9166
9522 9474 9473 9192 9280 9193
9523 9475 9474 9190 9279 9191
5831 9474 5829 9351 9350 5830
9538 9577 9541 8986 8983 8988
9451 2043 2045 9398 2044 9399
9446 9445 9499 9308 9244 9243
9468 5841 5843 9362 5842 9363
5817 9480 9481 9338 9273 9337
9441 9495 9442 9252 9251 9312
8856 9597 5286 8887 8889 8857
9436 8871 8861 9428 8872 9429
9587 9588 9552 8908 8962 8963
9460 2027 9459 9381 9382 9294
9464 5296 9597 9371 8888 8886
9597 8856 9488 8887 9322 8883
9557 9512 9556 9073 9074 9008
9578 9593 9560 8902 8949 8950
9592 9593 9557 8903 8952 8953
9502 9546 9547 9094 9018 9093
9503 9547 9548 9092 9017 9091
9582 9546 9581 8974 8975 8914

9571 9583 9582 8928 8913 8927
9548 9583 9584 8971 8912 8970
9584 9570 9569 8930 8995 8931
9528 9569 9570 9046 8995 9045
9460 9513 9514 9215 9139 9214
2051 9448 2049 9405 9404 2050
2049 9448 9449 9404 9305 9403
9447 9501 9448 9240 9239 9306
9486 5807 9485 9327 9328 9268
9565 9589 9588 8940 8907 8939
9534 9485 9533 9169 9170 9118
9534 9486 9485 9168 9268 9169
5831 9473 9474 9352 9280 9351
9530 9572 9531 9041 9040 9121
9530 9531 9482 9121 9175 9176
9449 9448 9502 9305 9238 9237
9566 9565 9588 8999 8939 8938
9509 9554 9510 9079 9078 9143
9446 2053 2055 9408 2054 9409
9468 9494 9469 9203 9202 9285
9595 8863 9440 8895 9420 8894
2065 9594 9441 8900 8884 9419
5296 5286 9597 5297 8889 8888
9547 9546 9582 9018 8974 8973
9547 9582 9583 8973 8913 8972
9564 9565 9523 9000 9055 9056
9502 9501 9546 9151 9095 9094
9581 9546 9545 8975 9019 8976
9526 9567 9568 9050 8997 9049
9512 9458 9511 9218 9219 9141
9447 9500 9501 9241 9152 9240
9501 9545 9546 9096 9019 9095
9591 9556 9555 8955 9009 8956
9574 9580 9579 8922 8916 8921
9587 9551 9586 8964 8965 8909
9439 9440 8865 9314 9421 9422
9558 9557 9593 9007 8952 8951
9513 9512 9557 9140 9073 9072
9567 9587 9586 8936 8909 8935
9456 9510 9457 9222 9221 9297
9500 9446 9499 9242 9243 9153
9589 9590 9554 8906 8958 8959
9534 9533 9575 9118 9035 9034
5803 9596 5797 8891 8893 5802
9596 9489 8859 8882 9321 8892
9511 9556 9512 9075 9074 9141
9557 9556 9592 9008 8954 8953
9499 9543 9544 9100 9021 9099
9545 9500 9544 9097 9098 9020
9456 9509 9510 9223 9143 9222
9457 9510 9511 9221 9142 9220
9543 9499 9498 9100 9154 9101
9497 9498 9444 9155 9246 9247
5823 9477 9478 9344 9276 9343
9589 9564 9590 8941 8942 8906
9511 9555 9556 9076 9009 9075

9543 9577 9579 8981 8917 8980
9455 9456 2035 9298 9389 9390
9579 9575 9574 8920 8990 8921
9589 9554 9553 8959 9011 8960
9437 9438 8869 9316 9425 9426
9539 9540 9493 9026 9108 9109
9573 9574 9532 8991 9037 9038
9541 9542 9497 9023 9103 9104
5815 9481 9482 9336 9272 9335
9509 9456 9455 9223 9298 9224
9472 5835 9471 9355 9356 9282
9468 5843 9595 9363 8896 8885
9559 9492 9515 9028 9111 9068
9492 9437 9491 9259 9260 9160
9462 2021 2023 9376 2022 9377
9450 9503 9504 9235 9149 9234
9492 9493 9438 9159 9257 9258
9550 9551 9506 9014 9085 9086
9554 9555 9510 9010 9077 9078
9595 5843 5801 8896 5844 8897
9476 9475 9524 9278 9189 9188
9459 9513 9460 9216 9215 9294
9502 9448 9501 9238 9239 9151
9478 9527 9479 9183 9182 9275
9478 5821 5823 9342 5822 9343
9499 9445 9498 9244 9245 9154
5839 9469 9470 9360 9284 9359
9526 9525 9567 9126 9051 9050
9499 9544 9500 9099 9098 9153
12 10 18688 13 18632 18645
18681 18679 18682 18671 18664 18663
18685 16920 16918 18655 16919 18639
18620 18682 18622 18668 18667 18621
18682 18687 18686 18651 18650 18629
18686 18689 18688 18637 18636 18646
12 18689 2 18641 18643 11
18680 18685 16918 18657 18639 18673
18684 16345 16343 18631 16344 18661
18686 18688 18683 18646 18648 18652
18684 18683 18685 18660 18656 18658
18684 18681 18683 18662 18630 18660
16924 16922 18688 16923 18638 18647
16298 16345 18680 16346 18669 18633
18680 18684 18685 18659 18658 18657
18679 18626 18624 18675 18625 18676
18679 16523 18626 18634 18627 18675
18687 18689 18686 18640 18637 18650
18688 18689 12 18636 18641 18645
18685 18683 16920 18656 18666 18655
18614 18689 18687 18642 18640 18644
18689 18614 2 18642 18615 18643
18684 18680 16345 18659 18669 18631
18682 18618 18687 18654 18649 18651
18681 18684 16343 18662 18661 18670
16924 18688 10 18647 18632 16925
16922 16920 18683 16921 18666 18665

18683 18688 16922 18648 18638 18665
16298 18680 16916 18633 18674 16915
18679 18624 18622 18676 18623 18672
18681 18686 18683 18653 18652 18630
18679 16525 16523 18678 16524 18634
18679 16343 16525 18677 16526 18678
18679 18622 18682 18672 18667 18664
18616 18614 18687 18628 18644 18635
18618 18616 18687 18617 18635 18649
18681 18682 18686 18663 18629 18653
18679 18681 16343 18671 18670 18677
16918 16916 18680 16917 18674 18673
18682 18620 18618 18668 18619 18654
6479 6507 6634 6325 5923 5932
6533 6532 6579 6197 6147 6146
6634 6507 5843 5923 6402 5934
6571 6523 6522 6211 6309 6212
6519 6567 6568 6219 6162 6218
6587 6588 6543 6055 6128 6129
5908 6481 6482 6455 6350 6454
6544 6545 6491 6186 6269 6270
6510 6511 5835 6321 6394 6395
6588 6589 6544 6054 6126 6127
5884 6494 5882 6430 6429 5883
6598 6554 6553 6107 6177 6108
6531 6477 6476 6297 6355 6298
6606 6563 6605 6091 6092 6038
6520 6568 6569 6217 6161 6216
6633 14 24 5939 25 5937
6494 5884 6493 6430 6431 6338
6494 6547 6548 6264 6183 6263
6523 5811 6522 6370 6371 6309
6547 6592 6548 6120 6119 6183
6547 6546 6591 6184 6122 6121
6547 6494 6493 6264 6338 6265
6481 6535 6482 6289 6288 6350
6572 6573 6524 6157 6208 6209
6560 6511 6559 6234 6235 6170
5837 5839 6509 5838 6398 6397
6592 6628 6593 5998 5997 6050
5900 6486 5898 6446 6445 5899
6624 6588 6623 6006 6007 5949
6528 5915 5796 6359 5916 6360
6599 6556 6575 6106 6151 6068
6474 5857 5864 5918 5863 6411
6528 5796 6575 6360 5919 6201
6606 6627 6626 5975 5946 5974
6473 6475 5845 6357 6468 6471
5884 5886 6493 5885 6432 6431
5823 5825 6516 5824 6384 6383
24 22 6503 23 6410 6409
6555 6534 6504 6175 6247 6245
5910 6480 6481 6457 6351 6456
6475 6502 6530 5917 6248 6300
6558 6600 6601 6102 6043 6101
16 6506 18 6404 6403 17

22 20 6504 21 6408 6407
6570 6521 6569 6214 6215 6160
6555 6599 6535 6105 6064 6145
6527 5796 5799 6361 5798 6362
6482 6535 6536 6288 6195 6287
6506 6505 18 6326 6406 6403
6536 6535 6580 6195 6144 6143
6563 6515 6514 6227 6317 6228
6572 6615 6573 6073 6072 6157
6620 6619 6613 5953 5960 5961
6485 6484 6538 6347 6283 6282
6619 6618 6614 5954 5958 5959
6537 6581 6582 6141 6061 6140
5874 6498 6499 6421 6333 6420
6479 6478 6533 6353 6294 6293
5874 6499 5872 6420 6419 5873
6501 6530 6502 6249 6248 6330
6533 6579 6557 6146 6104 6173
6536 6537 6483 6194 6285 6286
6483 6537 6484 6285 6284 6348
6583 6538 6582 6138 6139 6060
6561 6604 6562 6095 6094 6168
6616 6580 6577 6021 6025 6026
6549 6548 6593 6182 6118 6117
6579 6600 6557 6044 6103 6104
6498 6551 6552 6256 6179 6255
6494 6548 6495 6263 6262 6337
6594 6629 6630 5995 5943 5994
6574 6529 6527 6203 6304 6204
6562 6604 6605 6094 6039 6093
6584 6539 6583 6136 6137 6059
6550 6549 6594 6181 6116 6115
6619 6584 6583 6015 6059 6016
5902 6485 5900 6448 6447 5901
6477 6532 6478 6296 6295 6354
6532 6533 6478 6197 6294 6295
6473 6502 6475 6301 5917 6357
6508 6507 6533 6324 6242 6241
6611 6612 6569 6032 6079 6080
5823 6516 6517 6383 6315 6382
6566 6567 6518 6163 6220 6221
6610 6568 6567 6082 6162 6083
6609 6610 6567 6034 6083 6084
6609 6623 6610 5968 5967 6034
6582 6618 6583 6018 6017 6060
6485 6486 5900 6346 6446 6447
6538 6539 6485 6192 6281 6282
5841 5843 6507 5842 6402 6401
6521 6570 6522 6214 6213 6310
6621 6586 6585 6011 6057 6012
6542 6586 6587 6131 6056 6130
6486 6485 6539 6346 6281 6280
6498 6497 6551 6334 6257 6256
6553 6499 6552 6253 6254 6178
20 6505 6504 6405 6327 6408
6532 6578 6579 6148 6065 6147

5819 6518 6519 6379 6313 6378
6607 6565 6564 6088 6165 6089
6517 6566 6518 6222 6221 6314
6482 6483 5906 6349 6452 6453
6536 6581 6537 6142 6141 6194
6492 6545 6546 6268 6185 6267
6587 6543 6542 6129 6188 6130
6552 6551 6596 6179 6112 6111
6496 6495 6549 6336 6261 6260
6479 6634 5847 5932 5933 6459
5849 6479 5847 6460 6459 5848
6608 6609 6566 6035 6085 6086
6516 5825 6515 6384 6385 6316
6562 6513 6561 6230 6231 6168
6589 6588 6624 6054 6006 6005
6564 6516 6515 6225 6316 6226
6608 6625 6624 5971 5948 5970
6570 6613 6571 6077 6076 6159
6492 6493 5886 6339 6432 6433
6616 6615 6618 5956 5957 5955
5876 6498 5874 6422 6421 5875
6502 6473 6474 6301 6358 6329
6508 5841 6507 6400 6401 6324
5902 6484 6485 6449 6347 6448
5876 6497 6498 6423 6334 6422
6629 6594 6593 5995 6049 5996
6574 6576 6529 6155 6154 6203
5797 5803 6636 5802 5925 5927
5821 5823 6517 5822 6382 6381
6590 6546 6545 6123 6185 6124
5847 6634 5801 5933 5935 5846
6478 6479 5849 6353 6460 6461
5859 6474 5861 6470 6469 5860
6580 6535 6599 6144 6064 6063
6490 5892 6489 6438 6439 6342
5896 5898 6487 5897 6444 6443
6593 6548 6592 6118 6119 6050
5912 14 6633 5913 5939 5938
6633 24 6503 5937 6409 5936
5872 6500 5870 6418 6417 5871
6629 6603 6630 5980 5981 5943
6629 6628 6604 5944 5978 5979
6604 6603 6629 6040 5980 5979
6630 6631 6595 5942 5992 5993
6596 6551 6595 6112 6113 6047
6576 6615 6616 6028 5956 6027
6529 5796 6527 6303 6361 6304
6526 5803 5805 6363 5804 6364
6561 6603 6604 6096 6040 6095
6520 6569 6521 6216 6215 6311
5815 5817 6520 5816 6376 6375
6570 6569 6612 6160 6079 6078
6621 6620 6612 5952 5962 5963
6508 6557 6509 6240 6239 6323
6508 5839 5841 6399 5840 6400
6617 6632 6600 5940 5986 5987

6535 6534 6555 6196 6175 6145
6633 6480 5912 5922 6458 5938
6588 6544 6543 6127 6187 6128
6545 6492 6491 6268 6340 6269
6476 6475 6530 6356 6300 6299
6517 6518 5821 6314 6380 6381
6480 5910 5912 6457 5911 6458
6534 6481 6480 6290 6351 6291
6509 5839 6508 6398 6399 6323
6511 6510 6559 6321 6236 6235
6510 5837 6509 6396 6397 6322
5878 5880 6496 5879 6426 6425
5904 6484 5902 6450 6449 5903
6636 5799 5797 5926 5800 5927
6526 6527 6636 6305 5920 5924
5825 5827 6515 5826 6386 6385
6574 6527 6526 6204 6305 6205
6567 6566 6609 6163 6085 6084
6559 6602 6560 6099 6098 6170
6631 6632 6596 5941 5990 5991
6631 6601 6632 5984 5985 5941
6627 6592 6591 5999 6051 6000
6617 6579 6578 6022 6065 6023
6605 6563 6562 6092 6167 6093
6611 6569 6568 6080 6161 6081
6616 6581 6580 6020 6062 6021
6546 6493 6492 6266 6339 6267
6597 6632 6617 5989 5940 5988
6512 6560 6561 6233 6169 6232
6510 5835 5837 6395 5836 6396
6522 5811 5813 6371 5812 6372
5815 6521 5813 6374 6373 5814
6557 6558 6509 6172 6238 6239
6542 6489 6488 6274 6343 6275
6487 6486 6540 6345 6279 6278
6500 6553 6554 6252 6177 6251
6550 6497 6496 6258 6335 6259
6537 6538 6484 6193 6283 6284
6566 6517 6565 6222 6223 6164
18 6505 20 6406 6405 19
5915 6528 6635 6359 5921 5929
6528 6556 6506 6200 6244 6302
6483 6484 5904 6348 6450 6451
6497 5878 6496 6424 6425 6335
6627 6605 6628 5976 5977 5945
6567 6519 6518 6219 6313 6220
5819 6519 5817 6378 6377 5818
6474 5859 5857 6470 5858 5918
6506 6635 6528 5928 5921 6302
6635 6506 16 5928 6404 5930
16 10 6635 15 5931 5930
5866 6474 5864 6412 6411 5865
6527 5799 6636 6362 5926 5920
6585 6586 6541 6057 6132 6133
6632 6601 6600 5985 6043 5986
6600 6579 6617 6044 6022 5987

6607	6606	6626	6037	5974	5973
6573	6615	6576	6072	6028	6071
6572	6614	6615	6074	6029	6073
6622	6621	6611	5951	5964	5965
6565	6517	6516	6223	6315	6224
6500	6501	5870	6331	6416	6417
6489	6542	6543	6274	6188	6273
6488	6489	5894	6343	6440	6441
6520	6521	5815	6311	6374	6375
6520	6519	6568	6312	6218	6217
6607	6626	6625	5973	5947	5972
6508	6533	6557	6241	6173	6240
6495	6496	5880	6336	6426	6427
6605	6627	6606	5976	5975	6038
6478	5849	5851	6461	5850	6462
6588	6587	6623	6055	6008	6007
6627	6591	6626	6000	6001	5946
6622	6586	6621	6010	6011	5951
6515	6563	6564	6227	6166	6226
6563	6606	6564	6091	6090	6166
6580	6581	6536	6062	6142	6143
6547	6493	6546	6265	6266	6184
6601	6559	6558	6100	6171	6101
6559	6510	6558	6236	6237	6171
6577	6580	6599	6025	6063	6069
6509	6558	6510	6238	6237	6322
6619	6614	6613	5959	6030	5960
6489	6543	6490	6273	6272	6342
5894	5896	6488	5895	6442	6441
6530	6501	6554	6249	6250	6176
6628	6592	6627	5998	5999	5945
5868	6501	6502	6415	6330	6414
6500	6554	6501	6251	6250	6331
6483	5904	5906	6451	5905	6452
5882	6495	5880	6428	6427	5881
6495	5882	6494	6428	6429	6337
6613	6614	6571	6030	6075	6076
6629	6593	6628	5996	5997	5944
6491	6492	5888	6340	6434	6435
6611	6621	6612	5964	5963	6032
6620	6621	6585	5952	6012	6013
6613	6612	6620	6031	5962	5961
6587	6622	6623	6009	5950	6008
6631	6602	6601	5983	6042	5984
6504	6505	6555	6327	6246	6245
6609	6624	6623	5969	5949	5968
6575	6556	6528	6151	6200	6201
6575	6577	6599	6152	6069	6068
6565	6516	6564	6224	6225	6165
6556	6505	6506	6243	6326	6244
6598	6617	6578	6024	6023	6066
6487	5898	6486	6444	6445	6345
6575	5796	6529	5919	6303	6202
6556	6599	6555	6106	6105	6174
6477	6531	6532	6297	6198	6296
6482	6536	6483	6287	6286	6349

6574	6525	6573	6206	6207	6156
6489	5892	5894	6439	5893	6440
6591	6546	6590	6122	6123	6052
6586	6542	6541	6131	6189	6132
6622	6611	6610	5965	6033	5966
6577	6576	6616	6070	6027	6026
6529	6576	6577	6154	6070	6153
6607	6564	6606	6089	6090	6037
6553	6597	6598	6109	6045	6108
6560	6602	6603	6098	6041	6097
6560	6603	6561	6097	6096	6169
6572	6571	6614	6158	6075	6074
6523	6571	6572	6211	6158	6210
6524	5807	5809	6367	5808	6368
5886	5888	6492	5887	6434	6433
6474	5866	6502	6412	6413	6329
5866	5868	6502	5867	6414	6413
6503	6504	6534	6328	6247	6292
6513	6514	5829	6318	6388	6389
5801	6634	5843	5935	5934	5844
6473	5861	6474	6472	6469	6358
6475	6476	5855	6356	6466	6467
5853	6477	5851	6464	6463	5852
5855	5845	6475	5856	6468	6467
6521	6522	5813	6310	6372	6373
6584	6620	6585	6014	6013	6058
6598	6578	6531	6066	6149	6067
6597	6617	6598	5988	6024	6045
6584	6585	6540	6058	6134	6135
6552	6597	6553	6110	6109	6178
6540	6541	6487	6190	6277	6278
6585	6541	6540	6133	6190	6134
6487	6541	6488	6277	6276	6344
5896	6487	6488	6443	6344	6442
6573	6525	6524	6207	6307	6208
5805	5807	6525	5806	6366	6365
6590	6589	6625	6053	6004	6003
5870	6501	5868	6416	6415	5869
6503	6480	6633	6352	5922	5936
6534	6480	6503	6291	6352	6292
5833	6512	5831	6392	6391	5832
6512	5833	6511	6392	6393	6320
5835	6511	5833	6394	6393	5834
6523	6524	5809	6308	6368	6369
5890	6490	6491	6437	6341	6436
5831	6512	6513	6391	6319	6390
6526	5805	6525	6364	6365	6306
5861	6473	5845	6472	6471	5862
5855	6476	5853	6466	6465	5854
6635	10	5915	5931	5914	5929
6596	6632	6597	5990	5989	6046
6596	6597	6552	6046	6110	6111
6584	6619	6620	6015	5953	6014
6624	6609	6608	5969	6035	5970
6607	6608	6565	6036	6087	6088
6540	6486	6539	6279	6280	6191

6577 6575 6529 6152 6202 6153
6631 6630 6602 5942 5982 5983
6602 6559 6601 6099 6100 6042
6562 6514 6513 6229 6318 6230
6513 5829 5831 6389 5830 6390
6526 6525 6574 6306 6206 6205
6624 6625 6589 5948 6004 6005
6574 6573 6576 6156 6071 6155
5827 5829 6514 5828 6388 6387
6615 6614 6618 6029 5958 5957
6594 6630 6595 5994 5993 6048
6631 6596 6595 5991 6047 5992
6583 6618 6619 6017 5954 6016
6539 6584 6540 6136 6135 6191
6607 6625 6608 5972 5971 6036
6535 6481 6534 6289 6290 6196
5890 5892 6490 5891 6438 6437
6593 6594 6549 6049 6116 6117
6582 6616 6618 6019 5955 6018
6582 6581 6616 6061 6020 6019
6582 6538 6537 6139 6193 6140
6549 6550 6496 6181 6259 6260
6603 6602 6630 6041 5982 5981
6550 6595 6551 6114 6113 6180
6558 6557 6600 6172 6103 6102
6544 6491 6490 6270 6341 6271
6545 6544 6589 6186 6126 6125
6625 6626 6590 5947 6002 6003
5878 6497 5876 6424 6423 5877
6613 6570 6612 6077 6078 6031
6571 6522 6570 6212 6213 6159
5890 6491 5888 6436 6435 5889
6518 5819 5821 6379 5820 6380
6628 6605 6604 5977 6039 5978
6503 22 6504 6410 6407 6328
6477 6478 5851 6354 6462 6463
6532 6531 6578 6198 6149 6148
6479 6533 6507 6293 6242 6325
6545 6589 6590 6125 6053 6124
6511 6560 6512 6234 6233 6320
6550 6551 6497 6180 6257 6258
6547 6591 6592 6121 6051 6120
6499 6500 5872 6332 6418 6419
6636 5803 6526 5925 6363 5924
6595 6550 6594 6114 6115 6048
6530 6531 6476 6199 6298 6299
6562 6563 6514 6167 6228 6229
5827 6514 6515 6387 6317 6386
5809 5811 6523 5810 6370 6369
6524 6525 5807 6307 6366 6367
6552 6499 6498 6254 6333 6255
6555 6505 6556 6246 6243 6174
6626 6591 6590 6001 6052 6002
6623 6622 6610 5950 5966 5967
6568 6610 6611 6082 6033 6081
6499 6553 6500 6253 6252 6332

5817	6519	6520	6377	6312	6376
6495	6548	6549	6262	6182	6261
6541	6542	6488	6189	6275	6276
6531	6554	6598	6150	6107	6067
5908	6482	5906	6454	6453	5907
6586	6622	6587	6010	6009	6056
6530	6554	6531	6176	6150	6199
5853	6476	6477	6465	6355	6464
6481	5908	5910	6455	5909	6456
6523	6572	6524	6210	6209	6308
6566	6565	6608	6164	6087	6086
6561	6513	6512	6231	6319	6232
6544	6490	6543	6271	6272	6187
6539	6538	6583	6192	6138	6137

9

240	244	239	186	185	195
237	239	244	187	185	189
242	243	244	184	183	169
233	234	242	200	192	202
135	234	137	219	218	136
237	238	239	197	168	187
240	162	160	206	161	207
242	234	243	192	166	184
235	234	246	167	175	174
246	234	135	175	219	177
147	238	237	210	197	213
239	238	245	168	173	179
243	234	235	166	167	190
236	237	244	198	189	188
126	232	129	171	228	128
141	232	126	226	171	142
157	245	238	181	173	196
238	143	157	172	158	196
245	157	155	181	156	182
135	133	246	134	178	177
241	242	244	193	169	170
239	164	162	208	163	209
149	236	151	215	214	150
237	236	149	198	215	212
235	151	236	217	214	199
236	243	235	191	190	199
244	243	236	183	191	188
233	231	232	222	225	223
241	244	240	170	186	194
231	242	241	201	193	203
145	238	147	211	210	146
233	137	234	221	218	200
233	139	137	220	138	221
233	242	231	202	201	222
241	240	160	194	207	204
127	241	160	205	204	159
147	237	149	213	212	148

153 246 133 176 178 154
232 141 139 226 140 224
164 239 245 208 179 180
162 240 239 206 195 209
245 155 164 182 165 180
127 231 241 229 203 205
127 131 231 132 230 229
145 143 238 144 172 211
153 151 235 152 217 216
246 153 235 176 216 174
232 231 131 225 230 227
232 139 233 224 220 223
129 232 131 228 227 130
16572 16660 16649 16658 16661 16656
16652 16647 16660 16653 16657 16662
16652 16437 16384 16655 16436 16651
16428 16437 16660 16438 16659 16654
16572 16649 16563 16656 16648 16573
16647 16649 16660 16650 16661 16657
16660 16572 16428 16658 16571 16654
16437 16652 16660 16655 16662 16659
16356 16303 16675 16357 16670 16674
16303 16667 16675 16666 16677 16670
16536 16675 16527 16673 16671 16535
16356 16536 16347 16669 16537 16355
16356 16675 16536 16674 16673 16669
16664 16667 16647 16672 16668 16665
16664 16675 16667 16676 16677 16672
16664 16527 16675 16663 16671 16676
16687 16464 16500 16682 16501 16689
16394 16384 16687 16393 16683 16688
16464 16687 16679 16682 16686 16680
16652 16647 16679 16653 16678 16681
16652 16679 16687 16681 16686 16685
16384 16652 16687 16651 16685 16683
16687 16500 16394 16689 16684 16688
16392 16394 16500 16395 16684 16499
16647 16667 16696 16668 16694 16692
16466 16696 16311 16698 16691 16465
16313 16667 16303 16690 16666 16312
16667 16313 16696 16690 16695 16694
16679 16466 16464 16693 16467 16680
16696 16466 16679 16698 16693 16697
16696 16679 16647 16697 16678 16692
16311 16696 16313 16691 16695 16314
16313 16303 17061 16312 17016 17015
17054 17055 17053 17037 17004 17039
17052 17061 16991 17013 17014 17047
17053 17056 17051 17034 17033 17043
17052 16989 17055 17048 17005 17038
17060 17058 6640 17010 17021 17019
16998 17051 17056 17045 17033 17006
17052 17055 17054 17038 17037 17040
17057 17059 17055 17025 17028 17026
17052 17054 17061 17040 17012 17013
17059 17053 17055 17027 17004 17028

16989 17052 16991 17048 17047 16990
17053 17058 17056 17002 17003 17034
17056 16994 16996 17031 16995 17032
17056 16996 16998 17032 16997 17006
16464 17051 17000 17007 17046 17001
16466 17051 16464 17049 17007 16467
16311 17051 16466 17050 17049 16465
6640 17058 6637 17021 17008 6639
6756 17057 143 17024 17009 6755
16991 17061 16303 17014 17016 16992
17055 16985 17057 17036 17029 17026
16987 17055 16989 17035 17005 16988
17054 17053 16311 17039 17044 17041
17060 16994 17056 17018 17031 17017
6638 17060 6640 17020 17019 6641
16994 17060 6638 17018 17020 16993
16983 17057 16985 17030 17029 16984
17057 17058 17059 17011 17023 17025
6756 6637 17058 6757 17008 17022
17058 17053 17059 17002 17027 17023
17054 16311 16313 17041 16314 17042
16313 17061 17054 17015 17012 17042
143 17057 16983 17009 17030 16982
17000 17051 16998 17046 17045 16999
17055 16987 16985 17035 16986 17036
17056 17058 17060 17003 17010 17017
6756 17058 17057 17022 17011 17024
16311 17053 17051 17044 17043 17050
7391 7437 7390 6973 6972 7033
6644 7484 7365 6775 6773 7227
7417 7461 7416 6924 6923 7007
7418 7462 7417 6922 6921 7006
7354 7353 6668 7170 7251 7248
151 149 7373 150 7211 7210
7416 7460 7415 6926 6925 7008
7442 7481 7441 6839 6838 6896
7340 7339 6715 7185 7279 7276
7418 7421 7462 7002 6918 6922
7467 7459 7460 6807 6878 6808
7419 7463 7420 6920 6919 7004
7473 7453 7454 6819 6884 6820
6662 6660 7357 6661 7243 7242
7411 7455 7410 6936 6935 7013
7390 7389 7335 7034 7124 7121
7340 7341 7395 7184 7112 7111
6713 7341 7340 7274 7184 7277
7340 6715 6713 7276 6714 7277
7377 7419 7367 7005 7061 7062
7346 7400 7371 7100 7054 7154
7370 7421 7418 7056 7002 7055
7457 7458 7469 6880 6812 6811
7455 7411 7456 6936 6933 6882
7390 7436 7389 6975 6974 7034
7393 7392 7338 7031 7118 7115
7438 7437 7391 6900 6973 6970
6684 7346 7485 7264 6769 6770

6674 7350 6676 7257 7256 6675
7402 7447 7446 6951 6891 6954
6662 7357 7356 7242 7167 7245
6666 7355 7354 7246 7169 7249
7370 7418 7365 7055 7065 6759
7364 7417 7363 7067 7066 7160
7441 7481 7480 6838 6785 6841
7481 7446 7480 6836 6833 6785
147 145 7375 146 7207 7206
7413 7458 7457 6929 6880 6932
7365 6646 6644 7226 6645 7227
7471 7432 7472 6859 6856 6794
7472 7473 7454 6793 6820 6817
7455 7456 7471 6882 6816 6815
7472 7455 7471 6818 6815 6794
7395 7442 7441 6962 6896 6965
7445 7401 7446 6956 6953 6892
153 7372 7483 7212 6768 6778
7446 7447 7480 6891 6834 6833
7471 7456 7470 6816 6813 6795
7433 7386 7387 6980 7037 6981
7468 7459 7467 6810 6807 6798
7469 7429 7430 6862 6908 6863
7468 7428 7429 6864 6909 6865
7471 7470 7431 6795 6861 6858
147 7374 149 7209 7208 148
7345 6637 7376 7267 7180 7179
7431 7385 7432 6985 6982 6906
7429 7383 7430 6989 6986 6908
7456 7412 7457 6934 6931 6881
7469 7470 7457 6796 6814 6811
7414 7360 7361 7072 7163 7073
7481 7464 7445 6801 6873 6835
7478 7449 7477 6830 6827 6788
7434 7388 7435 6979 6976 6903
7433 7387 7434 6981 6978 6904
7433 7473 7472 6854 6793 6857
7333 7332 6729 7192 7293 7290
7421 7420 7462 7003 6760 6918
7466 7467 7460 6799 6808 6805
7462 7420 7463 6760 6919 6874
7434 7474 7473 6852 6792 6855
7355 7409 7408 7082 7015 7085
7326 7381 7380 7139 7043 7142
7382 7381 7327 7042 7140 7137
7365 7364 6646 7159 7229 7226
7344 6707 6705 7268 6706 7269
7364 7418 7417 7064 7006 7067
7404 7350 7351 7092 7173 7093
7401 7402 7446 7022 6954 6953
7405 7450 7449 6945 6888 6948
7352 7406 7405 7088 7018 7091
7406 7353 7407 7089 7086 7017
7337 6719 7338 7283 7280 7187
7342 7341 6711 7183 7275 7272
7378 7323 7324 7145 7201 7146

6743 7326 7325 7304 7199 7307
7366 7322 7377 6758 7147 7063
7350 7349 6676 7174 7259 7256
7408 7407 7354 7016 7087 7084
6672 7352 7351 7252 7172 7255
6715 7339 6717 7279 7278 6716
7442 7443 7464 6895 6872 6837
7396 7342 7397 7110 7107 7027
7443 7442 7396 6895 6963 6960
7331 7386 7385 7129 7038 7132
7330 6735 6733 7296 6734 7297
7332 7387 7386 7127 7037 7130
7370 7369 7421 7155 7057 7056
6737 7328 6739 7301 7300 6738
7369 6690 6692 7218 6691 7219
7421 7369 7420 7057 7058 7003
7343 7344 7398 7181 7106 7105
7342 7343 7397 7182 7108 7107
7331 7330 6733 7194 7297 7294
7330 7331 7385 7194 7132 7131
7330 7385 7384 7131 7039 7134
7332 6731 6729 7292 6730 7293
7387 7333 7388 7128 7125 7036
7331 6731 7332 7295 7292 7193
7481 7442 7464 6839 6837 6801
7338 6719 6717 7280 6718 7281
7342 6709 7343 7273 7270 7182
6707 7343 6709 7271 7270 6708
7326 7327 7381 7198 7140 7139
7383 7329 7384 7136 7133 7040
6739 7328 7327 7300 7197 7303
6640 7371 6637 7215 7214 6639
7371 7422 6637 7053 6763 7214
6637 7422 7376 6763 7052 7180
7346 7347 7400 7177 7101 7100
6672 6670 7352 6671 7253 7252
7353 7352 6670 7171 7253 7250
7364 6648 6646 7228 6647 7229
6664 7355 6666 7247 7246 6665
7356 6664 6662 7244 6663 7245
6702 7321 7320 7316 7205 7319
7370 6688 6690 7216 6689 7217
6690 7369 7370 7218 7155 7217
7370 7484 6688 6765 6774 7216
7484 6642 6688 6776 6687 6774
6698 6753 7321 6754 7314 6764
6739 7327 6741 7303 7302 6740
6745 6743 7325 6744 7307 7306
6751 7322 7321 7312 7203 7315
6707 7344 7343 7268 7181 7271
7456 7457 7470 6881 6814 6813
7324 6747 6745 7308 6746 7309
7469 7458 7468 6812 6809 6797
7469 7468 7429 6797 6865 6862
7429 7428 7382 6909 6991 6988
7439 7440 7479 6898 6843 6842

7440 7441 7480 6897 6841 6840
7467 7428 7468 6867 6864 6798
7359 7358 6658 7165 7241 7238
7457 7412 7413 6931 7011 6932
7407 7408 7452 7016 6942 6941
7335 7389 7334 7124 7123 7190
7438 7477 7437 6847 6846 6900
7356 7355 6664 7168 7247 7244
7354 7355 7408 7169 7085 7084
145 7482 7375 6783 6781 7207
7434 7387 7388 6978 7036 6979
7352 7405 7351 7091 7090 7172
6648 7364 7363 7228 7160 7231
7329 7383 7328 7136 7135 7196
7329 7328 6737 7196 7301 7298
7340 7395 7394 7111 7029 7114
7332 7333 7387 7192 7128 7127
7420 7369 7368 7058 7156 7059
7367 7419 7368 7061 7060 7157
6640 7485 7371 6771 6766 7215
7483 133 153 6780 154 6778
7433 7434 7473 6904 6855 6854
7472 7454 7455 6817 6883 6818
7406 7450 7405 6946 6945 7018
7412 7359 7413 7077 7074 7011
7444 7443 7397 6894 6961 6958
7396 7397 7443 7027 6961 6960
7444 7399 7424 6761 7024 6957
7374 7423 7373 7049 7048 7151
7424 7443 7444 6893 6894 6957
7472 7432 7433 6856 6905 6857
7433 7432 7386 6905 6983 6980
7384 7385 7431 7039 6985 6984
7427 7466 7426 6869 6868 6911
7377 7378 7419 7046 6998 7005
7419 7425 7463 6913 6875 6920
7468 7458 7459 6809 6879 6810
7416 7363 7417 7069 7066 7007
7403 7447 7402 6952 6951 7021
7479 7447 7448 6831 6890 6832
7351 6674 6672 7254 6673 7255
7337 7336 6721 7188 7285 7282
6747 7324 7323 7308 7201 7311
7395 7341 7396 7112 7109 7028
7442 7395 7396 6962 7028 6963
7368 6692 6694 7220 6693 7221
7419 7420 7368 7004 7059 7060
7331 6733 6731 7294 6732 7295
7375 7374 147 7150 7209 7206
7444 7423 7399 6914 6999 6761
6721 6719 7337 6720 7283 7282
7338 6717 7339 7281 7278 7186
7382 7327 7328 7137 7197 7138
6684 7485 6638 6770 6772 6685
6640 6638 7485 6641 6772 6771
7353 6670 6668 7250 6669 7251

7368 7369 6692 7156 7219 7220
7326 6743 6741 7304 6742 7305
6756 7345 7482 7266 6767 6782
6705 133 7483 6704 6780 6779
7485 7346 7371 6769 7154 6766
6684 6682 7346 6683 7265 7264
7479 7478 7439 6787 6845 6842
7427 7467 7466 6866 6799 6869
7474 7475 7452 6791 6824 6821
7406 7407 7451 7017 6944 6943
7349 7403 7402 7094 7021 7097
7413 7360 7414 7075 7072 7010
7451 7450 7406 6887 6946 6943
7379 7425 7378 6997 6996 7045
7325 7379 7324 7144 7143 7200
7325 7380 7379 7141 7044 7144
7391 7336 7337 7119 7188 7120
7365 7418 7364 7065 7064 7159
7330 7329 6735 7195 7299 7296
7330 7384 7329 7134 7133 7195
7342 7396 7341 7110 7109 7183
6711 7341 6713 7275 7274 6712
6678 7348 6680 7261 7260 6679
7336 7391 7390 7119 7033 7122
7345 7376 7399 7179 7104 7103
7482 7345 7375 6767 7178 6781
145 143 7482 144 6784 6783
7451 7452 7475 6886 6824 6823
7435 7475 7474 6850 6791 6853
7454 7453 7409 6884 6940 6937
7473 7474 7453 6792 6822 6819
7438 7392 7439 6971 6968 6899
7466 7461 7465 6806 6803 6800
7462 7463 7465 6874 6802 6804
7465 7426 7466 6871 6868 6800
7411 7410 7357 7013 7081 7078
7456 7411 7412 6933 7012 6934
7444 7397 7398 6958 7026 6959
7343 7398 7397 7105 7026 7108
7430 7431 7470 6907 6861 6860
7471 7431 7432 6858 6906 6859
7430 7384 7431 6987 6984 6907
7432 7385 7386 6982 7038 6983
7405 7449 7404 6948 6947 7019
7414 7361 7415 7073 7070 7009
7414 7459 7458 6927 6879 6930
6650 7363 7362 7230 7161 7233
7377 7323 7378 7148 7145 7046
7325 7324 6745 7200 7309 7306
7373 7398 7372 7051 7050 7153
7484 6644 6642 6775 6643 6776
7321 6700 6698 7317 6699 6764
7321 6702 6700 7316 6701 7317
7321 6753 6751 7314 6752 7315
6637 7345 6756 7267 7266 6757
7463 7425 7465 6875 6870 6802

7425	7419	7378	6913	6998	6996
7450	7451	7476	6887	6826	6825
7477	7450	7476	6828	6825	6789
7451	7407	7452	6944	6941	6886
7424	7376	7464	7025	6762	6915
7380	7325	7326	7141	7199	7142
7379	7378	7324	7045	7146	7143
7440	7480	7479	6840	6786	6843
7391	7392	7438	7032	6971	6970
7337	7392	7391	7117	7032	7120
7390	7335	7336	7121	7189	7122
7424	7399	7376	7024	7104	7025
7371	7400	7422	7054	7001	7053
7445	7422	7400	6917	7001	6955
7445	7400	7401	6955	7023	6956
6737	6735	7329	6736	7299	7298
7332	7386	7331	7130	7129	7193
7359	7412	7358	7077	7076	7165
7475	7436	7476	6851	6848	6790
7476	7451	7475	6826	6823	6790
7437	7477	7476	6846	6789	6849
7390	7437	7436	6972	6901	6975
7424	7464	7443	6915	6872	6893
7356	7357	7410	7167	7081	7080
7408	7409	7453	7015	6940	6939
7462	7465	7461	6804	6803	6876
7415	7362	7416	7071	7068	7008
7404	7351	7405	7093	7090	7019
7449	7478	7448	6830	6829	6889
7426	7465	7425	6871	6870	6912
7413	7414	7458	7010	6930	6929
6652	7362	7361	7232	7162	7235
153	151	7372	152	7213	7212
7361	6654	6652	7234	6653	7235
7403	7349	7350	7094	7174	7095
6680	7348	7347	7260	7176	7263
7335	6725	6723	7286	6724	7287
7334	6727	6725	7288	6726	7289
7320	7321	7322	7205	7203	7149
7423	7398	7373	7000	7051	7048
7445	7446	7481	6892	6836	6835
7320	7366	6686	7204	7225	7318
6696	6686	7366	6697	7225	7224
6694	6696	7367	6695	7223	7222
7352	7353	7406	7171	7089	7088
6694	7367	7368	7222	7157	7221
7438	7439	7478	6899	6845	6844
7408	7453	7452	6939	6885	6942
7380	7427	7426	6992	6911	6995
7338	7392	7337	7118	7117	7187
7445	7464	7422	6873	6916	6917
7374	7375	7399	7150	7102	7047
7348	6678	7349	7261	7258	7175
7349	7402	7348	7097	7096	7175
7361	7360	6654	7163	7237	7234
7360	6656	6654	7236	6655	7237

7336 6723 6721 7284 6722 7285
7398 7423 7444 7000 6914 6959
7372 7398 7344 7050 7106 7152
6756 7482 143 6782 6784 6755
7435 7389 7436 6977 6974 6902
7435 7436 7475 6902 6851 6850
7356 7409 7355 7083 7082 7168
7410 7409 7356 7014 7083 7080
7416 7461 7460 6923 6877 6926
7460 7461 7466 6877 6806 6805
7403 7448 7447 6949 6890 6952
7404 7448 7403 6950 6949 7020
7479 7448 7478 6832 6829 6787
7430 7470 7469 6860 6796 6863
6676 7349 6678 7259 7258 6677
7334 7333 6727 7191 7291 7288
7435 7388 7389 6976 7035 6977
7334 6725 7335 7289 7286 7190
7389 7388 7334 7035 7126 7123
7440 7394 7441 6967 6964 6897
7428 7381 7382 6990 7042 6991
7427 7428 7467 6910 6867 6866
7381 7428 7427 6990 6910 6993
7393 7339 7394 7116 7113 7030
7394 7339 7340 7113 7185 7114
7439 7393 7440 6969 6966 6898
7347 6682 6680 7262 6681 7263
7348 7401 7347 7099 7098 7176
7401 7400 7347 7023 7101 7098
7322 6751 6749 7312 6750 7313
7323 7322 6749 7202 7313 7310
7323 6749 6747 7310 6748 7311
6658 7358 6660 7241 7240 6659
6660 7358 7357 7240 7166 7243
6702 7320 6686 7319 7318 6703
7366 7367 6696 7158 7223 7224
7395 7441 7394 6965 6964 7029
7394 7440 7393 6967 6966 7030
7454 7410 7455 6938 6935 6883
7410 7454 7409 6938 6937 7014
7382 7328 7383 7138 7135 7041
7464 7376 7422 6762 7052 6916
7411 7357 7358 7078 7166 7079
7366 7320 7322 7204 7149 6758
7377 7322 7323 7147 7202 7148
7462 7461 7417 6876 6924 6921
7379 7426 7425 6994 6912 6997
7460 7459 7415 6878 6928 6925
7380 7381 7427 7043 6993 6992
7414 7415 7459 7009 6928 6927
7383 7384 7430 7040 6987 6986
7429 7382 7383 6988 7041 6989
7388 7333 7334 7125 7191 7126
7480 7447 7479 6834 6831 6786
7449 7448 7404 6889 6950 6947
7439 7392 7393 6968 7031 6969

7338 7339 7393 7186 7116 7115
7404 7403 7350 7020 7095 7092
7435 7474 7434 6853 6852 6903
7370 7365 7484 6759 6773 6765
7350 6674 7351 7257 7254 7173
6666 7354 6668 7249 7248 6667
7354 7407 7353 7087 7086 7170
151 7373 7372 7210 7153 7213
7373 149 7374 7211 7208 7151
7359 6658 6656 7238 6657 7239
7327 7326 6741 7198 7305 7302
6682 7347 7346 7262 7177 7265
7411 7358 7412 7079 7076 7012
7380 7426 7379 6995 6994 7044
7375 7345 7399 7178 7103 7102
7399 7423 7374 6999 7049 7047
7362 6652 6650 7232 6651 7233
7363 7416 7362 7069 7068 7161
7362 7415 7361 7071 7070 7162
7363 6650 6648 7230 6649 7231
7335 6723 7336 7287 7284 7189
7342 6711 6709 7272 6710 7273
7437 7476 7436 6849 6848 6901
7477 7449 7450 6827 6888 6828
7478 7477 7438 6788 6847 6844
7366 7377 7367 7063 7062 7158
7333 6729 6727 7290 6728 7291
7483 7372 7344 6768 7152 6777
6705 7483 7344 6779 6777 7269
6656 7360 7359 7236 7164 7239
7453 7474 7452 6822 6821 6885
7359 7360 7413 7164 7075 7074
7348 7402 7401 7096 7022 7099
5504 5402 5508 5471 5440 5438
5502 5408 5406 5474 5407 5475
5504 5404 5402 5470 5403 5471
5507 5497 5506 5452 5453 5442
5503 5507 5502 5444 5443 5457
5505 5504 5508 5449 5438 5433
5503 5502 5406 5457 5475 5472
5506 5501 5502 5445 5459 5446
5507 5504 5498 5429 5450 5451
5494 1999 1997 5482 1998 5483
5500 5499 1995 5460 5481 5478
5497 5498 5420 5464 5485 5486
5502 5501 5408 5459 5477 5474
5509 5501 5500 5432 5458 5434
5508 5402 5400 5440 5401 5441
5509 5500 1993 5434 5479 5436
5412 5505 5414 5431 5461 5415
5500 1995 1993 5478 1994 5479
5505 5508 5414 5433 5439 5461
5496 5506 5497 5454 5453 5465
5506 5502 5507 5446 5443 5442
5506 5496 5499 5454 5455 5447
5499 1997 1995 5480 1996 5481

5497 5507 5498 5452 5451 5464
5422 5416 5496 5423 5489 5488
5425 5427 5494 5426 5493 5492
5495 5499 5496 5467 5455 5466
5503 5406 5404 5472 5405 5473
1990 5410 5509 5411 5435 5437
5494 1997 5499 5483 5480 5468
5498 5418 5420 5484 5419 5485
5494 5495 5425 5469 5491 5492
5416 5425 5495 5424 5491 5490
1990 5509 1993 5437 5436 1992
5410 5501 5509 5476 5432 5435
5414 5508 5400 5439 5441 5413
5408 5501 5410 5477 5476 5409
5505 5412 5418 5431 5417 5462
5416 5495 5496 5490 5466 5489
5497 5422 5496 5487 5488 5465
5422 5497 5420 5487 5486 5421
5505 5418 5498 5462 5484 5463
1991 1999 5494 2000 5482 5430
1991 5494 5427 5430 5493 5428
5494 5499 5495 5468 5467 5469
5505 5498 5504 5463 5450 5449
5504 5503 5404 5456 5473 5470
5500 5506 5499 5448 5447 5460
5507 5503 5504 5444 5456 5429
5500 5501 5506 5458 5445 5448
9600 17615 9598 17582 17565 9601
17614 5400 17549 17566 17548 17586
16994 17613 16996 17589 17588 16995
17614 17551 17612 17587 17592 17580
17615 17610 17613 17559 17590 17560
17608 17613 17610 17591 17590 17601
17614 17615 9600 17568 17582 17579
9600 5400 17614 9599 17566 17579
17555 17612 17553 17562 17593 17554
16392 17611 16394 17599 17598 16395
16392 17610 17611 17600 17597 17599
16998 17608 17000 17605 17604 16999
17614 17549 17551 17586 17550 17587
6638 17617 16994 17577 17576 16993
17609 17557 17618 17603 17572 17570
17608 16464 17000 17564 17001 17604
17609 17555 17557 17602 17556 17603
17616 17615 17614 17583 17568 17581
17610 17616 17612 17585 17584 17561
17614 17612 17616 17580 17584 17581
16998 16996 17613 16997 17588 17563
17612 17611 17610 17595 17597 17561
17611 17618 16394 17569 17571 17598
17555 17609 17612 17602 17594 17562
17618 16384 16394 17573 16393 17571
17557 16384 17618 17558 17573 17572
17610 16392 17608 17600 17606 17601
16392 16500 17608 16499 17607 17606
16994 17617 17613 17576 17574 17589

17617 6638 9603 17577 9602 17575
16464 17608 16500 17564 17607 16501
16998 17613 17608 17563 17591 17605
9603 9598 17615 9604 17565 17578
17611 17612 17609 17595 17594 17596
17615 17617 9603 17567 17575 17578
17612 17551 17553 17592 17552 17593
17618 17611 17609 17569 17596 17570
17615 17613 17617 17560 17574 17567
17610 17615 17616 17559 17583 17585
18109 18108 18106 18071 18051 18072
18105 16437 16428 18054 16438 18083
18106 18101 18045 18080 18094 18084
18107 17551 17553 18076 17552 18053
5412 5414 18111 5415 18061 18063
18110 5414 5400 18066 5413 18067
18102 17557 16384 18096 17558 18056
16437 18105 18102 18054 18087 18089
18045 18047 18106 18046 18085 18084
16384 16437 18102 16436 18089 18056
18111 18036 5412 18062 18039 18063
17549 17551 18107 17550 18076 18075
18107 17553 18104 18053 18090 18081
16428 16572 18101 16571 18100 18099
18107 18104 18105 18081 18086 18082
18104 18102 18105 18088 18087 18086
17555 18102 18104 18095 18088 18091
18109 18049 18037 18069 18050 18057
18109 18036 18111 18068 18062 18060
17549 18110 5400 18065 18067 17548
18045 18101 18043 18094 18098 18044
18107 18105 18103 18082 18078 18052
18106 18103 18101 18079 18093 18080
17553 17555 18104 17554 18091 18090
17555 17557 18102 17556 18096 18095
16572 16563 18101 16573 18055 18100
18106 18049 18109 18077 18069 18072
18043 18101 18041 18098 18097 18042
18105 16428 18103 18083 18092 18078
18037 18036 18109 18038 18068 18057
18041 18101 16563 18097 18055 18040
18108 18110 18107 18059 18064 18073
18107 18103 18108 18052 18074 18073
18111 5414 18108 18061 18070 18058
18110 18108 5414 18059 18070 18066
18103 16428 18101 18092 18099 18093
18108 18103 18106 18074 18079 18051
17549 18107 18110 18075 18064 18065
18106 18047 18049 18085 18048 18077
18109 18111 18108 18060 18058 18071
10297 10334 10296 9706 9705 9760
10264 10263 10213 9878 9946 9943
10330 10331 10310 9657 9687 9684
10334 10335 10306 9653 9695 9692
10323 10322 10285 9665 9730 9727
10186 10187 10239 10057 9996 9995

10272 10273 10316 9869 9789 9788
10196 10248 10195 9978 9977 10048
10322 10318 10319 9668 9737 9669
10284 10322 10321 9729 9666 9731
10281 10235 10282 9860 9857 9776
10285 10322 10284 9730 9729 9772
10315 10272 10316 9791 9788 9740
10215 10216 10266 10027 9940 9939
10332 10331 10294 9656 9712 9709
10229 10258 10206 9911 9958 10012
10277 10280 10301 9864 9780 9623
10248 10196 10249 9978 9975 9893
10246 10247 10291 9895 9839 9838
10282 10235 10236 9857 9906 9858
6668 10216 10215 10098 10027 10101
10234 10235 10281 9907 9860 9859
10245 10193 10246 9984 9981 9896
10310 10331 10309 9687 9686 9746
10323 10318 10322 9671 9668 9665
10194 2098 2096 10142 2097 10143
10287 10286 10242 9770 9849 9846
10190 10243 10242 9987 9899 9990
10242 10241 10189 9900 9992 9989
10320 10301 10280 9735 9780 9753
10335 10297 10298 9703 9759 9704
10303 10280 10259 9815 9624 9816
10218 10269 10268 9933 9873 9936
9600 10228 10337 10074 9626 9648
10290 10291 10328 9766 9718 9717
10228 10232 10337 10014 9647 9626
10258 10230 10279 9912 9909 9862
2072 10206 2074 10119 10118 2073
10250 10197 10198 9973 10046 9974
10302 10277 10301 9779 9623 9755
10340 10179 10227 9635 10015 9629
10229 5408 10230 10073 10070 10013
2072 10338 10206 9645 9643 10119
10252 10253 10297 9889 9827 9826
10258 10302 10257 9622 9817 9884
10229 10206 10338 10012 9643 9628
10247 10292 10291 9836 9765 9839
10269 10313 10312 9794 9743 9797
10332 10294 10295 9709 9762 9710
10226 10227 10234 10016 9918 9917
10244 10288 10243 9845 9844 9898
10329 10312 10328 9683 9680 9659
10271 10270 10220 9871 9932 9929
10249 10197 10250 9976 9973 9892
10309 10331 10332 9686 9656 9689
10334 10297 10335 9706 9703 9653
10300 10255 10256 9820 9886 9821
10303 10259 10260 9816 9882 9814
10286 10285 10241 9771 9851 9848
10282 10236 10283 9858 9775 9774
10315 10316 10325 9740 9675 9674
10201 10200 2084 10043 10131 10128

10197 10249 10196 9976 9975 10047
10200 10253 10252 9967 9889 9970
10334 10333 10296 9654 9708 9705
10333 10295 10296 9707 9761 9708
10331 10293 10294 9711 9763 9712
10284 10321 10283 9731 9732 9773
10234 10227 10179 9918 10015 10007
10282 10283 10321 9774 9732 9734
10326 10327 10314 9661 9679 9676
10312 10311 10268 9744 9799 9796
10330 10292 10293 9713 9764 9714
10204 10205 10257 10039 9960 9959
10253 10298 10297 9824 9759 9827
10261 10305 10304 9810 9751 9813
10304 10336 10320 9696 9651 9698
10325 10324 10287 9663 9726 9723
10223 10224 10274 10019 9924 9923
10325 10316 10324 9675 9672 9663
6658 6656 10221 6657 10089 10088
10326 10288 10289 9721 9768 9722
10225 10275 10224 9922 9921 10018
10274 10275 10318 9867 9785 9784
10319 10281 10321 9736 9733 9667
10210 10261 10260 9949 9881 9952
10261 10210 10211 9949 10032 9950
10263 10262 10212 9879 9948 9945
10211 10262 10261 9947 9880 9950
10306 10262 10263 9808 9879 9809
10261 10262 10305 9880 9811 9810
10330 10293 10331 9714 9711 9657
10250 10295 10294 9830 9762 9833
10292 10247 10248 9836 9894 9837
10293 10248 10249 9834 9893 9835
10243 10288 10287 9844 9769 9847
10219 10270 10269 9931 9872 9934
10312 10268 10269 9796 9873 9797
10314 10313 10270 9742 9795 9792
6664 6662 10218 6663 10095 10094
10205 10258 10257 9957 9884 9960
10302 10301 10257 9755 9819 9817
10230 10258 10229 9912 9911 10013
10279 10278 10302 9861 9778 9777
10230 5406 10231 10071 10068 10011
10244 10245 10289 9897 9843 9842
10290 10245 10246 9840 9896 9841
10236 10238 10283 9856 9854 9775
10182 10236 10181 10004 10003 10062
10271 10272 10315 9870 9791 9790
10221 10271 10220 9930 9929 10022
10317 10273 10274 9786 9868 9787
10233 10280 10277 9883 9864 9916
2086 10199 2088 10133 10132 2087
2094 10195 2096 10141 10140 2095
10293 10249 10294 9835 9832 9763
10249 10250 10294 9892 9833 9832
10188 10241 10240 9991 9901 9994

10192 10193 10245 10051 9984 9983
10184 2118 2116 10162 2117 10163
2112 2110 10187 2111 10157 10156
10238 10236 10237 9856 9905 9904
10185 10238 10237 9997 9904 10000
6652 6650 10224 6651 10083 10082
10276 10275 10225 9866 9922 9919
10264 10213 10214 9943 10029 9944
2076 10204 2078 10123 10122 2077
10252 10296 10251 9829 9828 9890
10200 10199 2086 10044 10133 10130
2080 10202 2082 10127 10126 2081
10188 10187 2110 10056 10157 10154
10187 10188 10240 10056 9994 9993
5408 5406 10230 5407 10071 10070
10218 6662 10219 10095 10092 10024
10194 10193 2098 10050 10145 10142
10191 2102 10192 10149 10146 10052
10190 10191 10243 10053 9988 9987
10247 10246 10194 9895 9982 9979
10183 9605 10178 10167 10176 10065
5402 5400 10337 5401 9650 9649
10277 10302 10278 9779 9778 9863
5402 10337 10232 9649 9647 10067
10277 9598 10233 9625 10036 9916
10207 10233 9598 10037 10036 10116
9603 6638 10341 9602 9634 9633
10207 9603 10341 10117 9633 9631
6674 10213 10212 10104 10030 10107
10265 10266 10309 9876 9803 9802
6656 6654 10222 6655 10087 10086
6660 10220 10219 10090 10023 10093
6654 6652 10223 6653 10085 10084
6658 10220 6660 10091 10090 6659
10184 10178 2118 10060 10165 10162
9618 10178 9605 10177 10176 9617
9615 10179 10340 10174 9635 9636
10312 10313 10328 9743 9681 9680
10228 9600 9598 10074 9601 10075
2100 10193 10192 10144 10051 10147
10178 10184 10183 10060 10009 10065
10237 10236 10182 9905 10004 10001
10186 10185 2114 10058 10161 10158
10185 10186 10238 10058 9998 9997
2112 10186 2114 10159 10158 2113
10185 10237 10184 10000 9999 10059
10229 10338 5410 9628 9644 10072
10221 10222 10272 10021 9928 9927
10320 10299 10300 9699 9757 9700
10304 10303 10260 9752 9814 9812
10326 10315 10325 9677 9674 9662
10274 10318 10317 9784 9738 9787
10272 10271 10221 9870 9930 9927
10265 10309 10308 9802 9747 9805
10307 10263 10264 9806 9878 9807
10225 10224 6650 10018 10083 10080

10318 10275 10319 9785 9782 9737
10314 10327 10313 9679 9678 9742
10182 10183 10237 10061 10002 10001
6664 10218 10217 10094 10025 10097
6674 10212 6676 10107 10106 6675
6670 10215 10214 10100 10028 10103
10263 10212 10213 9945 10030 9946
10225 6650 6648 10080 6649 10081
10189 2108 2106 10152 2107 10153
10287 10242 10243 9846 9899 9847
2080 2078 10203 2079 10125 10124
2080 10203 10202 10124 10041 10127
6662 6660 10219 6661 10093 10092
10232 5404 5402 10066 5403 10067
10209 10260 10259 9951 9882 9954
10178 10339 2120 9630 9640 10164
10307 10334 10306 9693 9692 9749
10295 10333 10332 9707 9655 9710
10311 10310 10267 9745 9801 9798
10267 10216 10217 9937 10026 9938
10218 10268 10217 9936 9935 10025
10317 10323 10324 9670 9664 9673
10304 10260 10261 9812 9881 9813
10336 10299 10320 9702 9699 9651
10329 10292 10330 9716 9713 9658
10292 10329 10291 9716 9715 9765
10292 10248 10293 9837 9834 9764
10226 10276 10225 9920 9919 10017
10276 10234 10281 9865 9859 9781
10281 10282 10321 9776 9734 9733
10270 10313 10269 9795 9794 9872
10204 2076 10205 10123 10120 10039
10204 10257 10256 9959 9885 9962
10256 10301 10300 9818 9756 9821
10257 10301 10256 9819 9818 9885
10192 10245 10244 9983 9897 9986
5404 10231 5406 10069 10068 5405
10279 10230 10231 9909 10011 9910
10278 10232 10228 9913 10014 9914
10231 10232 10278 10010 9913 9908
10207 10259 10233 9956 9955 10037
10207 10208 10259 10034 9953 9956
10341 10208 10207 9627 10034 9631
10223 6652 10224 10085 10082 10019
10211 10212 10262 10031 9948 9947
6676 10212 10211 10106 10031 10109
10211 10210 6678 10032 10111 10108
6678 6676 10211 6677 10109 10108
10275 10274 10224 9867 9924 9921
5410 5408 10229 5409 10073 10072
10217 10268 10267 9935 9874 9938
10328 10327 10290 9660 9720 9717
2102 2100 10192 2101 10147 10146
2100 2098 10193 2099 10145 10144
10182 9609 9607 10168 9608 10169
10231 5404 10232 10069 10066 10010

10207 9598 9603 10116 9604 10117
10183 9607 9605 10166 9606 10167
10181 9611 9609 10170 9610 10171
10225 6648 10226 10081 10078 10017
2120 10339 2067 9640 9642 2121
9620 10339 9618 9641 9639 9619
10191 10192 10244 10052 9986 9985
2104 2102 10191 2103 10149 10148
10190 2106 2104 10150 2105 10151
1990 5410 10338 5411 9644 9646
10239 10283 10238 9855 9854 9903
10336 10305 10335 9697 9694 9652
10255 10254 10202 9887 9966 9963
10298 10254 10299 9825 9822 9758
10317 10318 10323 9738 9671 9670
10259 10208 10209 9953 10035 9954
10210 10260 10209 9952 9951 10033
10273 10272 10222 9869 9928 9925
10308 10332 10333 9688 9655 9691
10309 10332 10308 9689 9688 9747
2116 10185 10184 10160 10059 10163
10198 10199 10251 10045 9972 9971
6638 6684 10341 6685 9632 9634
10214 6672 6670 10102 6671 10103
10190 2104 10191 10151 10148 10053
10204 10256 10203 9962 9961 10040
10341 6684 10208 9632 10114 9627
6682 10208 6684 10115 10114 6683
6656 10222 10221 10086 10021 10089
10220 6658 10221 10091 10088 10022
2120 2118 10178 2119 10165 10164
10339 10178 9618 9630 10177 9639
2094 10196 10195 10138 10048 10141
10330 10310 10311 9684 9745 9685
10276 10281 10319 9781 9736 9783
10319 10321 10322 9667 9666 9669
10214 10215 10265 10028 9942 9941
10264 10308 10307 9804 9748 9807
10266 10267 10310 9875 9801 9800
10241 10242 10286 9900 9849 9848
10189 10190 10242 10054 9990 9989
10324 10316 10317 9672 9739 9673
10316 10273 10317 9789 9786 9739
10290 10246 10291 9841 9838 9766
10291 10329 10328 9715 9659 9718
10279 10231 10278 9910 9908 9861
10258 10279 10302 9862 9777 9622
10203 10256 10255 9961 9886 9964
10206 10205 2074 10038 10121 10118
10194 2096 10195 10143 10140 10049
10196 2094 2092 10138 2093 10139
2090 2088 10198 2089 10135 10134
9598 10277 10228 9625 9915 10075
10228 10277 10278 9915 9863 9914
6666 10217 10216 10096 10026 10099
10215 10266 10265 9939 9876 9942

6664 10217 6666 10097 10096 6665
6644 6642 10340 6643 9638 9637
10336 10304 10305 9696 9751 9697
6678 10210 6680 10111 10110 6679
10183 10182 9607 10061 10169 10166
9615 10340 6642 9636 9638 9616
10241 10285 10240 9851 9850 9901
10336 10335 10298 9652 9704 9701
10222 10223 10273 10020 9926 9925
10310 10309 10266 9746 9803 9800
10233 10259 10280 9955 9624 9883
10220 10270 10219 9932 9931 10023
2116 2114 10185 2115 10161 10160
10239 10238 10186 9903 9998 9995
10216 10267 10266 9937 9875 9940
10252 10199 10200 9969 10044 9970
2088 10199 10198 10132 10045 10135
2090 10198 10197 10134 10046 10137
10334 10307 10333 9693 9690 9654
10295 10250 10251 9830 9891 9831
10235 10234 10180 9907 10008 10005
6644 10340 10227 9637 9629 10077
10203 2078 10204 10125 10122 10040
6682 6680 10209 6681 10113 10112
10209 6680 10210 10113 10110 10033
6682 10209 10208 10112 10035 10115
10320 10303 10304 9754 9752 9698
10300 10301 10320 9756 9735 9700
10303 10320 10280 9754 9753 9815
10264 10265 10308 9877 9805 9804
10252 10297 10296 9826 9760 9829
10284 10283 10239 9773 9855 9852
10239 10187 10240 9996 9993 9902
10314 10271 10315 9793 9790 9741
10289 10245 10290 9843 9840 9767
10203 10255 10202 9964 9963 10041
10189 2106 10190 10153 10150 10054
10189 10241 10188 9992 9991 10055
6644 10227 6646 10077 10076 6645
10215 6670 6668 10100 6669 10101
9611 10181 10180 10170 10063 10173
10180 10234 10179 10008 10007 10064
10179 9613 10180 10175 10172 10064
10180 9613 9611 10172 9612 10173
10197 2092 2090 10136 2091 10137
10324 10323 10286 9664 9728 9725
10308 10333 10307 9691 9690 9748
10240 10285 10284 9850 9772 9853
10251 10199 10252 9972 9969 9890
10326 10325 10288 9662 9724 9721
10226 10234 10276 9917 9865 9920
10319 10275 10276 9782 9866 9783
10330 10311 10329 9685 9682 9658
10239 10240 10284 9902 9853 9852
10314 10270 10271 9792 9871 9793
10314 10315 10326 9741 9677 9676

10289 10327 10326 9719 9661 9722
10290 10327 10289 9720 9719 9767
10201 10253 10200 9968 9967 10043
10201 10202 10254 10042 9966 9965
2108 10188 2110 10155 10154 2109
6648 6646 10226 6647 10079 10078
10214 10265 10264 9941 9877 9944
6672 10213 6674 10105 10104 6673
9613 10179 9615 10175 10174 9614
10254 10253 10201 9888 9968 9965
10299 10254 10255 9822 9887 9823
10287 10288 10325 9769 9724 9723
10262 10306 10305 9808 9750 9811
5400 9600 10337 9599 9648 9650
2067 10339 9620 9642 9641 9621
10328 10313 10327 9681 9678 9660
10298 10253 10254 9824 9888 9825
10288 10244 10289 9845 9842 9768
10336 10298 10299 9701 9758 9702
10306 10335 10305 9695 9694 9750
10236 10235 10181 9906 10006 10003
10180 10181 10235 10063 10006 10005
10307 10306 10263 9749 9809 9806
2076 2074 10205 2075 10121 10120
10251 10296 10295 9828 9761 9831
10213 6672 10214 10105 10102 10029
2084 10200 2086 10131 10130 2085
10201 2084 2082 10128 2083 10129
10223 10274 10273 9923 9868 9926
10223 10222 6654 10020 10087 10084
10187 10186 2112 10057 10159 10156
2092 10197 10196 10136 10047 10139
10193 10194 10246 10050 9982 9981
10247 10194 10195 9979 10049 9980
10248 10247 10195 9894 9980 9977
10181 9609 10182 10171 10168 10062
10237 10183 10184 10002 10009 9999
10244 10243 10191 9898 9988 9985
10218 10219 10269 10024 9934 9933
10188 2108 10189 10155 10152 10055
10250 10198 10251 9974 9971 9891
10338 2072 1990 9645 2071 9646
10258 10205 10206 9957 10038 9958
6668 6666 10216 6667 10099 10098
10202 10201 2082 10042 10129 10126
10227 10226 6646 10016 10079 10076
10267 10268 10311 9874 9799 9798
10255 10300 10299 9820 9757 9823
10329 10311 10312 9682 9744 9683
10285 10286 10323 9771 9728 9727
10324 10286 10287 9725 9770 9726
18690 18702 18763 18703 18722 18711
143 18765 157 18717 18716 158
18764 18762 18763 18712 18725 18718
18755 18700 18698 18749 18699 18750
18692 18760 18694 18731 18739 18693

18761 18758 18759 18735 18740 18736
18758 18756 18759 18742 18741 18740
18759 16356 16347 18708 16355 18737
18765 16983 18761 18715 18729 18714
18756 16303 16356 18709 16357 18743
18758 16987 16989 18744 16988 18745
18757 18755 18760 18747 18734 18733
18755 16527 18700 18710 18701 18749
18755 18696 18760 18748 18738 18734
18702 18764 18763 18720 18718 18722
18761 16983 16985 18729 16984 18730
18755 18698 18696 18750 18697 18748
18763 18760 18692 18726 18731 18723
16356 18759 18756 18708 18741 18743
18761 16985 16987 18730 16986 18707
18756 16991 16303 18752 16992 18709
18756 18758 16989 18742 18745 18751
16991 18756 16989 18752 18751 16990
18702 155 18764 18704 18721 18720
155 157 18764 156 18719 18721
18755 16536 16527 18754 16535 18710
18765 143 16983 18717 16982 18715
18762 157 18765 18724 18716 18713
18694 18760 18696 18739 18738 18695
18755 18757 16347 18747 18746 18753
16987 18758 18761 18744 18735 18707
16347 16536 18755 16537 18754 18753
18765 18761 18762 18714 18727 18713
18763 18692 18690 18723 18691 18711
18759 16347 18757 18737 18746 18732
18763 18762 18760 18725 18705 18726
157 18762 18764 18724 18712 18719
18757 18760 18762 18733 18705 18728
18762 18761 18757 18727 18706 18728
18761 18759 18757 18736 18732 18706

5 63 5 63 37 37 5 63 63 5 19 19 5 17 9 17 17 17 5 19 19

1

26 326 327 328 126

2

126 142 141 140 139 138 137 136 135 134
133 6704 6705 6706 6707 6708 6709 6710 6711 6712
6713 6714 6715 6716 6717 6718 6719 6720 6721 6722
6723 6724 6725 6726 6727 6728 6729 6730 6731 6732
6733 6734 6735 6736 6737 6738 6739 6740 6741 6742
6743 6744 6745 6746 6747 6748 6749 6750 6751 6752
6753 6754 6698

3

5857 7564 7565 7566 6698

4

26 27 28 29 30 31 32 33 34
35 14 5913 5912 5911 5910 5909 5908 5907 5906
5905 5904 5903 5902 5901 5900 5899 5898 5897 5896
5895 5894 5893 5892 5891 5890 5889 5888 5887 5886
5885 5884 5883 5882 5881 5880 5879 5878 5877 5876
5875 5874 5873 5872 5871 5870 5869 5868 5867 5866
5865 5864 5863 5857

5

5857 5858 5859 5860 5861 5862 5845 5856 5855 5854
5853 5852 5851 5850 5849 5848 5847 5846 5801 8862
8863 8864 8865 8866 8867 8868 8869 8870 8871 8872
8861 8877 8876 8875 8874 8873 2015

6

6698 6699 6700 6701 6702 6703 6686 6697 6696 6695
6694 6693 6692 6691 6690 6689 6688 6687 6642 9616
9615 9614 9613 9612 9611 9610 9609 9608 9607 9606
9605 9617 9618 9619 9620 9621 2067

7

2015 2068 2069 2070 2067

8

2015 2016 2017 2018 2019 2020 2021 2022 2023 2024
2025 2026 2027 2028 2029 2030 2031 2032 2033 2034
2035 2036 2037 2038 2039 2040 2041 2042 2043 2044
2045 2046 2047 2048 2049 2050 2051 2052 2053 2054
2055 2056 2057 2058 2059 2060 2061 2062 2063 2064
2065 2066 2005 2014 2013 2012 2011 2010 2009 2008
2007 2006 2001

9

2067 2121 2120 2119 2118 2117 2116 2115 2114
2113 2112 2111 2110 2109 2108 2107 2106 2105 2104
2103 2102 2101 2100 2099 2098 2097 2096 2095 2094
2093 2092 2091 2090 2089 2088 2087 2086 2085 2084
2083 2082 2081 2080 2079 2078 2077 2076 2075 2074
2073 2072 2071 1990 1992 1993 1994 1995 1996 1997
1998 1999 2000 1991

10

2001 2002 2003 2004 1991

11

2001 5310 5311 5312 5313 5314 5302 5309 5308 5307
5306 5305 5304 5303 5298 17961 17960 17974 17962

12

1991 5428 5427 5426 5425 5424 5416 5423 5422 5421
5420 5419 5418 5417 5412 18039 18036 18038 18037

13

17962 18126 18127 18128 18037

14

17962 17963 17964 17965 17966 17967 17968 17969 17970
17971 17972 17973 16559 16613 16612 16611 16595

15

16647 16705 16704 16703 16702 16701 16700 16699 16595

16

18037 18050 18049 18048 18047 18046 18045 18044 18043 18042
18041 18040 16563 16648 16649 16650 16647

17

18690 18691 18692 18693 18694 18695 18696 18697 18698 18699
18700 18701 16527 16663 16664 16665 16647

18

18616 18617 18618 18619 18620 18621 18622 18623 18624 18625
18626 18627 16523 16598 16597 16596 16595

19

18616 18780 18781 18782 18690

20

18616 18628 18614 18615 2 9 8 7 6 5
4 3 1 40 39 38 37 36 26

21

18690 18703 18702 18704 155 165 164 163 162 161
160 159 127 132 131 130 129 128 126

CRACK3D.SIF

LOADING INCREMENT NUMBER = 1

Energy release rates & SIFs for crack front#: 1
(This is an open crack front)

Total crack extension so far: 0.00000E+00 Multiplicative factor used to scale loading: 0.10000E+01

SEGMT# X Y Z G1 G2 G3 K1 K2 K3
1 -0.63500E-01 0.00000E+00 -0.23812E-02 0.37165E-03 0.10656E-03 0.37377E-05 0.54455E+04 -0.29159E+04 0.44700E+03
2 -0.63500E-01 0.00000E+00 -0.79375E-03 0.39629E-03 0.10753E-03 0.46060E-06 0.56231E+04 -0.29291E+04 0.15692E+03
3 -0.63500E-01 0.00000E+00 0.79375E-03 0.37837E-03 0.10506E-03 0.34734E-06 0.54945E+04 -0.28952E+04 -0.13627E+03
4 -0.63500E-01 0.00000E+00 0.23812E-02 0.38625E-03 0.11748E-03 0.46666E-05 0.55514E+04 -0.30616E+04 -0.49947E+03

LOADING INCREMENT NUMBER = 1

Energy release rates & SIFs for crack front#: 1
(This is an open crack front)

Total crack extension so far: 0.20000E-02 Multiplicative factor used to scale loading: 0.10000E+01

SEGMT# X Y Z G1 G2 G3 K1 K2 K3
1 -0.62004E-01 0.13276E-02 -0.23812E-02 0.75121E-03 0.31880E-06 0.16848E-06 0.77420E+04 0.15949E+03 0.94904E+02
2 -0.62004E-01 0.13276E-02 -0.79375E-03 0.79535E-03 0.36949E-06 0.31913E-07 0.79662E+04 -0.17170E+03 0.41304E+02
3 -0.62004E-01 0.13276E-02 0.79375E-03 0.79535E-03 0.34982E-06 0.32934E-07 0.79662E+04 -0.16707E+03 -0.41959E+02
4 -0.62004E-01 0.13276E-02 0.23813E-02 0.77147E-03 0.29758E-06 0.19412E-06 0.78457E+04 0.15409E+03 -0.10187E+03

LOADING INCREMENT NUMBER = 1

Energy release rates & SIFs for crack front#: 1
(This is an open crack front)

Total crack extension so far: 0.40000E-02 Multiplicative factor used to scale loading: 0.10000E+01

SEGMT# X Y Z G1 G2 G3 K1 K2 K3
1 -0.60510E-01 0.26575E-02 -0.23812E-02 0.89194E-03 0.62888E-06 0.12236E-08 0.84361E+04 0.22400E+03 0.80879E+01
2 -0.60510E-01 0.26575E-02 -0.79375E-03 0.94345E-03 0.68460E-06 0.35363E-08 0.86762E+04 0.23372E+03 0.13749E+02
3 -0.60510E-01 0.26575E-02 0.79375E-03 0.94319E-03 0.84510E-06 0.33224E-08 0.86751E+04 0.25967E+03 -0.13327E+02

4 -0.60510E-01 0.26575E-02 0.23813E-02 0.91714E-03 0.75434E-06 0.40909E-08 0.85544E+04
0.24533E+03 -0.14788E+02

LOADING INCREMENT NUMBER = 1

Energy release rates & SIFs for crack front#: 1
(This is an open crack front)

Total crack extension so far: 0.60000E-02 Multiplicative factor used to scale loading: 0.10000E+01

SEGMT# X Y Z G1 G2 G3 K1 K2 K3
1 -0.58945E-01 0.39018E-02 -0.23812E-02 0.10424E-02 0.24602E-08 0.23384E-07 0.91198E+04 -
0.14011E+02 0.35356E+02
2 -0.58945E-01 0.39018E-02 -0.79375E-03 0.11053E-02 0.63708E-08 0.30365E-08 0.93908E+04 -
0.22546E+02 0.12741E+02
3 -0.58945E-01 0.39018E-02 0.79375E-03 0.11061E-02 0.71879E-08 0.57638E-08 0.93942E+04 -
0.23948E+02 -0.17554E+02
4 -0.58945E-01 0.39018E-02 0.23813E-02 0.10718E-02 0.37370E-07 0.32012E-07 0.92474E+04 -
0.54605E+02 -0.41368E+02

LOADING INCREMENT NUMBER = 1

Energy release rates & SIFs for crack front#: 1
(This is an open crack front)

Total crack extension so far: 0.80000E-02 Multiplicative factor used to scale loading: 0.10000E+01

SEGMT# X Y Z G1 G2 G3 K1 K2 K3
1 -0.57387E-01 0.51558E-02 -0.23812E-02 0.11912E-02 0.32908E-08 0.11088E-07 0.97489E+04 -
0.16204E+02 0.24346E+02
2 -0.57387E-01 0.51558E-02 -0.79375E-03 0.12643E-02 0.70049E-08 0.29710E-08 0.10044E+05 -
0.23641E+02 0.12603E+02
3 -0.57387E-01 0.51558E-02 0.79375E-03 0.12599E-02 0.12317E-07 0.38677E-08 0.10026E+05 -
0.31349E+02 -0.14379E+02
4 -0.57387E-01 0.51558E-02 0.23813E-02 0.12210E-02 0.15173E-07 0.23911E-07 0.98704E+04 -
0.34794E+02 -0.35752E+02

LOADING INCREMENT NUMBER = 1

Energy release rates & SIFs for crack front#: 1
(This is an open crack front)

Total crack extension so far: 0.10000E-01 Multiplicative factor used to scale loading: 0.10000E+01

SEGMT# X Y Z G1 G2 G3 K1 K2 K3
1 -0.55835E-01 0.64181E-02 -0.23812E-02 0.13308E-02 0.10571E-07 0.87559E-08 0.10305E+05 -
0.29042E+02 0.21635E+02
2 -0.55835E-01 0.64181E-02 -0.79375E-03 0.14127E-02 0.86960E-08 0.20416E-09 0.10617E+05
0.26341E+02 0.33036E+01

3 -0.55835E-01 0.64181E-02 0.79375E-03 0.14136E-02 0.24837E-08 0.10044E-08 0.10620E+05 -0.14077E+02 -0.73275E+01
4 -0.55835E-01 0.64181E-02 0.23813E-02 0.13692E-02 0.14156E-07 0.10934E-07 0.10452E+05 -0.33608E+02 -0.24177E+02

LOADING INCREMENT NUMBER = 1

Energy release rates & SIFs for crack front#: 1
(This is an open crack front)

Total crack extension so far: 0.12000E-01 Multiplicative factor used to scale loading: 0.10000E+01

SEGMT# X Y Z G1 G2 G3 K1 K2 K3
1 -0.54287E-01 0.76841E-02 -0.23812E-02 0.14626E-02 0.92988E-08 0.20640E-08 0.10803E+05 0.27239E+02 0.10504E+02
2 -0.54287E-01 0.76841E-02 -0.79375E-03 0.15574E-02 0.18122E-07 0.93540E-09 0.11147E+05 0.38026E+02 0.70714E+01
3 -0.54287E-01 0.76841E-02 0.79375E-03 0.15557E-02 0.26493E-07 0.37783E-09 0.11141E+05 0.45977E+02 -0.44943E+01
4 -0.54287E-01 0.76841E-02 0.23813E-02 0.15045E-02 0.11177E-08 0.29300E-08 0.10956E+05 0.94435E+01 -0.12515E+02

LOADING INCREMENT NUMBER = 1

Energy release rates & SIFs for crack front#: 1
(This is an open crack front)

Total crack extension so far: 0.14000E-01 Multiplicative factor used to scale loading: 0.10000E+01

SEGMT# X Y Z G1 G2 G3 K1 K2 K3
1 -0.52732E-01 0.89416E-02 -0.23812E-02 0.15860E-02 0.16973E-07 0.14073E-08 0.11249E+05 0.36800E+02 0.86736E+01
2 -0.52732E-01 0.89416E-02 -0.79375E-03 0.16916E-02 0.19714E-07 0.59647E-09 0.11618E+05 0.39661E+02 0.56468E+01
3 -0.52732E-01 0.89416E-02 0.79375E-03 0.16832E-02 0.10127E-07 0.18859E-08 0.11589E+05 0.28426E+02 -0.10041E+02
4 -0.52732E-01 0.89416E-02 0.23813E-02 0.16344E-02 0.22974E-07 0.12336E-08 0.11420E+05 0.42814E+02 -0.81208E+01

LOADING INCREMENT NUMBER = 1

Energy release rates & SIFs for crack front#: 1
(This is an open crack front)

Total crack extension so far: 0.16000E-01 Multiplicative factor used to scale loading: 0.10000E+01

SEGMT# X Y Z G1 G2 G3 K1 K2 K3
1 -0.51168E-01 0.10189E-01 -0.23812E-02 0.17012E-02 0.39117E-07 0.71751E-09 0.11651E+05 0.55867E+02 0.61933E+01

2 -0.51168E-01 0.10189E-01 -0.79375E-03 0.18082E-02 0.36286E-07 0.63876E-10 0.12011E+05 0.53807E+02 0.18479E+01
3 -0.51168E-01 0.10189E-01 0.79375E-03 0.18068E-02 0.82220E-07 0.81703E-09 0.12007E+05 0.80995E+02 -0.66089E+01
4 -0.51168E-01 0.10189E-01 0.23813E-02 0.17491E-02 0.21554E-07 0.11258E-08 0.11813E+05 0.41470E+02 -0.77578E+01

LOADING INCREMENT NUMBER = 1

Energy release rates & SIFs for crack front#: 1
(This is an open crack front)

Total crack extension so far: 0.18000E-01 Multiplicative factor used to scale loading: 0.10000E+01

SEGMT# X Y Z G1 G2 G3 K1 K2 K3
1 -0.49593E-01 0.11421E-01 -0.23812E-02 0.18029E-02 0.20153E-07 0.11729E-08 0.11994E+05 0.40100E+02 0.79183E+01
2 -0.49593E-01 0.11421E-01 -0.79375E-03 0.19172E-02 0.34006E-07 0.71986E-09 0.12368E+05 0.52089E+02 -0.62034E+01
3 -0.49593E-01 0.11421E-01 0.79375E-03 0.19172E-02 0.55772E-07 0.20859E-08 0.12368E+05 0.66708E+02 0.10560E+02
4 -0.49593E-01 0.11421E-01 0.23813E-02 0.18547E-02 0.26017E-07 0.19943E-09 0.12165E+05 0.45561E+02 -0.32652E+01

LOADING INCREMENT NUMBER = 1

Energy release rates & SIFs for crack front#: 1
(This is an open crack front)

Total crack extension so far: 0.20000E-01 Multiplicative factor used to scale loading: 0.10000E+01

SEGMT# X Y Z G1 G2 G3 K1 K2 K3
1 -0.48007E-01 0.12640E-01 -0.23812E-02 0.18917E-02 0.66330E-07 0.27124E-09 0.12286E+05 0.72749E+02 -0.38079E+01
2 -0.48007E-01 0.12640E-01 -0.79375E-03 0.20160E-02 0.71559E-07 0.14384E-09 0.12683E+05 0.75562E+02 -0.27730E+01
3 -0.48007E-01 0.12640E-01 0.79375E-03 0.20118E-02 0.88642E-07 0.24471E-08 0.12670E+05 0.84099E+02 0.11438E+02
4 -0.48007E-01 0.12640E-01 0.23813E-02 0.19478E-02 0.50861E-07 0.80686E-09 0.12466E+05 0.63703E+02 0.65676E+01

LOADING INCREMENT NUMBER = 1

Energy release rates & SIFs for crack front#: 1
(This is an open crack front)

Total crack extension so far: 0.22000E-01 Multiplicative factor used to scale loading: 0.10000E+01

SEGMT# X Y Z G1 G2 G3 K1 K2 K3

1 -0.46407E-01 0.13840E-01 -0.23812E-02 0.19787E-02 0.69089E-07 0.29344E-09 0.12565E+05
0.74246E+02 -0.39607E+01
2 -0.46407E-01 0.13840E-01 -0.79375E-03 0.21077E-02 0.85531E-07 0.31981E-09 0.12968E+05
0.82610E+02 -0.41348E+01
3 -0.46407E-01 0.13840E-01 0.79375E-03 0.21035E-02 0.13675E-06 0.24518E-08 0.12955E+05
0.10446E+03 0.11449E+02
4 -0.46407E-01 0.13840E-01 0.23813E-02 0.20370E-02 0.87836E-07 0.13225E-10 0.12749E+05
0.83716E+02 0.84083E+00

LOADING INCREMENT NUMBER = 1

Energy release rates & SIFs for crack front#: 1
(This is an open crack front)

Total crack extension so far: 0.24000E-01 Multiplicative factor used to scale loading: 0.10000E+01

SEGMT# X Y Z G1 G2 G3 K1 K2 K3
1 -0.44791E-01 0.15019E-01 -0.23812E-02 0.20479E-02 0.12539E-06 0.50449E-08 0.12783E+05
0.10002E+03 -0.16422E+02
2 -0.44791E-01 0.15019E-01 -0.79375E-03 0.21819E-02 0.18469E-06 0.57208E-09 0.13194E+05
0.12139E+03 0.55301E+01
3 -0.44791E-01 0.15019E-01 0.79375E-03 0.21824E-02 0.19846E-06 0.24257E-08 0.13196E+05
0.12584E+03 0.11387E+02
4 -0.44791E-01 0.15019E-01 0.23813E-02 0.21062E-02 0.15600E-06 0.52980E-09 0.12964E+05
0.11157E+03 0.53219E+01

LOADING INCREMENT NUMBER = 1

Energy release rates & SIFs for crack front#: 1
(This is an open crack front)

Total crack extension so far: 0.26000E-01 Multiplicative factor used to scale loading: 0.10000E+01

SEGMT# X Y Z G1 G2 G3 K1 K2 K3
1 -0.43155E-01 0.16168E-01 -0.23812E-02 0.21119E-02 0.88676E-07 0.30555E-08 0.12981E+05
0.84115E+02 -0.12781E+02
2 -0.43155E-01 0.16168E-01 -0.79375E-03 0.22547E-02 0.10418E-06 0.74047E-10 0.13413E+05
0.91173E+02 -0.19896E+01
3 -0.43155E-01 0.16168E-01 0.79375E-03 0.22510E-02 0.71895E-07 0.49060E-09 0.13402E+05
0.75739E+02 -0.51212E+01
4 -0.43155E-01 0.16168E-01 0.23813E-02 0.21712E-02 0.68106E-07 0.12286E-08 0.13162E+05
0.73717E+02 0.81041E+01

LOADING INCREMENT NUMBER = 1

Energy release rates & SIFs for crack front#: 1
(This is an open crack front)

Total crack extension so far: 0.28000E-01 Multiplicative factor used to scale loading: 0.10000E+01

SEGMT# X Y Z G1 G2 G3 K1 K2 K3
1 -0.41505E-01 0.17298E-01 -0.23812E-02 0.21698E-02 0.20511E-06 0.17686E-08 0.13158E+05 0.12793E+03 -0.97236E+01
2 -0.41505E-01 0.17298E-01 -0.79375E-03 0.23086E-02 0.25158E-06 0.96179E-09 0.13572E+05 0.14168E+03 -0.71705E+01
3 -0.41505E-01 0.17298E-01 0.79375E-03 0.23055E-02 0.34365E-06 0.18926E-08 0.13563E+05 0.16559E+03 0.10059E+02
4 -0.41505E-01 0.17298E-01 0.23813E-02 0.22313E-02 0.23404E-06 0.65428E-08 0.13343E+05 0.13665E+03 0.18702E+02

LOADING INCREMENT NUMBER = 1

Energy release rates & SIFs for crack front#: 1
(This is an open crack front)

Total crack extension so far: 0.30000E-01 Multiplicative factor used to scale loading: 0.10000E+01

SEGMT# X Y Z G1 G2 G3 K1 K2 K3
1 -0.39831E-01 0.18392E-01 -0.23812E-02 0.22169E-02 0.12940E-06 0.46224E-08 0.13300E+05 0.10161E+03 -0.15720E+02
2 -0.39831E-01 0.18392E-01 -0.79375E-03 0.23662E-02 0.18496E-06 0.40042E-09 0.13740E+05 0.12148E+03 -0.46266E+01
3 -0.39831E-01 0.18392E-01 0.79375E-03 0.23638E-02 0.18353E-06 0.38330E-08 0.13733E+05 0.12101E+03 0.14315E+02
4 -0.39831E-01 0.18392E-01 0.23813E-02 0.22830E-02 0.20926E-06 0.15014E-09 0.13497E+05 0.12922E+03 0.28331E+01

CRACK3D.CXT

Arcan 4 elem through thickness

INFORMATION OF LOAD VERSUS TOTAL CRACK INCREMENT

AT SPECIFIED MASTER NODE POSITION

(Reference Z-COORDINATE: 0.00000)

LOADING INCREMENT	CRACK FRONT NUMBER	TOTAL CRACK INCREMENT	TOTAL LOADS ON ALL SPECIFIED NODES X-LOAD	Y-LOAD	Z-LOAD	COMBINED
1	1	0.00000	0.21361E+02	-0.21362E+02	-0.29745E-12	0.30210E+02
1	1	0.00200	0.21236E+02	-0.21236E+02	-0.42413E-08	0.30033E+02
1	1	0.00400	0.21086E+02	-0.21086E+02	-0.39401E-08	0.29820E+02
1	1	0.00600	0.20909E+02	-0.20909E+02	0.35147E-08	0.29570E+02
1	1	0.00800	0.20704E+02	-0.20705E+02	-0.41428E-09	0.29281E+02
1	1	0.01000	0.20473E+02	-0.20473E+02	-0.12057E-08	0.28953E+02
1	1	0.01200	0.20216E+02	-0.20216E+02	-0.35862E-08	0.28590E+02
1	1	0.01400	0.19935E+02	-0.19936E+02	0.14178E-07	0.28193E+02
1	1	0.01600	0.19633E+02	-0.19633E+02	0.53847E-09	0.27765E+02
1	1	0.01800	0.19310E+02	-0.19311E+02	0.18068E-08	0.27309E+02
1	1	0.02000	0.18970E+02	-0.18971E+02	0.28869E-08	0.26828E+02
1	1	0.02200	0.18614E+02	-0.18614E+02	0.45479E-08	0.26324E+02
1	1	0.02400	0.18243E+02	-0.18244E+02	0.32076E-08	0.25800E+02
1	1	0.02600	0.17860E+02	-0.17861E+02	0.27318E-08	0.25259E+02
1	1	0.02800	0.17466E+02	-0.17467E+02	0.89362E-09	0.24701E+02
1	1	0.03000	0.17062E+02	-0.17063E+02	-0.32270E-08	0.24130E+02